

https://dspace.org/

# Exploring heatwaves and urban heat islands: implications for water wesource availability in Gauteng Province, South Africa

**Kuwaza, Tamiranashe**

**2025**
University of the Witwatersrand, Johannesburg
https://hdl.handle.net/10539/50288
Kuwaza, Tamiranashe. (2025). Exploring heatwaves and urban heat islands: implications for water wesource availability in Gauteng Province, South Africa [Master's dissertation PhD thesis, University of the Witwatersrand, Johannesburg]. WIReDSpace. https://hdl.handle.net/10539/50288

Downloaded from a DSpace repository. https://dspace.org/

# Exploring heatwaves and urban heat islands: implications for water wesource availability in Gauteng Province, South Africa

Tamiranashe Kuwaza
2428968

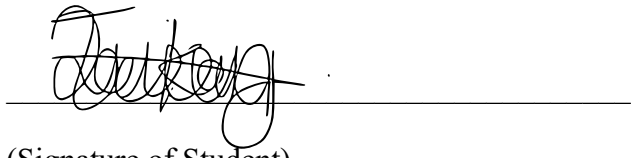
This thesis is submitted to the Faculty of Science, University of the Witwatersrand, Johannesburg, in fulfilment of the requirements for the degree of Master of Science (Environmental Studies) by Dissertation at the School of Geography, Archaeology & Environmental Studies.

Supervisor: Professor Paidamwoyo Mhangara
Co-Supervisor: Dr. Eskinder Gidey

December 2025
Johannesburg

# DECLARATION OF ORIGINALITY AND NO USE OF AI

I, Tamiranashe Kuwaza, 2428968, declare that this Dissertation is my own work. It is being submitted for the Degree of MSc Environmental Studies at the University of the Witwatersrand, Johannesburg. It has not been submitted before for any degree or examination at any other University.



(Signature of Student)

31 of December 2025 in Johannesburg

# DISSERTATION SUPERVISORS

Main Supervisor

- Prof. Paidamwoyo Mhangara, School of Geography, Archaeology and Environmental Studies, Faculty of Science, University of Witwatersrand, Private Bag: 2050, Johannesburg, Gauteng, South Africa

Co- Supervisor

- Dr. Eskinder Gidey, Department of Land Resources Management and Environmental Protection (LaRMEP), College of Dryland Agriculture and Natural Resources, Mekelle University, P.O Box: 231, Mekelle, Tigray–Ethiopia

# ACKNOWLEDGEMENTS

I would like to thank my supervisor Prof Paida Mhangara, for providing me with the necessary assistance, tools and guidance to complete my research. I am thankful to the Water Research Commission (WRC) for funding my tuition to complete this research. Additionally, Dr Eskinder Gidey, for assisting me and guiding me on producing outputs and editing. Additionally, to the institution (University of the Witwatersrand) and more specifically the school of Geography, Archaeology, and Environmental Studies for providing the relevant up-to-date resources, tools, network and professional staff that aid with any queries or technical issues in record time.

Lastly, to my mother and brother for their patience and unwavering support throughout my life. I owe everything to God and His mercy.

This MSc research proposal has been fully supported (financially and technically) by the Water Research Commission (WRC) research project (Number: 2024/2025-01657) as part of the project's human capacity development initiative.

# ABSTRACT

Surface water is a scarce resource in Gauteng, which leads to diverse research in analysing possible implications on water resources in the region. Further, heatwaves and urban heat islands are a prevalent topic in urban studies in an attempt to understand and curb urban heat stress in the future. The study analyses heat and water indices along vegetation and land use land cover dynamics to uncover spatio-temporal trends in Gauteng. Using Landsat 5TM and Landsat 8 OLI/TIRS at 30m resolution with NASA POWER over a period of 4 decades. This uncovered trends in urbanisation, surface water and urban heat. Maximum air temperature and NDVI displayed an increasing trend according to the Mann-Kendall analysis, with the water ratio index and precipitation decreasing over the years. Additionally, MNDWI and LST obtain a negative Spearman correlation of $\rho = -0.40$, $p < 0.001$. Similarly, NDVI and WRI observe a negative correlation of $\rho = -0.69$, reflecting the inverse spectral response of vegetation and water surfaces as detected by the sensors. Moreover, heatwaves in Gauteng have increased gradually, with average frequency being ~1 from 1984 to 2009; however, from 2014 to 2024, the average frequency is ~4. While the average UHII for Gauteng in 1984 was –2.18 °C, it increased to 0.25°C in 2024. This further highlights a negative result of UHII, indicating a cooling response in 1984 as opposed to the positive result in 2024, indicating a warming sensation in Gauteng.

The mean land surface temperature of vegetated areas exhibits a decreasing trend over time, corresponding with increasing NDVI trends in the region. The increase of NDVI by anthropogenic greening and cultivated land, with the increase of heatwave frequency and duration, contributes to thermal surface water stress.

The paper makes use of random forest classification to depict LULC trends over 40 years. The overall accuracy was ~ 96% while Kappa coefficients remained above 90% in general. However, the confusion matrix indicates comparatively higher misclassification among

waterbodies, grasslands, and barren land classes. This confusion is often attributed to spectral similarity in multispectral remote sensing data.

This study provides crucial insights into converging indicators of heat stress, as depicted by the increasing LST with decreasing WRI and precipitation. Additionally, the positive correlation between LST and WRI offers strong evidence that water resources in Gauteng are experiencing heat stress. Therefore, the region is vulnerable to climate-land cover interactions.

KEYWORDS: Heatwaves; Urban Heat Islands; Land Cover Change; Climate Impacts; Surface Water Resources; Gauteng Province; South Africa.

# LIST OF ACRONYMS

BT – Brightness

CBD – Central Business District

CSIR – Council for Scientific and Industrial Research

DWS – Department of Water and Sanitation

GHG – Greenhouse Gases

GIS – Geographic Information Systems

IVRS – Integrated Vaal River System

K – Kappa Coefficient

LST – Land Surface Temperature

LULC – Land Use Land Cover

MNDWI – Modified Normalised Difference Water Index

NASA POWER - National Aeronautics and Space Administration - Prediction Of Worldwide Energy Resources Project

NDVI – Normalised Difference Vegetation Index

NIR – Near Infrared (range of light)

OA – Overall Accuracy

OLI – Operational Land Imager

PA – Producer's Accuracy

RF – Random Forest

ROI – Region of Interest

SAWS – South African Weather Service

SWIR – Short Wave Infrared

TIRS – Thermal Infrared Sensor

TM – Thematic Mapper

TOA – Top Of Atmosphere

UA – User's Accuracy

UHI – Urban Heat Island

UHII – Urban Heat Island Intensity

USGS – United States Geological Survey

UTM – Universal Transverse Mercator

WRI – Water Ratio Index

# Table of Contents

*DECLARATION OF ORIGINALITY AND NO USE OF AI* ..... *i*

*DISSERTATION SUPERVISORS* ..... *ii*

*ACKNOWLEDGEMENTS* ..... *iii*

*ABSTRACT* ..... *iv*

*LIST OF ACRONYMS* ..... *vi*

*LIST OF FIGURES* ..... *xi*

*CHAPTER ONE: INTRODUCTION* ..... *1*

**1.1 Background** ..... **1**

**1.2 Problem Statement** ..... **5**

**1.3 Research Aims and Objectives** ..... **7**

1.3.1 Aim ..... 7

1.3.2 Objectives ..... 7

**1.4 Research Questions** ..... **8**

**1.5 The Structure of the Dissertation** ..... **8**

*CHAPTER TWO: LITERATURE REVIEW* ..... *9*

**Introduction** ..... **9**

**2.1 Global and Regional Climate Change Trends** ..... **10**

**2.2 Urban Climate Studies in Gauteng and South Africa** ..... **11**

**2.3 Urban Temperature Dynamics** ..... **13**

2.3.1 Urban Heat ..... 13

2.3.2 Land Surface Temperature (LST) and Urban Thermal Patterns ..... 16

2.3.3 Overview of Urban Heat Island (UHI) Effect ..... 18

2.3.4 Heatwaves and their Environmental Impacts ..... 19

**2.4 Natural Environmental and Urban Pressures** ..... **20**

2.4.1 Vegetation and Urban Pressures ..... 20

2.4.2 Urbanisation and Surface Water Depletion ..... 22

**2.5 Interconnections Between Urban Heat, Land Use Change, Vegetation, and Water** ..... **25**

**2.6 Integrating Remote Sensing and Empirical Research in Urban Environmental Studies** ..... **27**

2.6.1 Remote Sensing in Urban Cities ..... 27

2.6.2 Remote Sensing in Water and Heat Analysis ..... 29

**2.7 Land Use and Land Cover Classification and Machine Learning Approaches** ..... **30**

**Conclusion** ..... **32**

*CHAPTER THREE: DATA AND METHODOLOGY* ..... *36*

**3.1 Study Area** ..... **36**

**3.2 Data Acquisition** ..... **39**

**3.3 Image Processing and Analysis** ..... **46**

3.3.1 Assessment of LULC, Accuracy Assessment and NDVI Derivation ..... 46

3.3.2 Temperature and Urban Heat Calculations ..... 48

3.3.3 Surface Water Indices Calculation ..... 54

*CHAPTER FOUR: RESULTS AND DISCUSSION* ..... *57*
**4.1 Analysis Of Heatwaves and UHI Intensity Over Gauteng (1984 To 2020)** ..... **57**
4.1.1 Overview of Temporal Trends ..... 57
**4.2 Effects of Land Cover Types on Triggering Heatwaves and UHI** ..... **73**
4.2.1 Land Use Land Cover Trend ..... 73
4.2.2 Overview of Vegetation ..... 79
**4.3 Impacts of Land Cover Dynamics, Heatwaves, Urban Heat Islands on Surface Water Resources** ..... **84**
**4.4 Vegetation and Climate Indices Correlation** ..... **92**
**4.5 Trends of Climate, NDVI and Water Resources in Gauteng** ..... **93**
*CHAPTER FIVE: CONCLUSION AND FUTURE PROSPECTS* ..... *95*
5.1 Summary of Key Findings ..... 95
5.2. Synthesis of Urban Heat Implications on Surface Water Research ..... 96
5.3. Recommendations and Future Research Directions ..... 97
*REFERENCES* ..... *99*
*APPENDIX* ..... *119*

# LIST OF TABLES

*Table 1 1: Overview of Recent Literature on Urban Studies in Gauteng: Temporal, Spatial, and Variable Dimensions..... 5*

*Table 3.2 1: Spectral Index Table for the Satellite Imagery..... 41*
*Table 3.2 2:Kappa Coefficients..... 45*
*Table 3.2 3: MNDWI Interpretations. ..... 45*
*Table 3.2 4: NDVI Interpretations. ..... 46*

*Table 4.1 1: Relative Temperature in °C, Across Land Use Land Cover Types in Gauteng..... 65*
*Table 4.1 2: Urban Heat Island Intensity within Metropolises in Gauteng from 1984 to 2024 in °C..... 69*
*Table 4.1 3: Analysis of Heatwave Characteristics in Gauteng ..... 73*

*Table 4.2 1: Annual Land Use Land Cover Change Table from 1984 to 2024.. 77*
*Table 4.2 2:Land Use Class Analysis Table using CA, PA, F- S, OA, and K- K-coefficient values from 1984 to 2024. ..... 79*

*Table 4.4. 1: The Statistical Relationship Among Vegetation, Water and Climate Indices..... 93*

*Table 4.5. 1: Long-term Vegetation, Water and Climate Trends..... 94*

# LIST OF FIGURES

*Figure 3 1: Map of Gauteng. Source: Sintayehu & Mhangara (2023)..... 37*

*Figure 3.2 1: Schematic representation of the methodological framework..... 42*

*Figure 4.1 1: Spatiotemporal distribution of Land Surface Temperature in Gauteng..... 60*
*Figure 4.1 2: Localised long-term change analysis of Land Surface Temperature at a city-scale in Gauteng from 1984 to 2024..... 62*
*Figure 4.1 3: The map above displays the spatiotemporal distribution of Urban Heat Island Intensity in Gauteng..... 67*
*Figure 4.1 4: Localised long-term change analysis of Urban Heat Island Intensity at a city-scale in Gauteng from 1984 to 2024..... 71*

*Figure 4.2. 1: The map above displays the spatiotemporal variation of Land Use in Gauteng..... 75*
*Figure 4.2. 2: Spatiotemporal variation of NDVI in Gauteng..... 81*
*Figure 4.2. 3: Localised long-term change analysis of NDVI at a city-scale in Gauteng from 1984 to 2024..... 83*

*Figure 4.3. 1: The map above displays the spatiotemporal variation of MNDWI in Gauteng..... 85*
*Figure 4.3. 2: The map above displays a localised long-term change analysis of MNDWI at a city-scale in Gauteng..... 87*
*Figure 4.3. 3: The map above displays the spatiotemporal variation of WRI in Gauteng..... 89*
*Figure 4.3. 4: The map above displays a localised long-term change analysis of WRI at a city-scale in Gauteng..... 91*

*Figure 7 1: Ethics Waiver .....119*

# CHAPTER ONE: INTRODUCTION

The introduction introduces the research, the possible questions, gaps and outlines the background and study area. It is structured as the background first, containing the general idea of the topic in the setting of the study area. Secondly, the research objectives and the research aims of the research are examined. Thirdly, the aim and problem statement outline the reasoning for the research and plausible gaps in the literature surrounding this topic and its variables. Then follows the research questions that dive deeper into the literature of this topic, and whether the paper can answer these questions. These questions are to be answered through literature as well as the results of the paper. Lastly, a small paragraph is dedicated to the structure of the paper's contents.

## 1.1 Background

Climate change is a threat to the world's freshwater resources, altering precipitation, shrinking streamflow, accelerating glacier and snowpack loss undermining water security for communities, ecosystems and economies. The World Meteorological Organisation (WMO) confirm that the past decade is the warmest on record (WMO, 2025). Further, across Africa, these global trends translate into regionally amplified warming and heightened water stress. The Intergovernmental Panel on Climate Change (IPCC) documents that much of Africa is warming faster than the global average, with a substantial projected increase in the frequency of extreme heat, and greater variability in rainfall (IPCC, 2023). Moreover, many catchments that supply cities face reduced low flows while population growth and urbanisation have increased the water demand (Nhamo et al., 2021; IPCC, 2023; DWS, 2024).

Greenhouse gases exacerbate urban heat through mechanisms such as large-scale increases in mean and extreme air temperatures due to elevated greenhouse gas concentrations. Hence, the IPCC and WMO emphasise that anthropogenic emissions have made heat extremes more frequent and intense globally (IPCC, 2023; WMO, 2024). Further, empirical studies link increased impervious surfaces and tar with the loss of vegetation, leading to higher land surface temperatures to extreme urban heat intensification (Roba & Tabor, 2025). Moreover, remote-sensing and field analysis in African and global cities consistently show strong correlations between impervious surfaces, vegetation loss and increased land surface temperatures, which insinuates that urban design is a critical variable for water–heat management (Bokaie et al., 2016; Roba & Tabor, 2025).

These interacting changes between water, land use and urban temperature can trigger negative climatic events that amplify risk. Drastic climatic events can push natural systems toward thresholds where recovery becomes costly or slow, reinforcing the need for pre-emptive, integrated action. The IPCC's AR6 assessments synthesise robust findings on heat extremes, hydrological change and the benefits of near-term mitigation and adaptation without deep emissions cuts in targeted regions like Africa (IPCC, 2023). In South Africa, the Department of Water and Sanitation explicitly links climate change to stressed surface-water resources, thus prioritising augmentation of water storage that is cost-effective, and calls for sectoral climate-response strategies that combine infrastructure renewal, non-revenue water reduction and catchment protection (DWS, 2024). Furthermore, African governments and development partners confront these climatic burdens while also pursuing poverty reduction and infrastructure expansion. Taken together, the science and policy signals demand a forward-looking, integrated agenda.

The Gauteng City-Region refers to the broader continuous urbanised region encompassing Pretoria-Johannesburg-Vereeniging, in earlier definitions, which has grown in population over the past decades (Nhamo *et al.,* 2021). Gauteng is the smallest and most densely populated province in South Africa (Chakwizira et al*.,* 2018), with an area of about 18,176 km² and about 18,496 km² including the Vaal Catchment. The province is characterised by mixed land use and urbanised city centres. The metropolises in the area are Johannesburg, West Rand, Tshwane, Sedibeng and Ekurhuleni. In recent decades, the region has observed a rapid expansion of both formal and informal settlements (Nhamo *et al.,* 2021; Jombo et al., 2022). Moreover, unplanned development does not account for appropriate land use and green space planning, leaving areas barren and settlements scattered with structures as houses (Nhamo *et al.,* 2021; Jombo et al., 2022). This creates several implications, including infrastructure strain and service delivery challenges. Thus, lower socioeconomic areas usually suffer more, as evidenced in intra-urban studies such as Johannesburg, which show higher land surface temperature where vegetation is low (Jombo et al., 2022; Singh et al., 2023; Parker et al., 2025). Land surface temperature is the temperature of the surface skin sensed by remote sensors. While urban heat island effect is the phenomenon where urban areas are warmer than the surrounding rural areas. Surface urban heat islands are measured using land surface temperature. Furthermore, the region documents high urban heat islands and heatwaves mostly in Johannesburg and Ekurhuleni (Souverijns et al., 2022). Studies show that Johannesburg has experienced strong UHI effects due to dense built-up areas and impervious surfaces (Mudede et al., 2020; Souverijns et al., 2022). Another study during the COVID-19 pandemic found that urban heat island intensity in Tshwane, Johannesburg and Ekurhuleni reduced due to minimal industrial activity and vehicles on the roads (Shikwambana et al., 2020). Land use land cover is a terminology used in climate and environmental studies relating to how the land is occupied, used or covered, for example, vegetation, built-up areas, water or bare land. The use of remote sensing and time series

analysis allows for these changes (deforestation and urban expansion) to be tracked over time. Moreover, uneven vegetation cover disrupts the cooling in the region (Singh et al., 2023; Parker et al., 2025). Therefore, areas with low normalised difference vegetation index (NDVI) exhibit warmer temperatures, while greener suburbs offer cooling benefits (Jombo et al., 2022). Gauteng, as an inland province, is warm, with a temperate climate; however, dry compared to other provinces. Water sources are mainly from dams, rivers, catchments, and the Lesotho Highlands Water Project (indirectly) feeding into urban supply (Talanda et al., 2015; Muller et al., 2019; DWS, 2025; Maumela et al., 2025). Within this province, surface water storage often fluctuates widely depending on rainfall and temperature. The Vaal Dam is a core reservoir of the Integrated Vaal River System (IVRS), serving Gauteng's domestic, industrial, and agricultural water needs (Muller et al., 2019; Maumela et al., 2025). The province stretches northward from the Vaal River, bordered by the Free State. Additionally, numerous researchers apply water indices to local regions at a city scale. These indices include modified normalised difference water index (MNDWI) and the water ratio index (WRI), which are both used to detect waterbodies, moisture, presence and change in the environment. The region suffers the brunt of climate change with fluctuations in precipitation that lead to extreme evaporation in large shallow dams such as the Vaal (DWS, 2024; DWS, 2025) as well as flooding in unplanned or lowveld regions (Mawasha & Britz, 2022). Hence, when dam levels drop, that threatens water security for domestic, industrial, and agricultural use (DWS, 2024). Moreover, several studies in Gauteng have recorded the decrease of NDVI coupled with the increase of bare land and built-up areas, which reduces the cooling capacity, further exacerbating surface warming in the Jukskei catchment (Mawasha & Britz, 2022).

Further, the region observes detrimental urban patterns such as high-density urban structures and uncontrolled growth that precede sustainability interventions, including green infrastructure, parks, and wetland protection. These green and blue initiatives are often reactive

rather than proactive. Thus, it stands at the intersection of rapid urban growth, constrained natural water resources, and mounting climate pressures. Most research in the area makes use of Landsat and MODIS imagery; however, it is dominated by city-scale analysis as well as historical dates. Further, minor metropolises within Gauteng are underrepresented. Many studies focus on theme-based indices such as land surface temperature and land use land cover; NDVI and LST; or water/ moisture indices and LULC in pairings. Seldom are all variables researched over a region spanning 4 decades, including recent years.

*Table 1 1: Overview of Recent Literature on Urban Studies in Gauteng: Temporal, Spatial, and Variable Dimensions*

| Authors | Temporal Range | Variables | Spatial Scale |
|---|---|---|---|
| Mhangara, 2025 | 1993 to 2023 | NDVI, MSAVI2, PV, NDMI, LST, UHI and SMI | City Scale (Johannesburg) |
| Jombo *et al.* 2022 | 2001 to 2020 | NDVI, LST, UHI | City Scale (Johannesburg) |
| Masingi & Maposa, 2021 | 1900 to 2017 | Precipitation | Country Scale (South Africa) |
| Mawasha & Britz, 2022 | 1987 to 2015 | LULC | Catchment Scale (Jukskei) |
| Magidi & Ahmed, 2020 | 1997 and 2015 | LST | City Scale (Tshwane) |
| Mbokodo *et al.* 2020 | 1983 to 2099 | Heatwaves and Greenhouse gases | Country Scale (South Africa) |
| Mudede *et al.* 2020 | 2020 | LST, UHI, NDBI, NDVI | City Scale (Johannesburg) |

## 1.2 Problem Statement

Gauteng's water is serviced largely through Rand Water as the principal water board for the province's catchment and municipal supply systems, operating inside the country's designated Water Management Areas (WMAs) and under the custodianship of the Department of Water and Sanitation (DWS, 2016). Planned provincial and bulk-supply initiatives seek to increase treatment reliability and redistribute supply to high-demand municipalities in Gauteng (Rand

Water, 2024). At the national and provincial level, the government has publicly framed the challenge as one of renewing and expanding ageing infrastructure (DWS, 2024). These infrastructure and supply pressures are compounded by urban heat and land cover change in Gauteng's large metropolitan areas. Studies show pronounced urban heat island effects associated with high built-up areas and low vegetation and surface water, thus exacerbating evaporation, altering surface-water temperature dynamics, and increasing demand management in urban catchments (Mawasha & Britz, 2022; Souverijns et al., 2022). Comparable patterns have been documented across African cities where rapid urbanisation and climate change underline the need for integrated, climate-responsive catchment planning, green infrastructure (urban greening, permeable surfaces), and coordinated financing to bolster resilience in Gauteng and similar contexts (Nhamo et al., 2021; Li et al., 2022).

Furthermore, climate change and its implications on water resources in Gauteng. The province is landlocked and relies on dams from neighbouring provinces. Additionally, waterbodies in the province are scarce, and land planning enforces green and blue space degradation. Further, the challenges posed by urban heat and land use change are not unique to Gauteng but reflect global patterns in urbanising regions. Numerous studies across Africa and Europe demonstrate that increased urban development often results in a decline in green and blue spaces, accompanied by a measurable rise in land surface temperature (LST) and the urban heat island (UHI) effect (Uhrin & Onačillová, 2025). Moreover, research with relevant indices such as NDVI and MNDWI suggests negative correlations with LST. However, the availability of high-resolution, multi-temporal data and the integration of these indices with robust land cover classification methods vary substantially between regions. Additionally, Johannesburg, Tshwane and Ekurhuleni dominate in urban heat research, while other metropolises in the region lag in visibility. Thus, in comparison to the European areas, there is excess research and policy implementations in themes relating to multi-variable indices and variables denoting

urban heat and water stress. Similar to South Africa, African provinces, such as those in Ethiopia, Nigeria, and Kenya, echo similar concerns about the expansion of impervious surfaces, increase of urban heat and decrease in surface water. Additionally, like South Africa studies, which often focus on historical periods, shorter time periods, and are usually at city scales (Abimbola et al., 2025; Subhanil & Himanshu, 2025).

Moreover, there remains a critical research gap in synthesising green and blue space dynamics holistically in urban policy contexts. Few studies across the African continent have integrated UHI, LST, NDVI, and water-based indices like MNDWI and WRI into a comprehensive land use–climate–water framework. Gauteng presents an opportunity for such integrative research concerning urban thermal dynamics. Thus, this paper focuses on these gaps by researching the spatial and temporal analysis of land use land cover, green and blue space loss, as well as surface temperature increases in Gauteng, using consistent variables listed as LST, UHI, Heatwaves, NDVI, MNDWI and WRI. This would contribute not only to academic knowledge but also to actionable insights for climate adaptation, urban resilience, and environmental governance.

## 1.3 Research Aims and Objectives

### 1.3.1 Aim

This research aims to apply remote sensing to analyse the spatial and temporal distribution of land surface temperature, land use and water indices. Hence, to understand the interactions that urban heat islands and heatwaves have with vegetation, water indices, and land use in the Gauteng Province.

### 1.3.2 Objectives

- To analyse Heatwaves and UHI intensity over Gauteng from 1984 to 2024.
- To evaluate the effects of land cover types in triggering Heatwaves and UHI.

- To analyse the impacts of land cover dynamics, Heatwaves and Urban Heat Islands On Surface Water Resources.

## 1.4 Research Questions

- Is there evidence of a climate-induced trend in precipitation, reduced water availability, and rising maximum air temperatures in the region?
- How do urban expansion and impervious surface growth contribute to the intensification of UHIs in Gauteng?
- In what ways do heatwave events and urban warming relate to water resource indicators (WRI and MNDWI) in Gauteng?

## 1.5 The Structure of the Dissertation

Chapter 1 introduces the background of urban heat island intensity, heatwaves and land use's impact on water-related indices within the Gauteng province. The chapter is followed by the aims, objectives, research questions, and problem statement, which are detailed at the end of the chapter. Chapter 2 is the Literature Review. This chapter reinforces the need to incorporate remote sensing into surface water indices and urban heat island mapping within developing regions like South Africa. This section introduces literature that analyses the questions posed in Chapter 1. Chapter 3 describes the study area, data collection and pre-processing. Further, the Methodology through different software and formulas used is detailed in the paper. However, possible data implications can be expected due to internal temporal or spatial availability and access from Google Earth Engine. Furthermore, the Results and a Discussion are touched on in Chapter 4. Chapter 5 is the Conclusion. Lastly, Chapter 6, References.

# CHAPTER TWO: LITERATURE REVIEW

## Introduction

The acceleration of global warming has induced extreme climate trends such as heatwaves, urban heat islands (UHI) and decreased precipitation over long durations. This proves challenging for vulnerable regions over time. Urbanisation disrupts natural land cover and converts natural land into built-up and impervious surfaces. Thus, altering local climate and inducing climate variability through amplifying heat stress, lowering water availability, and affecting vegetation health. However, remote sensing provides powerful tools to monitor these changes and implement mitigation measures. The environmental indices in the paper focus on two water indices, the Water Ratio Index (WRI), Modified Normalised Difference Water Index (MNDWI), one vegetation index, Normalised Difference Vegetation Index (NDVI), land surface temperatures and urban heat island. These indices are calculated differently with various bands which derive either vegetation health, open water presence, and urban heat values. These indices are useful for detecting stress in vegetation and water due to heat.

South Africa offers a valuable case study because of its climatic heterogeneity, frequent droughts, and rapidly urbanising population centres. From emerging recent literature, several methodological insights seem particularly promising, such as multi-spectral index and high-resolution remote sensing data. This literature review aims to synthesise recent research globally and regionally on (i) climatic trends driving rising land surface temperatures in urban regions, (ii) the Urban Heat Island phenomenon with attention to land-use/land-cover changes (LULC), (iii) the use of water- and vegetation-based spectral indices (MNDWI, WRI, NDVI) to track how vegetation and water respond to heat stress and (iv) urban planning and research especially in Gauteng, South Africa to manage or mitigate these stresses through green and blue space initiatives focusing on water resilience, and vegetation restoration.

The literature review is structured as introducing global warming and climatic trends; the rise of urban heat from land surface temperature and maximum air temperature anomalies; the exacerbation of urban heat islands and UHI intensity relating to land use and land cover. Additionally, land cover changes over time on a global and local scale in favour of urbanisation are mentioned, followed by vegetation and water indices in tracking impacts of LULC and urban heat on NDVI, WRI and MNDWI. Lastly, initiatives about urban heat and the need for protective measures of green and blue space are discussed.

## 2.1 Global and Regional Climate Change Trends

Anomalies in climatic patterns are not new to Southern Africa (Rouault et al., 2024). Global challenges noticed at a national scale depict extensive climate variability due to sporadic climate trends (Xu et al., 2017; Ademe et al., 2020). Climate risk indicates the adverse consequences arising from climate change, which pose significant threats to socio-economic activities (Xu et al., 2017; Ngcamu, 2023). In response, researchers and policymakers are intensifying efforts to assess and mitigate these risks as extreme weather events contribute to heightened vulnerability in third-world countries (Xu et al., 2017; Ngcamu, 2023). Furthermore, climate change is making weather patterns more intense, increasing anomalies, and becoming less predictable. This exposes vulnerable communities to adverse climate trends (Ngcamu, 2023). Moreover, climate change represents one of the most pressing global challenges of the 21st century, with evidence indicating that global surface temperatures have been increasing at an unprecedented rate due to greenhouse gas emissions, primarily from anthropogenic activities (IPCC, 2023). Developing countries struggle with priorities of development and impacts of climate change (Xu et al., 2017; Simpson et al., 2024). In Africa, rising temperatures are particularly acute, with temperature increases above the global mean in many regions, especially southern Africa, which is recognised as a climate change hotspot

(Scholes & Engelbrecht, 2021). Moreover, South Africa has already experienced significant warming trends of approximately 0.02 °C per year over the past century, and projections suggest further intensification by mid- and late century (Scholes & Engelbrecht, 2021).

Global warming is due to the increase in greenhouse gas and pollution emissions within the atmosphere (Azizi & Azizi, 2024; Bhatti et al., 2023). This leads to excess heating and changes in weather patterns. Additionally, anthropogenic activities such as industries and the burning of fossil fuels are not sustainable for the environment. Moreover, recent climate science journals (Stringer et al., 2021) state that sub-Saharan Africa is heating faster than most global regions. Meanwhile, South Africa over the decades has experienced drastic weather conditions, and the South African weather service projects even more frequent climatic anomalies (Rouault et al., 2024). This exacerbates the vulnerabilities and risk within South Africa and Gauteng specifically. Additionally, this warming, coupled with population growth and industrial demand, has led to significant declines in water availability, public health and threatens sustainability (Souverijns, 2022; Rouault et al., 2024). Due to climate variability, there is an urgency for urban adaptation (Nhamo et al., 2021). Moreover, in spite of global warming and rapid urbanisation, urban heat islands and heatwaves are a prevalent subject. Over time, there have been noticeable temperature disparities between urban areas and rural, less developed regions (Rinner & Hussain, 2011; Senevirathne et al., 2021; Nevers et al., 2025). The land surfaces heat up rapidly during the day, and due to poor planning, heating is concentrated in areas saturated with concrete (Senevirathne et al., 2021), high traffic and minimal green space (Love et al., 2025). The 20th and 21st centuries are characterised by development replacing vegetation (Jabbar et al., 2023), which further exacerbates heating (Nhamo et al., 2021).

## 2.2 Urban Climate Studies in Gauteng and South Africa

Urban climate studies examine how urbanisation alters local climate. In Gauteng, the country's most densely populated and industrialised province, climate studies are important for water, health, and urban planning. Urban climatology refers to the systematic investigation of climatic processes in urban areas, including interactions of land cover and surface energy exchanges and how these diverge from non-urban or rural settings. Urban climate research encompasses phenomena such as Urban Heat Islands (UHI), surface temperatures and water cycles impacted by impervious surfaces, vegetation loss, and anthropogenic heat sources. Globally, there is strong intra-urban variation in heat exposure (Venter & Sydenham, 2021). This is observed in informal settlements and poorer neighbourhoods often have less green cover (Maconnachie & Shackleton, 2010; Jamalishahni *et al.,* 2023), more heat-absorbing surfaces, therefore, suffer more severe heat impacts than wealthier suburban counterparts (Astell-Burt *et al.,* 2014; Venter & Sydenham, 2021)

Some key characteristics observed in urban climate studies in Gauteng and South Africa include cities like Johannesburg and Ekurhuleni display elevated surface and air temperatures relative to surrounding rural or peri-urban areas. Low vegetation cover and high albedo differences contribute to UHI effects (Li *et al.,* 2022; Souverijns *et al.,* 2022). Additionally, Adeyemi (2015) noted that rapid urbanisation has converted natural or vegetated land into built or impermeable surfaces in metros like Tshwane. This increases heat storage, reduces evapotranspiration, and raises surface temperatures (Adeyemi, 2015). Moreover, heat stress and heat waves in South Africa have been increasing over decades due to climate variability (Ncongwane *et al.,* 2021). Urban climate studies are critical in Gauteng as the province has distinct dry and wet seasons, temperature and moisture fluxes. Thus, rainfall variability, soil moisture, and vegetation moisture status play roles in moderating UHI intensity and surface temperature dynamics (Li *et al.,* 2022; Yu *et al.,* 2025).

Urban climatic changes have diverse impacts, such as heat stress and increased morbidity, likely due to poorly insulated dwellings (Parker *et al.,* 2025). Additionally, increased temperatures lead to heightened energy demands, which in turn exacerbate load pressures, leading to loadshedding or blackouts (Liang et al, 2025). While direct South African studies on energy are fewer, general UHI literature for Africa points to these effects (Li *et al.,* 2022). Further, urban heat can amplify evaporation losses. For example, in the Mangaung metropolis, urbanisation led to vegetation loss, rising temperatures and a reduction in surface water quantity and quality (Senbore & Oke, 2021).

Developing cities such as those in South Africa need urban climate studies for several reasons, such as protecting vulnerable populations, be it species or humans, as well as the agenda of future generations, and sustainability. Additionally, failures to account for urban climate can lead to health crises, infrastructure damage and increased energy/water costs (Salimi & Al-Ghamdi, 2020; Das *et al.,* 2024). Gauteng, being semi-humid to semi-arid in parts, is highly urbanised and faces constraints on water supply and strong heat exposure. Introducing multi-index variables allows researchers and planners to examine how urban warming is not just an air or land issue but has direct implications for surface water.

## 2.3 Urban Temperature Dynamics

### 2.3.1 Urban Heat

Greenhouse gases such as carbon dioxide, methane, and nitrous oxide trap heat in the atmosphere, known as the greenhouse effect (Bhatti et al., 2023). This is due to the blanket nature of greenhouse gases (Bhatti et al., 2023). These gases are a major concern for developing regions (Ngcamu, 2023). Not only do these emissions pollute and degrade the air quality, but they also increase city temperatures (Azizi & Azizi, 2024). Thus, it increases the probability and formation of heatwaves and urban heat islands. Anthropogenic activities such as industries,

vehicles and burning of fossil fuels increase the concentration of greenhouse gases within the atmosphere (Bhatti et al., 2023; Azizi & Azizi, 2024). This can disrupt local weather and climate patterns. In Los Angeles, multi-decadal remote-sensing work links urban sprawl and vegetation loss to rising land surface temperature patterns and persistent heat islands, often using Landsat-derived LST and NDVI to map change (LaDochy et al., 2021). Similarly, Streutker in 2003 observed the association with expanding impervious surfaces and UHI growth over 12 years. Moreover, Toronto studies frequently combine NDVI, LST and land-use classifications to show higher LSTs over industrial and dense built environments and cooling where contiguous tree canopy exists (Rinner & Hussain, 2011; Nevers et al., 2025). Additionally, Kagabo et al. (2024) observe in Kigali, Rwanda and surrounding districts with the use of Sentinel-2 and Landsat imagery that built-up areas, agricultural land loss and declining vegetation indices (NDVI) correlate with rising land surface temperature trends (Mugiraneza et al., 2022; Kagabo et al., 2024). Kagabo et al. (2024) and Mugiraneza et al. (2022) emphasise that even modest increases in impermeable surfaces and reductions in local water bodies produce strong local thermal responses. Thus, dense urban areas have a higher rate of pollution and consumption than rural counterparts (Azizi & Azizi, 2024). This is solely due to the dense development and technological advancements that are solely focused on urban cities (Nhamo et al., 2021). This is noticed in Gauteng as there is an uneven distribution of urbanisation across the province. Moreover, urban regions, due to major vehicle dependence and concrete characteristics, have an increased greenhouse gas concentration and heating in the atmosphere (Bhatti et al., 2023; Azizi & Azizi, 2024). This reinforces the temperature difference between rural and urban areas. While urban areas demand more power than surrounding areas, it is noted by Li et al. (2019) that urban areas have an increased energy demand during heatwaves or within the urban heat island phenomenon. The effect of urban heat islands on energy resources is a known correlation in the literature (Magli et al., 2015).

Due to increased concentrated temperatures and a lack of cooling mechanisms in urban cities. This, in turn, puts a strain on power demands while increasing the cost for citizens (Magli et al., 2015). This issue is noticed across Gauteng, and research is being conducted quite fervently in districts such as Johannesburg and Ekurhuleni. During late 2022, the province experienced persistent heat temperatures (Fazel-Rastgar et al., 2025). Most South African heatwave studies focus on atmospheric dynamics and neglect the aspect of a systems approach. This approach will highlight the interconnectedness of environmental systems such as water, vegetation and development in contributing to climate variability. Further acknowledging the impact heatwaves have on water and the environment is essential for developing cities. Heatwaves fall under a climate anomaly defined as an extended period of unusually hot temperatures for at least 3 consecutive days (Chawanda et al., 2024). While UHIs are the effects of a metropolitan being warmer than surrounding rural areas (Hulley, 2012; Mughal et al., 2020; Munawar et al., 2025). In other words, urban heat islands occur when there is a loss of vegetation to urban characteristics and built-up regions, with materials like tar that store and re-emit heat increasing local land surface temperature (Munawar et al., 2025). Systematic reviews have emphasised the widespread occurrence of UHIs and that there is no universal standard for measuring UHI intensity or magnitude (Kim & Brown, 2021). Methods vary in data types, spatial scale, temporal resolution, and how LST or air temperature anomalies are defined (Kim & Brown, 2021; Chawanda et al., 2024). In Dallas, Texas, heat disparity is large, with green spaces being about – 11.11 °C cooler than residential areas (Streutker, 2003). Further, it suggests that vegetation cover is a strong influence on local temperature dynamics. Moreover, similar to Gauteng, in Chicago, green cover is uneven, causing intricate climatic sensitivity (Love et al., 2025).

Regional reports indicated that southern Africa experienced record high temperatures in early 2024, contributing to heat anomalies across the region (WMO, 2024). This was noticed in late 2022, South Africa experienced a heatwave coincident with an extreme drought (SPI < –2) (Fazel-Rastgar et al., 2025). Moreover, heatwaves are ambiguous and are amplified by urban heat islands and precipitation anomalies (Perkins & Alexander, 2013; Quante et al., 2022). For example, detailed analyses of station-level data from 1981–2020 reveal an increase in the number of hot days exceeding defined thresholds, along with extended multi-day heatwave periods (Mbokodo et al., 2023). This aligns with findings from national-scale studies, which confirm that maximum air temperature trends are particularly pronounced in interior provinces such as Gauteng (Fazel-Rastgar & Sivakumar, 2024).

In rapidly urbanising regions such as Gauteng, the conversion of natural land into built environments exacerbates land surface temperatures, thus inducing heatwaves and an urban heat island (Quante et al., 2022; Munawar et al., 2025). Therefore, deciphering heatwaves and their impact on water resources is essential for urban planning and water management. Moreover, prolonged exposure to extreme temperatures induces thermal pollution and a dependency on energy for cooling (Azizi & Azizi, 2024; Souverijns, 2022). Therefore, the unsustainable expansion of cities contributes to the spatial extent and intensity of urban heat islands and heatwaves, degrading the environment and public health (Nhamo et al., 2021).

### 2.3.2 Land Surface Temperature (LST) and Urban Thermal Patterns

Land Surface Temperature primary indicator of the urban thermal environment. Understanding land surface temperature and its spatial patterns is critical for urbanising cities. Land surface temperature is the radiative skin temperature of the Earth's surface to touch. It can be measured by radiometers on aircraft or satellites or derived from thermal infrared radiation bands within satellite imagery after correction for emissivity and atmosphere (Petitcolin & Vermote, 2002;

Diaz et al., 2021). Land surface temperature is heterogeneous and varies at fine spatial scales according to material, land cover, and urban morphology (Wu, Yao & Ren, 2020). Furthermore, materials such as tar and concrete cool differently from vegetation and water, producing significant day-to-night contrasts (Wu, Yao & Ren, 2020; Diaz et al., 2021). Thus, vegetation cover, soil moisture, water and surface albedo modulate Land surface temperatures (Wu, Yao & Ren, 2020). Hence, land surface temperature is a direct metric of urban thermal patterns (Wu, Yao & Ren, 2020; Diaz et al., 2021). Further, elevated LST has a dire effect on environmental and social systems. The increase of heat stress in vegetation and a rise in energy demand for cooling using fossil fuels can alter the local climate and increase air pollution. In other words, at the city scale, increased LST amplifies the intensity and spatial extent of heatwaves and can change local circulation, which in turn affects air quality and precipitation patterns (Peng et al., 2016).

There is an increase in research of satellite-based studies documenting the rising LST and pronounced intra-urban thermal heterogeneity across African cities in recent years (Li, Stringer & Dallimer, 2022; Parker et al., 2024). For instance, analyses in Addis Ababa report several degrees Celsius increase in mean surface temperature associated with built-up expansion, while Nairobi studies have used local sensors and Landsat LST to show that informal settlements can be thermal hotspots relative to greener districts (Negesse, Hishe & Getahun, 2024). Gauteng Province has attracted focused LST and UHI research because it is one of South Africa's economic hubs and is experiencing rapid urban growth. High-resolution studies show substantial present and projected heat stress across Gauteng, with spatial patterns that align with built-up density, bare land and industrial land uses. Further, recent analysis combining Landsat LST, urban indices and socio-demographic layers has begun to quantify intra-urban

heat vulnerability in Johannesburg, identifying wards where environmental exposure and social vulnerability overlap (Souverijns *et al*., 2022).

### 2.3.3 Overview of Urban Heat Island (UHI) Effect

Urban Heat Island (UHI) describes the phenomenon of urbanised areas recording warmer temperatures than surrounding rural areas due to land use change and human activity. The effect arises from heat-absorbing materials like tar and concrete, coupled with reduced surface water and vegetation loss. Urban heat islands can either be surface urban heat islands (SUHI), the higher land-surface temperatures detectable by thermal remote sensing or air-temperature urban heat islands, the elevated temperatures experienced by people at street level. Moreover, surface urban heat islands concentrate where built density, impervious cover and lack of vegetation coincide, therefore in city centres and industrial zones. Urban heat islands intensify at night due to urban materials slowly releasing stored solar radiation. Further, topography, wind patterns and proximity to water bodies modulate urban heat island intensity and footprint. Thus, remote sensing studies routinely show UHI magnitudes from <1°C to >8°C depending on the study area, season and methodology used (Li, Stringer & Dallimer, 2021).

Urban heat islands amplify heat exposure and energy demand in regions. Higher urban temperatures raise electricity demand for cooling, burdening grids and increasing emissions where electricity is fossil-fuel-based. This can also change local meteorology through pollution (coal energy) and altered circulation (urban form blocking), thus creating urban extremes. These impacts are already identified as critical threats to urban liveability in global development assessments (Roberts *et al.,* 2023). Developing regions face an acute UHI vulnerability and risk for several reasons. Firstly, rapid urbanisation and urban sprawl expand bare land and impervious surfaces while densifying built-up areas, which limits urban cooling

due to a lack of green and blue space. Secondly, municipal budgets and competing development priorities limit investments in urban greening.

Research on UHIs in Africa has grown rapidly in the last decade, driven by satellite remote sensing advances and a rising awareness of heat vulnerability. Case studies from Kampala, Accra, Lagos, Nairobi and other cities document substantial SUHI expansion coinciding with urban growth (Gyimah, 2023). Further, Gauteng province is one of the economic heartlands of the country. It has been the subject of several detailed UHI investigations using both remote sensing and station networks (Monama, 2016; Souverijns *et al.,* 2020). High-resolution assessments show that Johannesburg, Ekurhuleni and Tshwane display clear SUHI patterns linked to built-up areas and low vegetation indices (Monama, 2016; Souverijns *et al.,* 2020). These studies project that future warming and urban expansion will increase heat stress across the province (Monama, 2016), especially in low-income suburbs and peri-urban settlements where adaptive capacity is limited (Souverijns *et al.,* 2020). Thus, these findings align with broader African evidence and stress the need for targeted greening and measures to protect surface water.

### 2.3.4 Heatwaves and their Environmental Impacts

Heatwaves are increasingly recognised as one of the most consequential climate extremes for human societies and ecosystems (WMO, 2023). A heatwave is a period of extremely hot weather lasting from days to weeks and including warm night-times (WMO, 2023). However, the exact threshold varies from location and is framed in relative terms such as anomaly over a percentile (WMO, 2023). These conditions arise under persistent high-pressure systems that reduce cloudiness and ventilation, allowing solar heating and adiabatic warming to raise surface and air temperatures (Barriopedro *et al.,* 2023*;* WMO, 2023). Moreover, climate change globally has increased the frequency, duration and intensity of observed heatwaves

since the mid-20th century (Yin *et al.*, 2022; WMO, 2023). Additionally, the South African Weather Service documents an increasing frequency of early and intense heat events in recent years (SAWS, 2023). Further, urban regions, due to impervious surfaces, concrete and high density, exacerbate heatwaves via the urban heat island (UHI) effect. Heatwaves produce cascading impacts across health, infrastructure, economy and ecosystems. For example, extreme continual heat stresses water supplies and agriculture through evapotranspiration and crop failure. Hence, cities in Africa are more vulnerable to increased food insecurity and limited public health due to heatwaves (Kunda, Gosling & Foody, 2024). Research into heat and urban heat islands in African settings has expanded but remains unevenly distributed compared to Western regions. Recent systematic reviews and case studies emphasise that African cities experience strong heat–pollution synergies that require localised diagnostics. Thus, Gauteng research should prioritise open access datasets, multi-city-scale modelling and evaluations to scale the best practice.

## 2.4 Natural Environmental and Urban Pressures

### 2.4.1 Vegetation and Urban Pressures

Land use and land cover (LULC) change has emerged as a critical driver of urban climate dynamics, especially in regions experiencing rapid urbanisation (Rao et al., 2023). Over the past four decades, urban expansion in Gauteng has significantly altered natural landscapes, replacing vegetation with impervious surfaces and thereby amplifying land surface temperature (Nhamo et al., 2021). The reduction of green spaces through rapid urban expansion diminishes evapotranspiration, thus reducing the cooling effect (Kikon et al., 2023; Roba & Tabor, 2025). In recent decades, land use and land cover change have become a critical element in urban climate dynamics. Urban expansion globally has altered the environment, replacing vegetation and water bodies with impervious surfaces that amplify land surface temperature (Kikon et al.,

2023; Rao et al., 2023; Munawar et al., 2025) and disrupt ecosystems. Thus, this increases vulnerability and risk as increasing trends in unplanned settlements prohibit proper planning for green infrastructure (Parker et al., 2025). Additionally, global comparative studies provide further evidence that land use land cover (LULC) changes amplify UHI effects (Elbertse, 2021; Kabanda & Kabanda, 2019; Munawar et al., 2025). In western regions, Chicago is often criticised for lacking dramatic natural topography compared with cities like San Francisco or Denver. By contrast, Dallas, Texas, is improving in terms of parks and green space, but lags behind Chicago in several respects. Dallas has a humid subtropical climate that brings very hot summers, which can exacerbate heatwaves and UHIs. Moreover, a 40-year remote sensing study in Chicago found that green space quantity varies across neighbourhoods (Azizi & Azizi, 2024). Further, Azizi & Azizi (2024) observe a negative correlation between NDVI and land surface temperature (LST), meaning more vegetation helps cool its surface environment (D'Ercole et al., 2024). Many papers supplement surface UHI with air-temperature observations or modelled urban canopy fluxes to better represent human exposure (Cheval et al., 2024; Yang et al.,2024).

Further, remote sensing tools, particularly vegetation indices such as the normalised difference vegetation index (NDVI), have proven essential for quantifying these changes in natural surface degradation. NDVI is a metric used to quantify vegetation health and density through the near infrared and red spatial bands (Rahimi et al., 2025). In other words, this index serves as a proxy for vegetation greenness and biomass. The values range from −1 to +1, with higher values (positives) indicating denser vegetation. Hence, higher temperatures and decreased moisture due to heat stress result in lower chlorophyll content, thus reducing NDVI values (Kikon et al., 2023; Kliengchuay et al., 2025). The higher the NDVI value, the assumption of positive water content and reduced heat stress (Kikon et al., 2023; Kliengchuay et al., 2025). Additionally, many studies show a strong negative correlation between land surface

temperature (LST) and NDVI across spatial scales (Hulley, 2012; Kikon et al., 2023). Numerous studies confirm that areas with higher NDVI values typically exhibit lower LST, demonstrating the cooling role of vegetation in urban and peri-urban areas (Singh et al., 2023; Love et al., 2025). Furthermore, due to recent urban sprawl, there has been a reduction in vegetation area, and its cooling effects have diminished (Love et al., 2025). Moreover, as developed as Gauteng is, there are still numerous outdated buildings, corridors and structures, which correlates to a lack of sustainable modern green buildings and planning. This emphasises the need for cooling systems like blue and green infrastructure for the reduction of greenhouse gases. Moreover, affluent neighbourhoods with abundant green space remain cooler (Piketh et al., 2025), whereas city centres and informal settlements exhibit higher surface and air temperatures (Raj et al., 2020; Dinda & Chatterjee, 2022). Gauteng has prioritised industrial and residential development over green infrastructure, reducing the ecological resilience of urban landscapes, thus reaping challenges from the pressures of urban form and function (Nhamo et al., 2025; Parker et al., 2025).

### 2.4.2 Urbanisation and Surface Water Depletion

Urbanisation is a spatial process by which people concentrate in towns and cities centres and in turn, built environments expand to accommodate growing urban populations and activities. If unmanaged urbanisation is coined urban sprawl, and propagates inequalities, environmental injustice and stress (UN-Habitat, 2021). Urbanisation has several defining characteristics, such as spatial expansion and central density, functional specialisation from industries, transit networks, and natural land conversion to built-up areas (Angel, 2023). As planned growth occurs with urban sprawl, these characteristics are usually uneven (Angel, 2023). Furthermore, urbanisation reshapes ecological cycles through fragmentation of habitats, degradation of vegetative cover, loss of surface water bodies and alters hydrology by increased runoff from

impervious surfaces (Abdullah et al., 2022). Many developing regions fail to safeguard blue and green space in the midst of urbanisation (Abdullah et al., 2022; Bille et al., 2023). Thus, sustainability becomes an afterthought once the development of buildings is set (Abdullah et al., 2022). Governments prioritise short-term housing and economic needs over ecological conservation and riparian buffers (Graziano et al., 2022; Majumdar & Avishek, 2025). Additionally, institutional and fiscal constraints limit municipal capacity to plan and maintain public open spaces (Palliwoda et al., 2022). Thus, the unequal distribution of green space is carried over to current and future times (Venter & Sydenham, 2021; Bille et al., 2023; Ngan et al., 2025). The interactions between heatwaves, urbanisation, land surface temperature (LST), and vegetation dynamics have direct implications for water resources in Gauteng. The implication of climate variability on surface water availability is a complex dilemma that impacts regions differently. Therefore, observing climate variability in urban cities and its effect is essential to water management and availability in Gauteng (Zubaidi et al., 2020; Rasebechele et al., 2025). In South Africa, most rural and urban areas are prone to water scarcity due to precipitation decreasing and urbanisation pressures, respectively (Zubaidi et al., 2020; Stringer et al., 2021). Gauteng is one of South Africa's most densely populated provinces, experiencing heatwaves and water shortages. Further, rising temperatures and altered precipitation patterns intensify evaporation rates, reduce surface water availability, and place additional stress on the province's already limited water supply (Stringer et al., 2021; Gidey & Mhangara, 2023). Remote sensing indices such as the Modified Normalised Difference Water Index (MNDWI) and Water Ratio Index (WRI) have been widely applied to quantify changes in surface water extent, further providing insight into water stress and climate change (Gidey & Mhangara, 2023; Günen & Atasever, 2024; Kareem et al., 2023). Similarly, Belhaj et al. (2022) observe long-term surface water in New Mexico and determine that climate change, coupled with rapid population growth in the metropolitan areas of El Paso, Ciudad

Juárez, and Las Cruces, has intensified water demand and altered land-use practices. Additionally, at a long-term analysis, city-scale MNWI values observe a consistent decline for urbanised regions, indicating reduced surface water bodies over the past several decades (Belhaj et al., 2022; Haight et al., 2024). This reduction is closely associated with both increasing LST and declining vegetation cover, suggesting that urban expansion exacerbates water scarcity by limiting infiltration, increasing runoff, and raising thermal stress (Kikon et al., 2023; Haight et al., 2024). Further, the province is landlocked and relies on inter-basins, dams and the Lesotho Highlands project, with no internal large source of water. Moreover, climate variability affects weather patterns by increasing the frequency of weather anomalies, which disrupt the hydrological cycle while increasing the sporadic trends of rainfall (McBride et al., 2022; Mengistu et al., 2023). Bonetti et al. (2022) state that South African climate models project decreasing rainfall as heatwaves amplify these effects by increasing evapotranspiration rates, which in turn lower the volume of surface water in dams, rivers, and reservoirs (McBride et al., 2022). Studies in Gauteng indicate that prolonged hot periods coincide with reduced water indices, posing risks to both municipal water supply and agricultural irrigation (Stringer et al., 2021). Furthermore, the reduced water availability affects energy production, sanitation, and urban green space, creating cascading impacts on urban sustainability. Nonetheless, urbanisation compounds these pressures (Nhamo et al., 2021). Still, impervious surfaces prevent infiltration, accelerate runoff, and reduce natural storage of rainwater, directly affecting MNDWI and WRI measurements (Haight et al., 2024).

In provinces such as Gauteng, infrastructure and land-use policy are being revised to integrate resilience, green-economy objectives, and ecosystem protection, but often after significant land conversion has already reduced natural assets (Nhamo et al., 2021; Parker et al., 2025). Specific research on Gauteng points to the expansion of impermeable surfaces modifying catchment hydrology, thus contributing to surface-water stress (Mawasha & Britz, 2022). Hence, meta-

analysis, according to Sarfo *et al.* (2024), of land-use systems in Africa corroborates that urban growth is among the dominant drivers of vegetation degradation and water-cycle disruption. Furthermore, remote sensing and hydrological studies increasingly document the environmental footprint of urbanisation across Africa. Continental-scale modelling finds that land-use land-cover change with climate variability alters evapotranspiration, reducing surface water availability and increasing runoff (Chawanda *et al.,* 2024). Additionally, degraded vegetation and shrinking wetlands are linked to settlement expansion and urban agricultural encroachment (Chaemiso *et al.,* 2021; Chawanda *et al.,* 2024). Therefore, moving from reactive sustainability after development to integrated sustainable planning during urban growth is the critical shift that can deliver resilient, just and liveable cities in Gauteng for the coming decades.

## 2.5 Interconnections Between Urban Heat, Land Use Change, Vegetation, and Water

By combining LST and NDVI with water indices, the research allows for a better understanding of UHIs on urban vegetation and surface water. Thus, linking insights for urban planning, public health, and climate resilience. Water resource availability is a prominent issue in Gauteng (Maumela et al., 2025). The high temperatures dry the soils, and increased evapotranspiration reduces the natural cooling effect from the green and blue space (Mengistu et al., 2023; Love et al., 2025). Hence, drought often accompanies heatwaves, making poorly planned regions more vulnerable and at risk (Stringer et al., 2021; Mengistu et al., 2023). Areas with low NDVI values tend to experience higher LST (D'Ercole et al., 2024), with low MNDWI, highlighting the interconnectedness of urban heat, vegetation loss, and water. Moreover, the combined effect of increased temperatures and decreased precipitation leads to a decrease in soil moisture, which reduces groundwater recharge and exacerbates water stress

during dry seasons (Masingi & Maposa, 2021; Haight et al., 2024). Research demonstrates that enhancing urban greenery can mitigate both thermal and water stress (Love et al., 2025). Further, increased vegetation cover has positive compounded effects. It improves soil moisture retention, reduces runoff, and lowers surface temperatures, which collectively help maintain water availability (Singh et al., 2023). Furthermore, the change in land use from natural vegetative areas to impervious surfaces leads to reduced water retention in urban centres, hence, limited cooling in city centres (Ncongwane et al., 2021; Singh et al., 2023; Haight et al., 2024).

Therefore, sustainable water planning requires an integrated systems approach analysing climate and urban factors. Further, the province is a relatively small area and the smallest province in terms of size in South Africa (Chakwizira et al., 2018). However, it is a booming economic hub plagued by unplanned urban sprawl (Chakwizira et al., 2018; Nhamo et al., 2021). The rapid growth of urban structures that replace vegetation and water leads to the elevation of local temperatures (Nhamo et al., 2021; Senevirathne et al., 2021; Love et al., 2025). The city centres are characterised by concrete, vehicle dependency and major industries. This region's urban expansion has outpaced cooling infrastructures and green space. Studies have shown that vegetation, unlike urban structures, can cool by evapotranspiration (Mughal et al., 2020; Love et al., 2025), whereas dense buildings and concrete absorb and radiate heat, thus creating strong UHI effects (Senevirathne et al., 2021). The urban form of a city influences pollution intensity as well as local temperature fluctuations (Azizi & Azizi, 2024). Gauteng is a heterogeneous region with areas characterised as forest-dense, such as the city of Johannesburg, and areas that are overdeveloped, lacking green spaces, such as informal settlements and business districts. The neglect of certain districts within Gauteng in UHI research means adaptation and vulnerability contexts lack detailed analysis and understanding.

## 2.6 Integrating Remote Sensing and Empirical Research in Urban Environmental Studies

### 2.6.1 Remote Sensing in Urban Cities

The use of advanced geospatial and computational techniques is popular in modern studies relating to climate trends and variability (Günen & Atasever, 2024). Remote sensing and Google Earth Engine (GEE) have simplified climate monitoring in African provinces. The free and open-source access to multiple datasets allows for on-demand processing and trend analysis in data-scarce regions. Additionally, random forest (machine learning) algorithms can learn complex trends in land cover and climate variables. For example, Erol (2023) combines high-resolution land surface temperature retrievals with socio-demographic heat-vulnerability mapping to tie LST and urban heat island hotspots to health risk during extreme heat events. Furthermore, the use of remote sensing in climate trends will fast-track initiatives and programme-specific ideals for Sedibeng and West Rand while also improving the gaps in implementation and understanding within the other districts. Remote sensing proves valuable in analysis and data collection due to its being significantly cheaper and quicker than ground truthing. This will allow the province to have updated continuous data on land surface temperatures, vegetation and precipitation to gauge trends and prepare vulnerable communities for climate anomalies like Love et al. (2025). Therefore, the wide use of remote sensing can mitigate the research disparities between districts in Gauteng. This method is not a rigid application that is specifically developed for resource-favoured cities. Other methods, such as applying machine learning, have grown in popularity for predictions and complex analysis. Western studies have successfully applied ML and climate models to predict UHI intensity from variables such as building density, albedo, NDVI, population, and local climate factors (Rinner & Hussain, 2011; Kagabo et al., 2024; Mutani et al., 2024; Li et al., 2025). Using

remote sensing and machine learning allows for real-time statistical analysis and monitoring. For example, in Nigeria, Kaduna, studies observed aggressive urbanisation in conjunction with shrinking water bodies from 1987 to 2020 using numerous machine learning models (Durowoji et al., 2025), suggesting unsustainable urban planning may worsen heat exposure and deplete water sources.

Moreover, Gauteng has seen uneven spatial development, highlighting certain districts as more vulnerable to heatwaves and other climate anomalies. This proves problematic as resources are not evenly distributed, increasing the risk in poorer districts. There are disproportional analyses and research done across the province, with certain areas more capable of researching and applying countermeasures to environmental trends. Furthermore, districts such as the City of Johannesburg, Ekurhuleni and Tshwane have developed vast research and initiated programmes to curb climate change and reduce climate-related risks. However, Sedibeng and West Rand still feel the brunt of climate change, with less research on urban heat islands and climate anomalies, which perpetuates their vulnerability. Additionally, numerous challenges arise from spatial data, especially in research concerning developing countries (Zhao et al., 2013; Du et al., 2015). Ramakreshnan et al. (2018) review UHI trends in Malaysia, emphasising methodological shortcomings such as inconsistent site classifications and outdated data. This is often the case in developing regions. Case studies using remote sensing have focused on major cities such as Johannesburg and Pretoria, leaving smaller counterparts and informal settlements understudied and further at risk. Nonetheless, there is a need for a combination of high-resolution and ground-validated urban heat island measurements (Hu & Uejio, 2024) in regions such as Gauteng. This will promote local collaboration while identifying the most at-risk regions in the province and the relevant initiatives applicable.

### 2.6.2 Remote Sensing in Water and Heat Analysis

Remote Sensing is the acquisition of information about Earth's surface from sensors on satellites. It provides spatially comprehensive measurements of land dynamics such as surface temperature, vegetation and water at scales that in-situ networks cannot match (Yu & Fang, 2023). Modern platforms such as Google Earth Engine (GEE) combine vast archived imagery (like Landsat or MODIS) with cloud computing to enable researchers and planners to compute various environmental indices, then to map change or run time-series analysis rapidly and reproducibly (Yu & Fang, 2023). Land Surface Temperature represents the radiative skin temperature of the land and is widely used to quantify urban heat islands and surface energy balance changes (Li *et al.,* 2023). LST can be derived from thermal infrared bands after atmospheric correction and emissivity estimation (Li *et al.,* 2023). Further, LST, according to research, correlates strongly with impervious surfaces and vegetation loss in cities (Naserika *et al.,* 2023; Kara & Yavuz, 2025; Roba & Tabor, 2025). Moreover, Normalised Difference Vegetation Index (NDVI) is a vegetation health index calculated from NIR and red bands to indicate plant biomass and greenness (Martinez & Labib, 2023). This is used to identify green space or vegetation within an area (Martinez & Labib, 2023). Water indices such as the Normalised Difference Water Index (NDWI), Modified Normalised Difference Water Index (MNDWI), and Water Ratio Index (WRI). The distinction between the indices is that NDWI (McFeeters, 1996) uses green and NIR bands to enhance open water, while the modified NDWI (MNDWI; Xu, 2006) replaces NIR with SWIR to better separate built and turbid water in urban scenes. Additional metrics like the Water Ratio Index help map water extent in complex urban and peri-urban environments. These indices are essential to resource planning as accurate water detection is essential for flood risk, drainage planning and blue-green infrastructure design. Developing cities face rapid urban sprawl; thus, remote-sensed datasets provide objective,

repeatable measures to diagnose environmental stressors over time (Yu & Fang, 2023). However, many areas in Africa face the issue of data quality due to loud contamination, sensor noise, and seasonal bias (Yu & Fang, 2023).

Across Africa, researchers have used Landsat, MODIS and Sentinel imagery, often implemented in GEE. In South Africa, several studies examine urban thermal patterns and surface cover in major metros like Cape Town, eThekwini, Johannesburg, and Tshwane (Monama, 2016; Ngie *et al.,* 2016; Rogalski & Ilunga, 2025). For example, multi-sensor LST analyses in the City of Tshwane document rising surface temperatures associated with impervious expansion (Magidi & Ahmed, 2020). These studies illustrate both the power of satellite indices and the practical challenges, particularly the need for local validation and temporally consistent processing (Magidi & Ahmed, 2020). Hence, GEE's archive and computing power make localised multi-decadal change analysis feasible even for institutions without heavy local computing resources.

Thus, remote sensing, when combined with cloud platforms like Google Earth Engine, allows developing regions affordable, and scalable instruments for environmental monitoring, heat-risk management, water security initiatives and urban planning. For provinces such as Gauteng, the path forward is pragmatic in developing a localised scheme to aid climate vulnerability and implement sustainable infrastructural interventions. By doing so, Gauteng planners and researchers can turn satellite insight into equitable, climate-resilient urban action.

## 2.7 Land Use and Land Cover Classification and Machine Learning Approaches

Land Use Land Cover (LULC) is a foundational concept in geography, urban planning and remote sensing. Land cover refers to the physical material on the surface of the earth, like

grassland, water bodies, built surfaces and bare soil (Nedd *et al.,* 2021). While land use refers to anthropogenic uses of the land, such as agriculture, residential, commercial or infrastructure (Lesslie *et al.,* 2006; Nedd *et al.,* 2021). Therefore, the land cover land use defines the status of an area in both environmental and socio-economic terms. LULC is not uniform and varies sharply over space, especially near urban–rural interfaces. Changes in LULC have a wide array of consequences. In developing cities, especially, rapid and often unregulated change leads to environmental degradation such as soil erosion, reduced water infiltration and loss of green space. Further, as natural land cover and vegetation are replaced by built-up areas, regions tend to warm, hence, in many studies, built-up expansion correlates with rising land surface temperature (Chen *et al.,* 2022; Debnath *et al.,* 2025; Vahid & Aly, 2025). Conversion to built-up areas reduces the natural cooling effect of the environment and natural water regulation (Jandaghian & Colombo, 2024; Soltanifard & Amani-Ben, 2025). Sustainable planning that preserves green spaces and manages water bodies is essential to help steer growth and minimise environmental degradation (Nhamo *et al.,* 2021; Fadda, 2024). Moreover, machine learning, and especially Random Forest (RF), combined with remote sensing and cloud platforms like Google Earth Engine (GEE), has become a powerful tool for LULC mapping and change detection. Random Forest is a supervised classification model that builds an ensemble of decision trees using random subsets of features and training samples (Belgiu & Drăguț, 2016). It tends to be robust to overfitting and works well with many input variables like spectral bands. Google Earth Engine enables large-scale access to satellite imagery in addition to the ease of implementing classification workflows. This method is widely used in research, for example, in the Upper Tekeze River Basin, Ethiopia, Fentaw & Abegaz (2024), mapped LULC changes over thirty-one years and found high overall accuracy (~ 0.83) and Kappa (~ 0.75) results. This analysis showed forest, bushland, shrubland, and bare land decreased while farmland, settlement and dry river feature increased. Additionally, Matarira *et al.* (2022) added spectral

and textural data to the model to improve discriminability in Durban (Matarira *et al.,* 2022). Furthermore, in one Bangladesh study, RF and Artificial Neural Network achieved overall accuracies above 0.91, with RF among the top performers (Chowdhury, 2024). In many African contexts, field data or reference data are scarce or expensive; sample areas may not well represent all classes, or there is class imbalance (more on one class than the other), which becomes a problem (Meyer *et al.,* 2019; Zhao *et al.,* 2023). For places such as Gauteng, which is under pressure from rapid urbanisation and climate change, high-quality LULC research can inform zoning, infrastructure investment, and green space preservation. Therefore, combining sustainable urban planning with advanced machine learning based LULC mapping is both urgent and promising.

# Conclusion

In conclusion, urban regions are facing major challenges due to climate change globally. However, developing regions are on the brunt of heat stress and water scarcity. Climate change represents the daunting pressures of the 21st century. Research evidence indicates that the land surface temperatures are increasing at significant rates due to greenhouse gas emissions and LULC change, which is primarily derived from anthropogenic activities (McBride *et al.,* 2022; Fuentes et al., 2024). In South Africa, research shows recent warming trends of approximately 0.02°C per century over the past century, with projections of further intensification later on in the century (Ncongwane et al., 2021). Hence, the province's growing vulnerability to extreme temperatures underscores the urgent need for adaptation strategies that integrate remote sensing data and urban planning specific to the region. This province consists of major urbanised cities that have seen noticeable shifts in both maximum average air temperature and land surface temperature (Rastgar & Sivakumar, 2024). Between 1984 and 2020, Gauteng's maximum air temperatures showed a rising trend, closely linked to an increase in the frequency and duration

of heatwaves (Mbokodo et al., 2023). Additionally, further research shows station-level analysis from the years 1981 to 2020 depicting an increase in the number of heat waves or hot days exceeding defined thresholds (Mbokodo et al., 2023). The states with the national scale findings of increased maximum temperatures, especially in interior provinces like Gauteng (Rastgar & Sivakumar, 2024). A city-scale remote sensing study showed that land surface temperatures in built-up areas are consistently higher than those in surrounding rural zones, often by several degrees Celsius (Parker et al., 2025). Additionally, for South Africa, research on water and vegetation being impacted by urban heat is limited, and available research usually has a focus on historical timescales. Further, research indicates that intra-urban heat exposure is unevenly distributed, with wealthier neighbourhoods often benefiting from tree cover while vulnerable populations are usually situated in areas with less vegetation (Umeh & Gil-Alana, 2024; Parker et al., 2025). Various techniques are applied in research to monitor temperature and urban heat island intensity at a city scale (Bhamjee et al., 2024). Gauteng has prioritised industrial and residential development over green infrastructure, reducing the ecological resilience of urban landscapes, thus reaping pressures from urban form and function (Nhamo *et al.,* 2021; Parker *et al*., 2025). Additionally, the spatial distribution of UHI in Gauteng also reflects legacies of apartheid-era planning, where segregated neighbourhoods were constructed with limited green space (Parker et al., 2025). These historical inequities continue to shape contemporary vulnerability patterns in the region, making UHI an environmental justice concern. Ultimately, UHI intensity in Gauteng represents the intersection of global warming and localised urban pressures. While climate change raises baseline temperatures, urban planning and land cover changes determine how these global shifts manifest at the local level (Bhamjee *et al*., 2024; Parker *et al*., 2025). International comparative studies provide further evidence that land use land cover (LULC) changes amplify UHI effects (Kabanda & Kabanda, 2019; Elbertse, 2021). Therefore, the functional relationship between NDVI and LST has

important implications for urban planning, as higher vegetation density reduces heat re-emission and induces urban cooling, which helps lower surface and near-surface air temperatures (Kikon et al., 2023). The interactions between heatwaves, urbanisation, land surface temperature (LST), and vegetation dynamics have direct implications for water resources in Gauteng. Additionally, increasing temperatures intensify evaporation rates and reduce surface water availability, which puts additional stress on the area with a limited water supply (Sintayehu & Mhangara, 2023). Ultimately, Gauteng relies on extensive dam infrastructure and inter-basin transfers; therefore, any reduction in surface water availability from heat-driven losses threatens urban water security (Zubaidi et al., 2020; Stringer *et al.,* 2021). The long-term analysis of MNDWI values in urbanised regions demonstrates a decreasing trend (Tuan et al., 2019; Sintayehu & Mhangara, 2023). Thus, the integration of multi-variable remote sensing indices is crucial for quantifying trends in land use and LST. Furthermore, the uneven research coverage mirrors spatial inequality and vulnerability (Rasebechele et al., 2025) within the region. This gap hampers effective water management and climate resilience planning across the province, necessitating advanced analytical tools and predictive models. Hence, limited high-resolution data and research on UHII (urban heat island intensity) are attributed to the whole province (Souverijins et al., 2022; Rasebechele et al., 2025; Afuye et al., 2024). The rise in research on urban heat islands has initiated work in South Africa; however, it is still an underdeveloped topic within certain metropolises. This makes the province a relevant site for studying urban heat islands and water availability through rainfall patterns and water-related indices. Gauteng has five metropolitan districts, all dealing with urban heat stress and water scarcity; however, some metros lag behind in research and visibility. This leads to a spatial disparity in mitigation and resource distribution.

This study therefore pursues three objectives: (i) to analyse heatwaves and UHI intensity in Gauteng between 1984 and 2024; (ii) to evaluate the effects of land cover types in triggering

heatwaves and UHI; and (iii) to investigate the impacts of land cover dynamics, heatwaves, and UHIs on surface water resources. The use of remote sensing multi-variable indices will provide essential data for monitoring these trends over time. Thus, allowing for this paper to track both LST, vegetation and water indices over a decadal period, capturing the impacts urban heat has on vegetation and water resources as well as land use in propagating urban heat intensity. The research is guided by the following questions: Is there evidence of climate-induced LST increase and reduced water availability? How do urban expansion and impervious surface growth contribute to the intensification of UHIs? In what ways do heatwave events and urban warming relate to water resource indicators such as precipitation deficits and water indices in Gauteng?

# CHAPTER THREE: DATA AND METHODOLOGY

## 3.1 Study Area

Gauteng contributes a major share of the national gross domestic product (GDP) and employment, thus higher migration and urban sprawl. This leads to higher consumption, industrial emissions, pollution and waste (Jacobs et al., 2023). Hence, contributing to higher air temperatures, wastewater and pollution (Piketh et al., 2025). Gauteng is mostly urbanised and economically diverse. It harbours finance, trade, mining, urban agriculture and major manufacturing industries. This contributes to concentrated populations and socio-economic activities. Gauteng experiences rising heatwave frequency, compounding socio-economic inequalities and intensifying water demand. This increases water supply stress (Piketh et al., 2025). Moreover, this creates climate-driven variability and vulnerability.

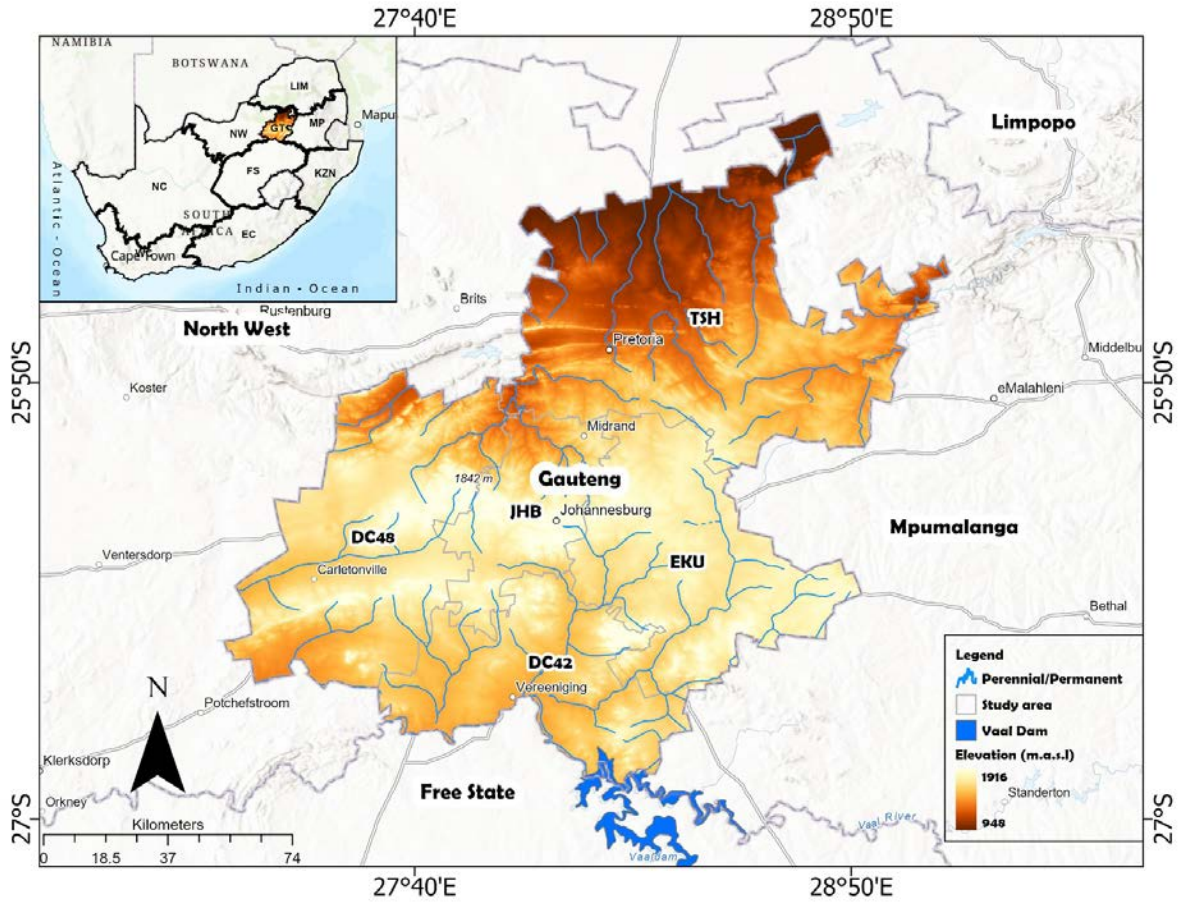



*Figure 3 1: Map of Gauteng. Source: Sintayehu & Mhangara (2023).*

Figure 3.1, Gauteng province was used as the study area to analyse the relationship between land surface temperature, maximum air temperature and vegetation and water indices. The province is characterised by mixed land use and ample vegetation. Additionally, it is a small province situated on the Highveld at about 25° 50' latitude South and 28° 50' longitude East.

It is the smallest province in South Africa; however, it is densely populated and one of the top economic hubs of the country. This province includes the city of Johannesburg (JHB), Tshwane (TSH), Ekurhuleni (EKU), West Rand (DC48) and Sedibeng (DC42) districts. The province's total area is an estimated 18,176 $km^2$. According to the Cwb in Köppen, the climate in the area is a temperate subtropical highland, with wet summers from December to February and dry winters from June to August. Due to climate variability and seasonal rain, Gauteng's water

supply is vulnerable (Zubaidi *et al.,* 2020). This urban province is characterised by industries, major transportation networks and is scattered with mining and cultivated lands. Moreover, it has a juxtaposition of residential zones – wealthier suburbs fitted with ample green space and jarring informal settlements with dense housing and sparse greenery (Hardy & Nel, 2015; Souverijins *et al.,* 2022). South Africa has a significant racial and economic segregation history, influencing current land cover and infrastructure patterns within all cities. Gauteng's water supply relies on several dams and surface water, which are both vulnerable to heatwaves and urban planning patterns (Zubaidi *et al.,* 2020). Moreover, with rising temperatures and water scarcity in the province (Gauteng Provincial Government, 2010; Zubaidi *et al.,* 2020; Souverijns, 2022), methods deployed to analyse the phenomenon are mostly qualitative, field surveys and basic geographic information systems for mapping that lack advanced geospatial analysis. Hence, the use of remote sensing to observe a current phenomenon, which has the attention of many municipalities in the province, increases accuracy and efficiency in urban studies and can aid city-specific urban planning and mitigation measures(Gauteng Provincial Government, 2010). Thus, given its rapid growth and uneven development (Rasebechele *et al.,* 2025), Gauteng is an ideal region to study urban heat impacts on vegetation and water indices. Gauteng's geology has extensive dolomite formations that underlie regions between Johannesburg and Pretoria. These areas have karstic aquifers suitable for groundwater recharge and flow due to high permeability. These aquifers are susceptible to instability in water levels due to infrastructure leaks (Dippenaar et al., 2018). Moreover, the surface water in Gauteng interacts with dolomite aquifers in exchanging water throughout the seasons, depending on groundwater levels (DWA, 2010). The hydrogeology in the province has significant implications for water resources under climate stress (DWA, 2010). Moreover, dolomite aquifers provide a buffer during dry seasons by supplying groundwater when surface inflows are reduced.

Across the study area, the mean annual rainfall is ~ 363mm, and temperatures average between 20.3 °C and 26.3 °C, highlighting the region as climate vulnerable to heatwave intensification (Mbokodo et al., 2023). Additionally, recent research has revealed trends in rising maximum air temperature and more intense heatwaves in inland provinces like Gauteng (Mbokodo et al., 2023). Remote sensing studies reflect these changes in the landscape, such as reduced vegetation towards more impervious urban surfaces in Gauteng, which have contributed to increasing land surface temperatures (LST), as revealed by Landsat-derived thermal analyses over time (Adedayo, 2015; Magidi & Ahmed, 2020).

## 3.2 Data Acquisition

To analyse the relationship between urban heat factors and vegetation and water indices, the method employed the use of multiple sensors and variables. This allowed for the capturing of land-vegetation-water dynamics over four decades in Gauteng for the summer seasons of 1984, 1989, 1994, 1999, 2004, 2009, 2014, 2020, and 2024. Region-based Landsat 5 TM (1984 to 2009) and Landsat 8 OLI TIRS (2014 to 2024) imagery at 30m multispectral were accessed through Google Earth Engine Data Catalogue – USGS Collection (U.S Geological Survey, nd).

Long-term analysis using both Landsat 5 TM and Landsat 8 OLI/TIRS enables consistent spatial coverage but is affected by several uncertainties. Pixel gaps even after computation and cleaning remain due to cloud cover and shadow masking. However, excluding either sensor would create temporal gaps, undermining long-term trends. Despite sensor differences, both Landsats are designed for continuity and work well in GEE, reducing inter-sensor bias. Moreover, the study applies a consistent LST retrieval framework to both sensors, thus minimising inconsistencies. Additionally combined use of Landsat 5 and 8 for long-term climate and UHI studies is well established, proving methodological validation.

From this imagery, the variables were derived and calculated as surface temperature from thermal bands, Normalised difference vegetation index (NDVI) to quantify vegetation in an area, water ratio index (WRI) to detect surface water and modified normalised difference water index (MNDWI), which enhances open-water detection in urban settings. All indices were computed on the same five-year cadence to align with land use land cover (LULC) and LST layers. Daily precipitation and maximum air temperature (Tmax) were extracted from the NASA POWER (Data Access Viewer/API), which supplies analysis-ready, station-independent NASA reanalysis/satellite-driven fields suitable for climate applications (NASA POWER Data Access Viewer, n.d). The maximum air temperature and precipitation data for the research were collected from 1984 to 2024. Further, the use of Python was implemented to compute heatwave metrics following the threshold of $\geq 3$ consecutive days exceeding a baseline high-temperature threshold of the 90th percentile to characterise heatwave frequency, duration, and intensity throughout 40 years. The chosen periods allow both a long-term perspective and recent intensification of warming and its impacts on water and vegetation indices. NASA POWER can be more useful than relying on local station data, as it is consistent and offers continuous spatial coverage. Moreover, station areas are at points with more developed regions having clusters, while rural areas are sparse (Skrynyk et al., 2025). Additionally, for long-term analysis, NASA POWER is better as all grid cells use the same methodology over time while stations relocate, break down, or change instruments. Therefore, using NASA POWER allows for large area analysis in simultaneous extreme heat mapping (Mankin et al., 2025). Additionally, finer scales may not have the same temporal consistency (Mankin et al., 2025).

*Table 3.2 1: Spectral Index Table for the Satellite Imagery.*

| Index | Formula | Bands | Source |
|---|---|---|---|
| Normalised Difference Vegetation Index | $(NIR - Red) / (NIR + Red)$ | B5, B4 (Landsat 8) | Rouse *et al.,* 1973; Tucker, 1979 |
| Modified Normalised Difference Water Index | $(Green - SWIR1) / (Green + SWIR1)$ | B3, B6 | Xu, 2006 |
| Water Ratio Index | $(Green + Red) / (NIR + SWIR)$ | B3+B4 / B5+B6 | McFeeters, 1996 |
| Land Surface Temperature | _ | Band 6 or Band 10 | Sekertkin & Bonafoni, 2019; De Almeida *et al*., 2023 |

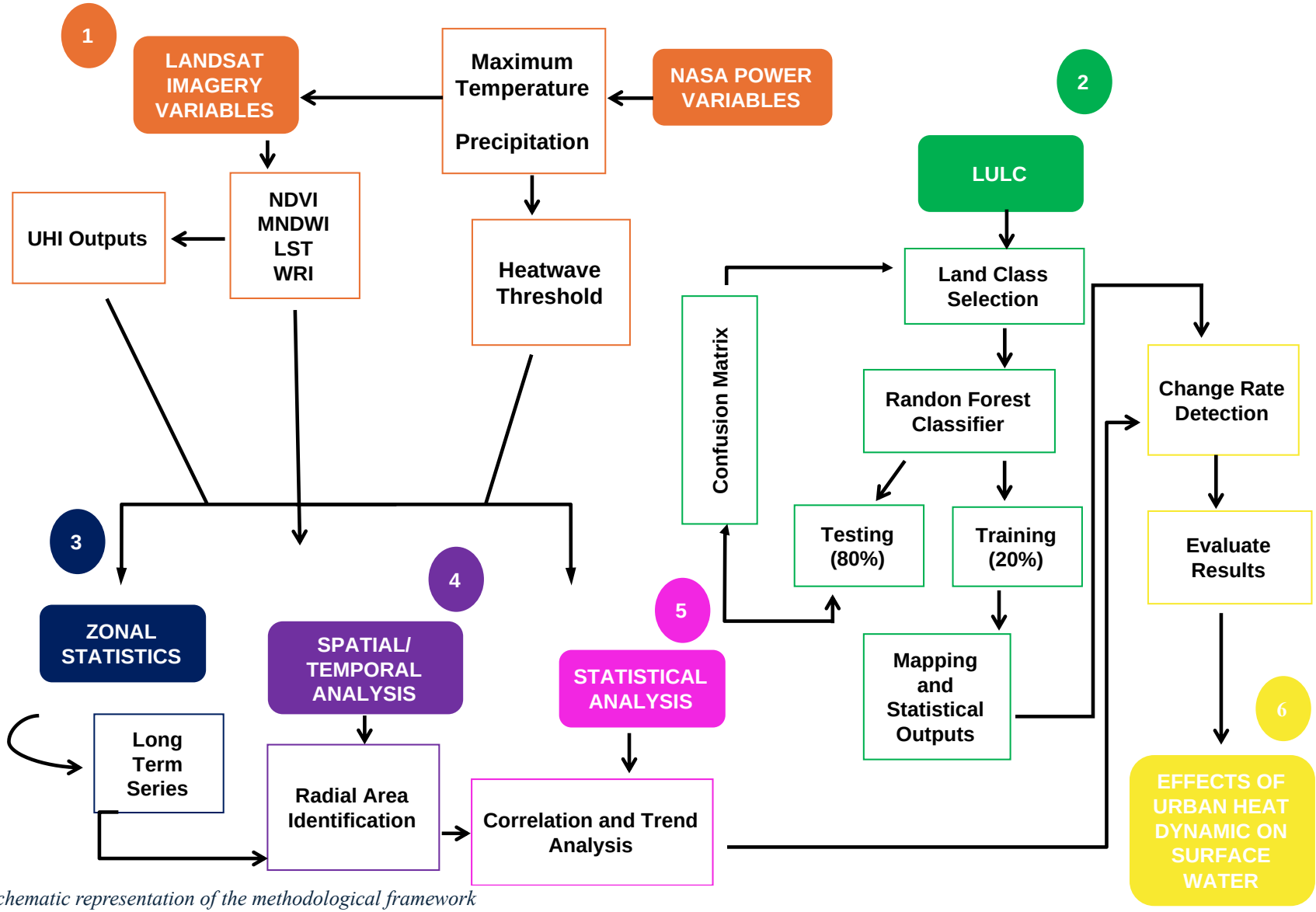



*Figure 3.2 1: Schematic representation of the methodological framework*

Confusion metrics derive the error or accuracy level, thus making it indispensable in rigorous research pertaining to assessing classification accuracy and reliability of land use and land cover. A confusion matrix systematically compares predicted land-cover classes to reference ground truth (Phan et al., 2020). Ground truthing in Google Earth Engine involves selecting points and polygons per land cover across all bands to ensure and allow that the random forest correctly applies certain pixels to a specific land cover for land use land cover mapping (Shafizadeh-Moghadam et al., 2021). The confusion metrics calculate indicators such as overall accuracy, producer's accuracy, user's accuracy, and the Kappa coefficient, offering both regional and per-class performance insights and accounting for chance agreement (Hsiao & Cheng, 2016; Phan et al., 2020). Furthermore, the F-score is a harmonic mean of precision and recall, the user's accuracy and the producer's accuracy, respectively. This metric is especially valuable when dealing with class imbalance, as it fairly balances both correctness and completeness for each class.

The confusion matrices used to ensure accuracy in the LULC are Overall Accuracy (OA), Consumer's Accuracy (CA), Producers' Accuracy (PA), F-Score and Kappa Coefficients (K) (Table 3.2.2). The equations for each are as follows: Eq. 1 to 5:

$$CA = \frac{xii}{xi}_{+} \times 100 \qquad (Eq.1)$$

$$PA = \frac{xii}{x+i} \times 100 \qquad (Eq.2)$$

$$OA = \frac{D}{V} \times 100 \quad (Eq.3)$$

$$F - Score = 2 \times \frac{(PA \times CA)}{(PA + CA)} \quad (Eq.4)$$

$$k = \frac{N \Sigma_{i=1}^{k} x_{ii} - \Sigma_{i=1}^{k} (x_i + \times x + i)}{N^2 - \Sigma_{i=1}^{k} (x_i + \times x + i)} \quad (Eq.5)$$

Where k is the Kappa coefficient, $x_{ii}$ is the total number of observations in row *i* and column *i*; $x_{i+}$ and $x_{+i}$ are the marginal totals of row *i* and column *i*, respectively; *N* is the total number of observations; D is the total number of correct pixels (diagonal); V is the total number of pixels in the error matrix; F-Score is the harmonic mean of PA and CA (Islami *et al.,* 2022; Sintayehu & Mhangara, 2023).

The Kappa coefficient (Cohen's Kappa) is used in remote sensing to assess classification accuracy by comparing observed versus predicted class agreements. Islami *et al* (2022) report LULC Kappa values of 0.74 to 0.80 across multiple years, reinforcing good-quality classification.

*Table 3.2 2: Kappa Coefficients.*

| Kappa values | Description |
|---|---|
| 0.8 to 0.6 | Substantial agreement |
| 0.6 to 0.2 | Moderate agreement |
| 0.4 to 0.2 | Fair agreement |
| 0.2 to 0.01 | Slight agreement |
| ≤ 0 | No agreement |

*Table 3.2 3: MNDWI Interpretations.*

| MNDWI values | Description |
|---|---|
| 1 to 0.66 | Blue Water |
| 0.34 to 0.66 | Green Water |
| 0.007 to 0.34 | Shallow or Vegetation Water |

NDVI values range from -1 to 1. Negative values indicate non-vegetated areas like water, low positive values (0.12 to 0.22) indicate barren or sparsely vegetated areas, moderate values (0.22 to 0.42) indicate shrubs, bushes and grasslands and lastly, high NDVI values (0.72 to 1) depict dense and healthy vegetation such as forests.

*Table 3.2 4: NDVI Interpretations.*

| NDVI values | Description |
|---|---|
| 0.72 to 1 | Very Good |
| 0.42 to 0.72 | Good |
| 0.22 to 0.42 | Normal |
| 0.12 to 0.22 | Poor |
| -1 to 0.12 | Very Poor |

## 3.3 Image Processing and Analysis

### 3.3.1 Assessment of LULC, Accuracy Assessment and NDVI Derivation

Random Forest (RF) was chosen for long-term land use and land cover classification in Google Earth Engine due to its high accuracy, robustness and suitability for handling large-scale remote sensing data (Sultan et al., 2025). RF effectively mitigates overfitting and handles high-dimensional and noisy data—key advantages when processing time-series imagery over extended periods (Gislason et al., 2006; Macarringue et al., 2023; Bhungeni et al., 2024; Sultan et al., 2025 ). Additionally, numerous studies report high classification accuracy—studies report overall accuracies exceeding 90% and Kappa indices above 0.9 in diverse contexts such as complex European landscapes and southern Spain (Venter & Sydenham,

2021). While in South Africa, the coastal ecosystem yields an average overall accuracy of 82.3 % and an average Kappa coefficient of approximately 0.81, demonstrating reliable performance (Bessinger et al., 2022). Furthermore, random forest in cloud environments like GEE proves to be less complicated than methods such as SVMs or neural networks (Venter & Sydenham, 2021; Sultan et al., 2025).

In this study, a Random Forest (RF) classifier was applied in GEE on Landsat 5 TM and Landsat 8 TIRS imagery (1984 to 2024) to map LULC. The training and validation samples were used with known LULC points and spectral bands (from Band 1 to Band 7). A Random Forest (RF) classifier was used for land cover classification. The model constructs an ensemble of decision trees, where the final classification is determined by majority voting.

Random Forest (RF) Classifier Eq. 6:

$$\hat{y} = \text{mode}\{\text{T1}(\chi), \text{T2}(\chi), \ldots, \text{TN}(\chi)\} \qquad (Eq. 6)$$

Where $T_i(x)$is the class predicted by the $i^{th}$decision tree. $N$is the number of trees in the forest, and $\hat{y}$is the final predicted land cover class.

The Normalised Difference Vegetation Index is useful in assessing urban heat island effects. Urban areas typically replace vegetated landscapes with impervious, low-NDVI surfaces. Therefore, the use of NDVI assesses the amount of cooling in the region (Ahmad et al., 2025). Empirical studies consistently demonstrate a negative correlation between NDVI and LST (Yuan & Bauer, 2007; Roba & Tabor, 2025). Hence, areas with higher NDVI generally exhibit lower surface temperatures (Yuan & Bauer, 2007; Roba & Tabor, 2025). Additionally, barren land in Ethiopia correlates with low NDVI values below 0.1, indicating both built-up areas and barren land contribute to increasing LST over time (Roba & Tabor,

2025). Hence, NDVI was applied in this study to evaluate the impacts of heat stress and vegetation density using Landsat 5 TM and Landsat 8 OLI TIRS in Google Earth Engine (GEE) for the years 1984 to 2024. NDVI was computed in GEE and visualised in ArcGIS and QGIS as follows (Eq. 7):

$$NDVI = \frac{(NIR - RED)}{(NIR + RED)} \qquad (Eq. 7)$$

Where Band 5 and Band 4 represent NIR from Landsat 5 TM and Landsat 8 OLI TIRS, respectively. And Band 4 and Band 3 for RED from Landsat 5 TM and Landsat 8 OLI TIRS, respectively.

Further, the RED Band is (0.63 – 0.69 μm), and the NIR band is (0.76–0.90 μm), while for Landsat OLI TIRS, the RED band is Band 4 (0.64–0.67 μm) and the NIR band is Band 5 (0.85–0.88 μm). The NDVI values range between −1 and +1. Negative values represent non-vegetated surfaces such as water, bare land, or built-up areas, while positive values indicate vegetation. Low vegetation or stressed vegetation cover is typically represented by NDVI values of 0.12 – 0.22, whereas healthy and dense vegetation corresponds to higher values between 0.72 – 1 (Gidey *et al.,* 2018).

### 3.3.2 Temperature and Urban Heat Calculations

Landsat 5 TM band 6 and Landsat 8 TIRS band 10 are commonly used in land surface temperature retrieval in Google Earth Engine due to their appropriate thermal infrared bands. These bands have spectral coverage which allows conversion from digital number to top-of-atmosphere spectral radiance and brightness temperature (Sekertkin & Bonafoni, 2019; Macharia et al., 2022). Once the top of atmosphere radiant is calculated, it is converted to brightness temperature using sensor-specific Planck's constant K-1 and K2, which are about 607.76 and 1260.56, respectively, for Landsat 5 TM band 6 and approximately 774.89 and 1321.08, respectively, for Landsat 8 Band 10 (Du et al., 2015; Sekertkin & Bonafoni, 2019; Macharia et al., 2022). Planck's law is for the adjustments of thermal emission (Akomolafe & Rosazlina, 2022). Furthermore, emissivity is calculated from the formulas of proportion vegetation (PV), which is derived from NDVI, which is the normalised difference vegetation index (Parastatidis et al., 2017; Sekertkin & Bonafoni, 2019).

This paper used Landsat 5 TM and Landsat 8 T1_ RT TOA to derive land surface temperature through the thermal band, brightness and proportion of vegetation (PV). The equations for each are listed below from Eq. 8 to 14:

Conversion of DN to TOA Radiance (Eq. 8):

$$L\lambda = ML \times Qcalc + AL \qquad (Eq. 8)$$

Where L$\lambda$ = Top-of-Atmosphere (TOA) spectral radiance, ML = multiplicative scaling factors, Qcalc = Quantised and calibrated pixel value, AL = Radiance additive factor for band x (band 6 for Landsat 5 and band 10 for Landsat 8 OLI TIRS)

Spectral Radiance of Brightness Temperature (BT)

The paper used the same methodology as Gidey & Mhangara (2025) to calculate the spectral radiance of brightness temperature (BT) from Kelvin to Celsius using the Landsat algorithm based on the Planck curve (Eq. 9):

$$BT = \left(\frac{K2}{ln}\left(\frac{K1}{L\lambda}\right)\right) - 273 \qquad (Eq. 9)$$

Where BT = Brightness temperature in Celsius, K 2 and K 1 = Calibration constant 2 and 1 for band 6 in Landsat 5 and 10 in Landsat 8, L$\lambda$ = calculated TOA spectral radiance.

NDVI is commonly used in GEE and research in climate studies as a vegetation proxy for land surface emissivity and temperature calculation. Since vegetated areas have higher emissivity than bare soil or urban materials, NDVI-derived vegetation proportion (Pv) enables more accurate emissivity modelling (Feng et al., 2020; Albut, 2024; Ahmad et al., 2025). The Proportion of vegetation calculation is derived from the NDVI formula (Eq. 7 ):

Proportion of Vegetation (Eq. 10):

$$PV = \left( \frac{(NDVI - NDVI_{min})}{(NDVI_{max} - NDVI_{min})} \right)^2 \quad (Eq. 10)$$

Land Surface Emissivity (LSE) based on the proportion of vegetation (PV) from NDVI, using constant soil and vegetation emissivity coefficients for both satellite imageries.

Land Surface Emissivity (Eq. 11):

$$LSE = 0.004 \times PV + 0.986 \quad (Eq. 11)$$

Land surface temperature (LST) band 6 (Landsat 5 TM) and band 10 (Landsat 8 OLI TIRS) were applied (Eq. 12):

$$LST = \left( \frac{BT}{\left(1 + \left(0.00115 \times \frac{BT}{1.4388}\right) \times ln\,(LSE)\right)} \right) \quad (Eq. 12)$$

Surface urban heat island effect is calculated from the normalised standard deviation of land surface temperature values. This demonstrates anomalies in heating according to the area trends in temperature. This method was used in previous papers (Albut, 2024; Sintayehu & Mhangara,

2025). Standard statistical anomaly methods in UHI calculations are prevalent in remote sensing. The foundational methods established by Voogt and Oke (2003) and altered versions by Mosia and Gemeda (2022) streamline UHI spatial compatibility of heat intensity over decades, making it a suitable calculation for this research. Additionally, many authors acknowledge this formula as a basis for comparing surface UHI against morphological and biophysical indices in climate studies (de Almeida et al., 2021). Thus, applicable in context for this paper, similarly used by researchers in Thailand (Kliengchuay et al., 2025) and in Addis Ababa (Mosia and Gemeda, 2022).

Urban heat island (Eq.13):

$$UHI = LSTi - \frac{LSTmean}{LSTStdev} \quad (Eq.13)$$

Where UHI = Urban Heat Island, LST i = Land Surface Temperature Value of i period, LST mean = Mean Land Surface Temperature Value of i– i-period, Stdev = Standard Deviation value of Land Surface Temperature for– i-period (Sintayehu & Mhangara, 2023).

Heatwave detection:

The maximum temperature at 2 meters above the Earth's surface acquired from NASA POWER was used to detect heatwaves and their characteristics in the province. This dataset is ~50km resolution, which is much coarser than municipal data. However, it captures spatially coherent large-scale temperature patterns without station distribution bias and data gaps (Mistry et al., 2022).

To identify extreme heat events, this paper applied a threshold-based approach using daily maximum air temperature (*T2M_MAX*) values. First, thresholds were established for each day of the year (*DOY*) based on a moving-window percentile method. For each DOY (1–366), a temporal window was defined as ± WINDOW_DAYS. All historical temperature observations within this window across the baseline period were extracted, and the PERCENTILE (e.g., $90^{th}$) of these values was computed. Further, the resulting thresholds were then merged with the daily temperature dataset. For each day, we assessed whether T2M_MAX exceeded its corresponding threshold. Days above threshold were flagged as potential heat-event days. To identify discrete events, we tracked consecutive exceedances. A new event identifier (*EventID*) was assigned whenever one or more consecutive days surpassed the threshold. Events shorter than the minimum required duration (*MIN_DURATION days)* were discarded, ensuring that only sustained periods of anomalously high temperature were retained as heat events, as shown in Eq. 14.

Moreover, a sensitivity analysis was done to assume the appropriate heatwave threshold across percentiles $85^{th}$ to $95^{th}$ and minimum durations of 2 to 5 days. The analysis indicated that thresholds below the $90^{th}$ percentile dramatically increased short-lived events, while thresholds above the $95^{th}$ percentile yielded scarce heatwave occurrences. Further, the duration of three consecutive days effectively excluded transient warm anomalies and retained sufficient events for robust analysis across Gauteng.

$$If\ length\ (EventID) <\ Dmin, EventID\ =\ 0 \qquad (Eq. 14)$$

Where EventID is the event identifier locating heatwaves, and *Dmin* is the minimum duration of a possible heatwave.

### 3.3.3 Surface Water Indices Calculation

MNDWI only shows identified water bodies. The Modified Normalised Difference Water Index (MNDWI) is applied in urban environmental studies to distinguish water bodies through green and shortwave-infrared (SWIR) bands (Xu, 2006). MNDWI improves on the traditional NDWI (normalised difference water index) by replacing the near-infrared (NIR) band with SWIR.

MNDWI was calculated from Landsat imagery (Eq. 15):

$$MNDWI = Green - \frac{SWIR\ 1}{Green} + SWIR\ 1 \qquad (Eq.\ 15)$$

where for Landsat TM, G = Band 2 (green) and SWIR = Band 5; for Landsat 8, G = Band 3 and SWIR = Band 6 for the green band in Landsat 5.

WRI shows wetness and shares the same band as NDVI (NIR); therefore, WRI identifies surface moisture rather than solely water bodies. In this index (water ratio index), positive values typically correspond to surface moisture, while negative values indicate non-water surfaces such as barren land and built-up areas.

WRI is derived from the formula (Eq. 16):

$$\frac{(Green\ +\ NIR)}{(SWIR\ 1\ +\ SWIR\ 2)} \qquad (Eq.16)$$

Where for Landsat TM, G = Band 2 (green); SWIR 1 = Band 5; for Landsat 8, G = Band 3 and SWIR 1 = Band 6 and SWIR 2 Band 7 for both satellite imageries.

3.3.4 The Statistical Relationship and Trend of the Climatic Variables and Indices

Spearman Correlation and Mann-Kendall are used to assess the trend of variables. Spearman correlation is a non-parametric method that assesses monotonic relationships between variables without requiring normality (Braunisch et al., 2013; Zhang et al., 2021). This method is robust to non-normal distributions and outliers, making it suitable for this dataset. Moreover, studies using Landsat-8 data from 2016 to 2020 found that LST demonstrated a strong inverse correlation with NDVI (Taloor et al., 2024).

Spearman Correlation (Eq. 17):

$$\rho = 1\ -\ \frac{6\Sigma d_i^2}{n(n^2-1)} \qquad (Eq.17)$$

where $\rho$ = Spearman's rank correlation coefficient,

$d_i$= difference between the two ranks of each observation and n = number of observations.

Testing monotonic trends in climate and environmental data as a time series, a non-parametric method is used, such as the Mann-Kendall test. This test does not require normal distribution assumptions, while being robust against outliers, thus efficient for environmental data. Using Python to perform Mann-Kendall simplifies the functions. This test was applied using the significance level of α = 0.05 implemented in the pymannkendall package. The Mann–Kendall trend test was applied to detect monotonic trends in the time series. The standardised test statistic $Z$ is defined below.

Mann-Kendall (Eq. 18):

$$Z_{MK} = \begin{cases} \dfrac{S-1}{\sqrt{\mathrm{VAR}(S)}} & \text{if } S > 0 \\ 0 & \text{if } S = 0 \\ \dfrac{S+1}{\sqrt{\mathrm{VAR}(S)}} & \text{if } S < 0 \end{cases} \qquad (Eq. 18)$$

Where,

S: Mann–Kendall test statistic

Var $(S)$: variance of $S$

$Z$: standardised normal statistic used to determine trend significance

# CHAPTER FOUR: RESULTS AND DISCUSSION

This section presents the main findings of remote sensing and GIS algorithms described in the methodology to explore the interactions between heatwaves, urban heat island (UHI) intensity, land cover dynamics, and surface water resources within the Gauteng province from 1984 to 2024. The results are organised into three main sections: firstly, the analysis of Heatwaves and UHI Intensity over the province; secondly, the effects of land cover types in triggering Heatwaves and UHI; thirdly, the impacts of land cover dynamics, heatwaves, and UHI effects on surface water resources; and lastly, the conclusion of the findings at the end of the chapter.

## 4.1 Analysis Of Heatwaves and UHI Intensity Over Gauteng (1984 To 2024)

### 4.1.1 Overview of Temporal Trends

Figure 4.1 is a provincial depiction of land surface temperature over the years. The maps show the seasonal (summer) characteristics of maximum temperature in Gauteng. Moreover, Figure 4.1 depicts a somewhat homogenous trend across the province throughout the period from 1984 to 2024. Land surface temperature in Gauteng reaches highs of 45°C. While the average of the 40 years is 53.06°C, with the lowest temperature

recorded in the five-year intervals was an average of 4.78°C from 2004, 2009 and 2014. Trends in LST are sparse within this region due to mixed land use as well as dominant land use land cover classes such as barren land, cultivated and forested land. The South African weather service documented high temperatures and heatwave events in 1983 to 84 (Mbokodo *et al.,*2023). Thus, the 1984 image shows an average higher LST; however, Landsat 5 during those years held a mild image bias within the band, therefore, the mean is subtly higher. The maps display no trend in land surface temperature over time. There is a subtle increase in average LST; this relates to global trends of regionally variable increases (Li *et al.,* 2022). This aligns with Kapwata *et al.* (2022), stating that regional average maximum temperatures have increased. From 1984, there has been a gradual increase in LST with a slight decrease during 2004 and 2009. However, recent years have seen warmer temperatures. Furthermore, the LST range is monotonous throughout the whole period with minor fluctuations and rare LST. The colour scale is limited to 20°C to 50°C to enhance visual representation, as the isolated pixels reaching temperatures of 60°C and above account for less than 0.001% of the study area. In other words, the colour ramp is based on the 95$^{th}$ percentile of land surface temperature. Moreover, similar to Martin (2019), the analysis of land surface temperature mapping displayed gaps and pixels which are linked to cloud contamination or atmospheric interference in the thermal infrared bands. This limitation is inherent to LST products since thermal sensors cannot penetrate cloud cover, resulting in reduced spatial continuity in the datasets. Similar challenges have been reported in international studies of the uncertainties of consistency in the retrieval of land surface temperature maps (Sekertekin & Bonafoni, 2020; Chen *et al.,* 2020). Moreover, the mean land surface difference between MODIS and the Landsat for the study ranges from 2.52°C to 5.07°C. However, the land surface temperatures experienced temporal sensitivity as an abnormal maximum was 68°C from 2019 to 2020 summer period, while reducing to 63°C from 2018 to 2020 summer periods. In the South African context, most recent

work has focused on individual metropolitan areas, such as Johannesburg (Sintayehu & Mhangara, 2025) and Durban (Ngie *et al.,* 2016). While these city-level studies do not explicitly report pixel loss, they illustrate how LST mapping is being applied locally. At the provincial scale, such as in Gauteng, these atmospheric contamination effects are equally evident, but remain under-reported in regional literature.

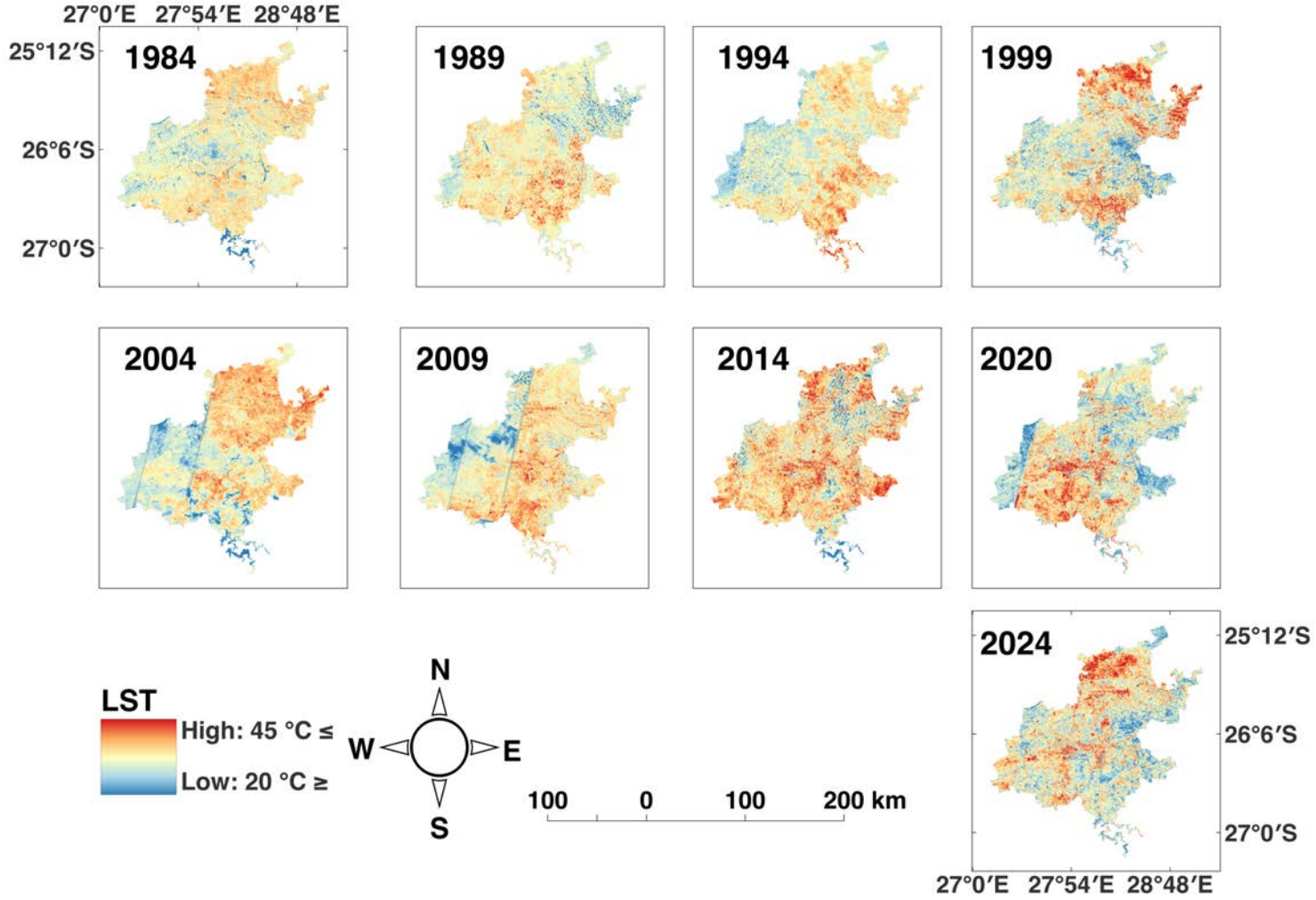



*Figure 4.1 1: Spatiotemporal distribution of Land Surface Temperature in Gauteng.*

The long-term land surface temperature at a city scale (Figure 4.1.2) analyses the centre of the province and its thermal distribution. The centre is attributed to be hotter than its surrounding areas. At 5km and 10km, this region averages 26.1°C and 25.9°C, respectively. While 15km and 20km average 25.4°C and 26.4°C respectively, demonstrating that further out from the centre, the temperatures usually decrease due to improved urban planning further from the central business district. The north-eastern areas of the city centres have lower land surface temperature beyond 20km. Additionally, beyond 20km, the south-western region depicts cooler trends. As expected, city centres exhibit high land surface temperature due to urban density and concrete and tarmac characteristics. This highlights poor urban cooling and poor urban planning that exacerbate temperatures in the city centres. Moreover, the white pixels, even at high cloud-masking, demonstrate that the further away from the centre, the cooler the land surface temperatures. Thus, this alludes to less density, urban fabric and pollution that are attributed to city centres. In general, land surface temperature behaviour is homogeneous temporally in Gauteng. The Mann-Kendall analysis indicated no trend in land surface temperature over 40 years for the province. It is noticed that both the Vaal and Bronkhurstspruit Dams, as water sources, exhibit slight warming as displayed by the coverage of reddish pixels.

The province experiences warmer average temperatures in the southeastern and southwestern areas. This highlights Johannesburg and the West Rand as areas experiencing sporadic long durations of heatwaves and intense UHIs. Considering the satellite-derived images, the northern areas of Gauteng have thermal contamination throughout the whole period (40 years). Thus, insinuating intense or continuous cloud cover, which can lower LST and thus the northern region can have fewer heatwaves. Overall, the results report TMAX and LST having similar trends over time, noted additionally by de Almeida *et al.*(2023) for Bragança, Portugal. Upon further visual inspection of Figure 3, Gauteng shows cooler

temperatures in the north-eastern regions for the early years 1989 to 2004. However, more recent years show the south-western regions to be cooler. Furthermore, Bronkhurstspruit Dam notices a decrease in land surface temperature over 40 years by an average of 0.5°C. While the Vaal increases by ~0.11°C, city centres observe a significant increase of ~4.24°C.

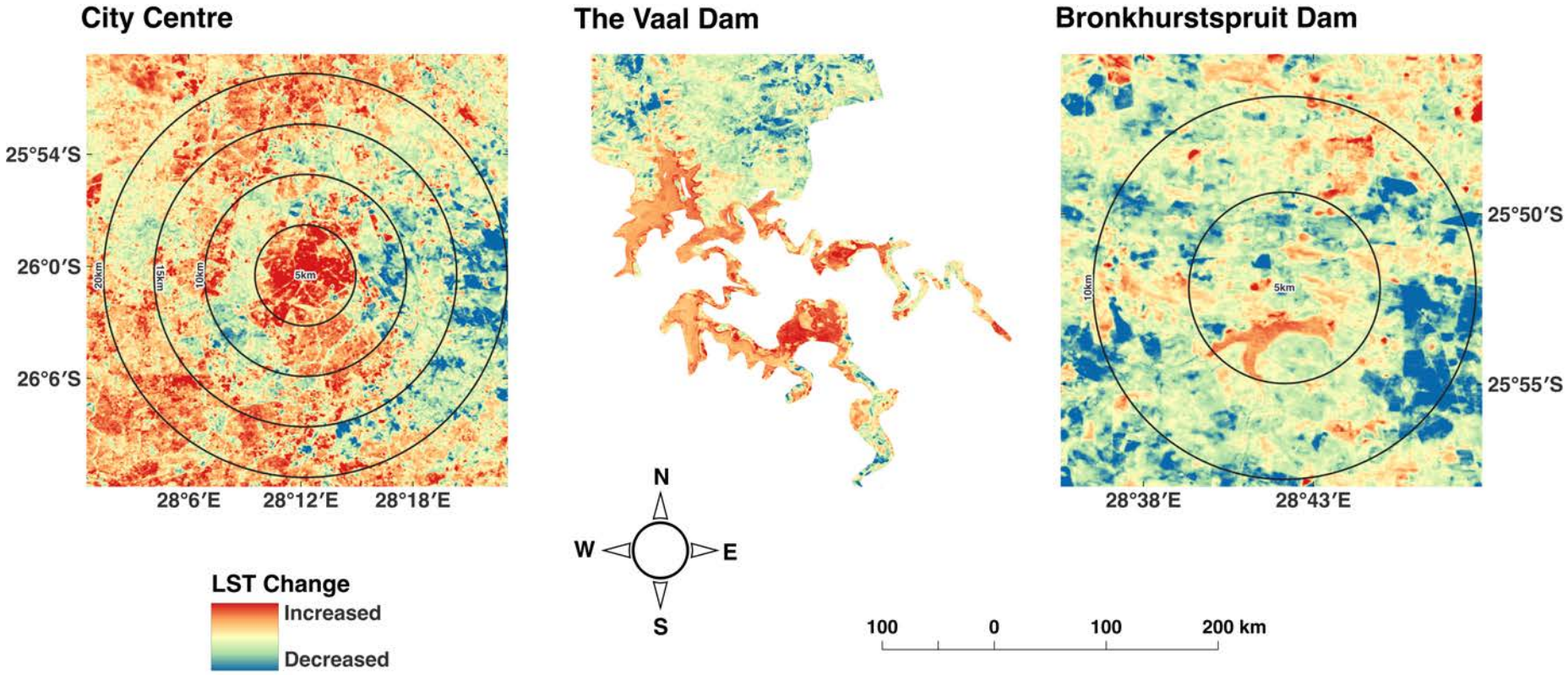



*Figure 4.1 2: Localised long-term change analysis of Land Surface Temperature at a city-scale in Gauteng from 1984 to 2024.*

Table 4.1.1 depicts the relative temperature per land use class. The table summarises observed temperature deviations across land cover categories. Built-up areas (BU) consistently showed values higher than 46°C, while water(WB)/vegetation (FL, CL, GL) sites recorded values mostly within 40°C. These results highlight the contrasting thermal behaviour of impervious versus vegetated surfaces. Thus, the results reveal clear and persistent temperature differences between these two LULC classes over the 40 years. The temperature values demonstrate that built-up areas generally recorded higher values, and vegetated/water sites recorded lower values. Across all observation years, built-up areas consistently recorded higher mean LSTs than vegetated areas, confirming the thermal contrast associated with urbanisation. In 1984, built-up areas exhibited a mean LST of 54.35 °C, compared to 50.68 °C for vegetated surfaces, indicating a substantial temperature differential at the beginning of the study period. This highlights the relative warming of impervious surfaces compared to cooler, green/blue areas. This aids in identifying which land cover exacerbates land surface temperatures and which reduces LST or offers a cooling effect. Urbanisation characteristics lead to reduced surface water and vegetation area, as well as degradation of such natural environments. This is evident in the values of water bodies and vegetated areas, which have a cooling effect (lower LST values) while built-up and barren land induce higher LST. Moreover, land-use change significantly influences both surface water and vegetation area, often leading to their reduction and degradation. This deterioration of land use diminishes the cooling capacity of these natural surfaces, thereby reducing the occurrence of lower surface temperatures in the region. Within urban contexts, the expansion of impervious surfaces and built-up areas, bare or barren land and mines contributes to elevated land surface temperature, which subsequently intensifies UHII. Both land cover types display notable temporal variability. A marked decline in LSTs is evident in 1989 for both vegetation (42.90 °C) and built-up areas (41.70 °C), followed by fluctuations through the 1990s and early 2000s. Despite these variations, built-

up areas generally maintained higher temperatures relative to vegetation, except for minor convergence during cooler years. Further, the increase in LST further undermines the cooling effects provided by water bodies and vegetation. Forest Land showed relatively moderate temperatures, decreasing from 48.01 °C in 1984 to 45.80 °C in 2024. Furthermore, built-up areas in this region depict an average of ~ 48.28°C, while waterbodies have an average of 44.70°C and vegetation an average of 46.72°C. Oyeniyi et al (2024) corroborate this paper's result of a strong relationship between land cover change, LST fluctuations and recent times, notice an average within 50°C for built-up areas. Cultivated Land (CL) displayed intermediate thermal behaviour, with mean LSTs ranging between 42.20 °C and 52.48 °C across the study period. Mining areas (MN) also showed notable variability, with relatively lower temperatures in the early 2000s (37.48 °C in 2009) followed by a sharp increase in later years, reaching 51.03 °C in 2024, likely reflecting changes in surface exposure and land management practices. As expected, waterbodies and vegetation exhibit cooler temperatures than land surface temperatures; this corroborates Mushore et al (2019). Water Bodies (WB) consistently recorded the lowest mean LST values in the earlier years, such as 42.86 °C in 1984 and 38.59 °C in 2004. However, from 2014 onwards, WB exhibited an apparent increase in mean LST, reaching 49.97 °C by 2024. In some years, water bodies appear to exhibit temperatures comparable to or exceeding those of certain built-up or vegetated classes. This counterintuitive pattern is attributed to minor misclassification effects arising from the Random Forest land cover classification implemented in Google Earth Engine (GEE). Mixed pixels, seasonal water level fluctuations, shadows, turbid waters, shallow wetlands and green waters or spectral confusion with dark impervious or mining surfaces. The land covers are abbreviated as WB: Waterbodies, BU: Built Up, FL: Forested Land, BL: Barren Land, CL: Cultivated, SL: Shrubland, GL: Grassland, MN: Mines. This persistent

disparity underscores the role of land use and land cover change in shaping surface thermal patterns and contributes to the observed Urban Heat Island effects discussed in subsequent sections.

*Table 4.1 1: Relative Temperature in °C, Across Land Use Land Cover Types in Gauteng*

| LC | 1984 | 1989 | 1994 | 1999 | 2004 | 2009 | 2014 | 2020 | 2024 |
|---|---|---|---|---|---|---|---|---|---|
| FL | 48.01 | 42.28 | 45.52 | 41.68 | 44.80 | 43.62 | 47.13 | 45.30 | 45.80 |
| SL | 53.06 | 46.34 | 52.08 | 46.72 | 51.94 | 46.89 | 51.68 | 48.76 | 50.39 |
| GL | 51.55 | 44.22 | 47.67 | 45.28 | 50.16 | 46.44 | 48.81 | 49.00 | 50.70 |
| WB | 42.86 | 40.63 | 51.62 | 41.31 | 38.59 | 42.49 | 46.05 | 48.77 | 49.97 |
| BL | 55.04 | 42.36 | 46.56 | 45.60 | 50.99 | 46.32 | 48.40 | 49.45 | 53.36 |
| CL | 52.48 | 42.20 | 47.17 | 42.52 | 49.42 | 43.05 | 49.58 | 49.15 | 47.99 |
| BU | 55.10 | 41.74 | 49.59 | 46.27 | 48.27 | 48.59 | 51.93 | 51.70 | 51.33 |
| MN | 52.90 | 40.99 | 46.85 | 44.96 | 42.98 | 37.48 | 52.20 | 51.61 | 51.03 |
| Vegetation LST Mean | 50.68 | 42.90 | 46.79 | 43.16 | 48.12 | 44.37 | 48.51 | 47.82 | 48.16 |
| Built-up LST Mean | 54.35 | 41.70 | 47.67 | 45.61 | 47.41 | 44.13 | 50.84 | 50.92 | 51.91 |

Figure 4.1.3 displays the spatial distribution of the urban heat island intensity across Gauteng. The year 2004 exhibits the lowest maximum UHI intensity of 2.65°C. Additionally, from 2014 to 2024 UHI intensity maximum is not lower than 4.69°C. Thus, an increase in average UHI intensity can be deduced from the results. The UHI intensity spatial patterns follow paths of Built-up areas, which are central to Gauteng. Moreover, the

periphery zones depict more hues of blue pixels (minimum UHI intensity) or a negative UHII indicating a cooler zone; in other words, possible waterbodies and vegetation. In 1984, the urban heat island intensity was a high of 0.98°C, and in 2024, the UHI intensity was 5.3°C, while the lowest UHI intensity recorded was in 2004 with -1.47°C, and the highest was in 2024, reaching 5.30°C. Moreover, the West Rand is predominantly cooler on average over the whole study period (1984 to 2024), while Tshwane, Ekurhuleni and the City of Johannesburg exhibit a higher urban heat island intensification seen by the spatially consistent reddish pixels. Further, the central part of Gauteng notices constant positive (shades or red) UHI intensity, indicating a warming trend in UHI and land surface temperatures from urban centres. Thus, the results indicate a concentrated approach to development for the Gauteng province. Therefore, major metropolises are at a higher risk of urban warming extremes due to poor urban planning, lack of green and blue space planning, as well as continual urban sprawl. Additionally, the province struggles with water resource availability and the increased heating burdens this issue further. Similar to this paper's results, Mbombela, Mpumalanga, observed via long-term satellite-based analysis, land surface temperatures (LST) increase from approximately 28.3 °C in 2008 to 30.1 °C in 2023, indicating a gradual intensification of surface heat conditions over time (Magagula, 2024).

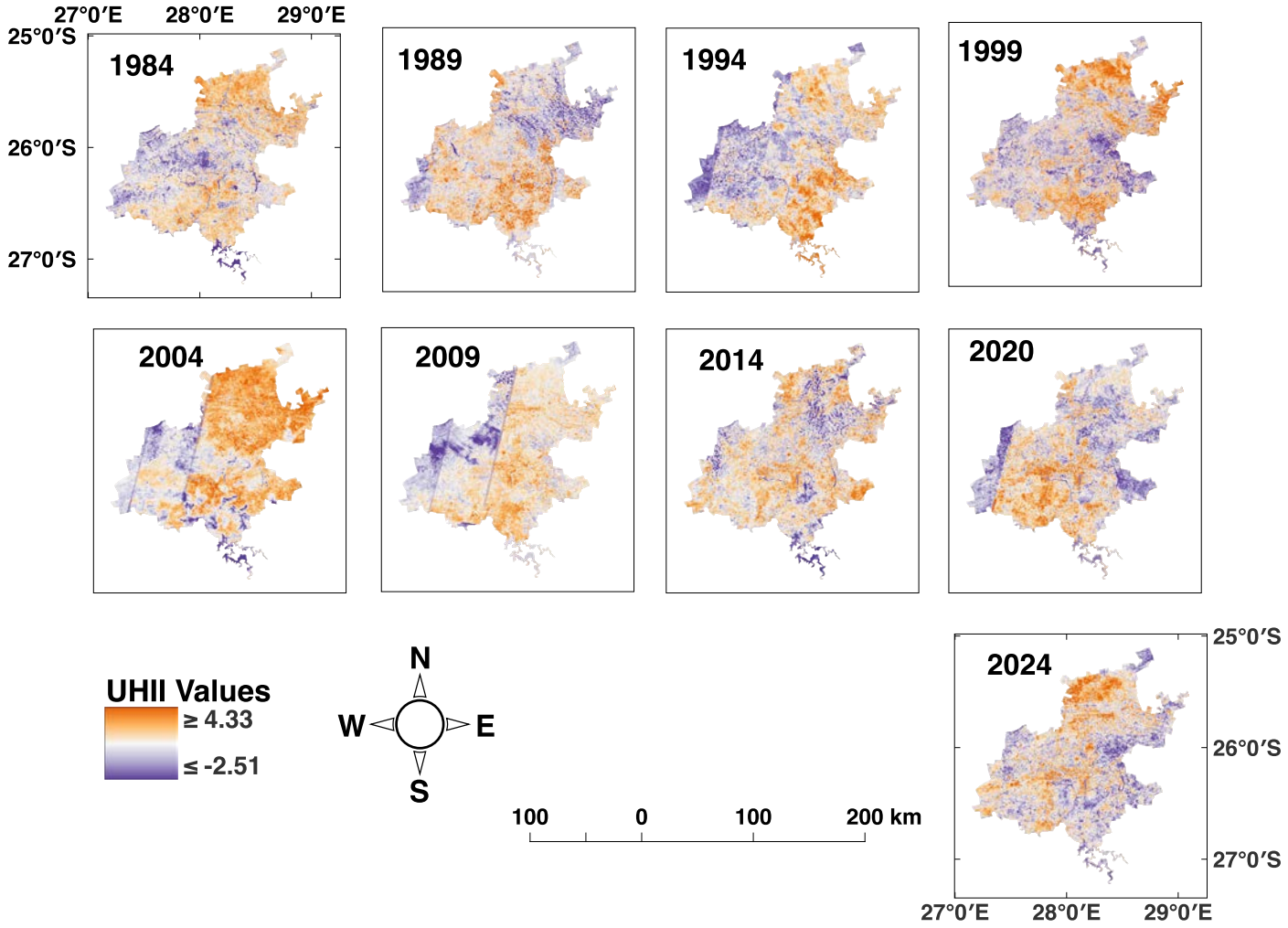



*Figure 4.1 3: The map above displays the spatiotemporal distribution of Urban Heat Island Intensity in Gauteng*

Table 4.1.2 demonstrates that over time, UHII values become less negative, pointing toward increasing urban warming. These results suggest 1984 shows predominantly negative UHII values, for example, -2.46°C in Johannesburg. Thus, indicating that, at the time, the urban areas were cooler than the surrounding regions. Further, the results indicate a consistent increase in UHII across all studied areas, although the magnitude of change varies spatially. Positive UHII values, on the other hand, suggest urban areas are warmer than surrounding rural areas. Moreover, in Table 4.1.2, UHII values transitioned from predominantly negative (cooler than surrounding rural areas) in the earlier years (1984 to 2009) to values closer to zero or positive in later years (2014 to 2024), indicating a gradual intensification of the UHII effect. Further, the City of Tshwane and Ekurhuleni (average + 2.24°C) are warming at a rate faster than Sedibeng and West Rand (average +1.29°C ). Additionally, the City of Johannesburg displayed a shift from -2.46°C in 1984 to 0.32°C in 2024, with a mean UHII change of +2.2°C. This suggests a substantial intensification of urban heat conditions over the study period. Similarly, the City of Tshwane experienced a pronounced increase, with a mean UHII change of 2.49 °C, closely followed by the West Rand, which showed an increase of 2.47 °C. These patterns suggest a consistent upward trend in UHII, particularly in the more urbanised municipalities. The Ekurhuleni Metropolitan Municipality exhibited a moderate rise in UHII, with a mean change of 2.20 °C over the same period. In contrast, Sedibeng District Municipality recorded the lowest increase in UHII, at 1.79 °C, indicating comparatively less intensification of urban heat effects relative to the other regions. Furthermore, similar to the results of this paper, recent studies in South Africa provide valuable context for interpreting Urban Heat Island (UHI) intensity trends. For example, in eThekwini (Durban), simulation data reported a seasonal UHI intensity of approximately 4 °C during summer, measured as the temperature difference between urban and rural areas using MODIS-derived land surface and air temperature data (Maisha et al., 2023). Additionally, at a country scale, the Council for Scientific and

Industrial Research (CSIR) green book estimated that urban temperatures in South African cities exceed those of surrounding areas by ~ 3 °C and ~10 °C, depending on specific land cover and urban morphology (CSIR, 2019). Overall, the results in Table 4.12 demonstrate that all metropolises in Gauteng experienced an increase in Urban Heat Island Intensity from 1984 to 2024, with the most pronounced changes observed in the highly urbanised metropolitan areas. Furthermore, these findings highlight notable spatial differences in the degree of UHII change within the province over the four-decade period. These results align with the increasing UHII trends observed in Gauteng municipalities from this paper, supporting the broader conclusion that urban expansion and land surface modification contribute significantly to localised warming in metropolitan areas.

*Table 4.1 2: Urban Heat Island Intensity within Metropolises in Gauteng from 1984 to 2024 in °C*

| Year | City of Johannesburg | City of Tshwane | Ekurhuleni | Sedibeng | West Rand |
|---|---|---|---|---|---|
| 1984 | -2.46 | -1.88 | -2.20 | -1.95 | -2.42 |
| 1989 | -0.23 | -0.64 | 0.10 | 0.24 | -0.14 |
| 1994 | -0.47 | -0.06 | 0.28 | 0.34 | -0.76 |
| 1999 | 0.05 | 0.75 | -0.18 | 0.43 | -0.16 |
| 2004 | -0.27 | 0.75 | 0.29 | 0.07 | -0.26 |
| 2009 | -0.20 | -0.12 | 0.42 | 0.29 | -0.64 |
| 2014 | -0.06 | -0.22 | 0.05 | -0.27 | -0.31 |
| 2020 | 0.45 | -0.32 | -0.26 | 0.36 | -0.23 |
| 2024 | 0.32 | 0.61 | 0.00 | -0.16 | 0.05 |
| Mean UHII change from 1984 to 2024 | 2.78 | 2.49 | 2.20 | 1.79 | 2.47 |

Figure 4.1.4 shows a local scale buffer analysis on consistent water bodies in Gauteng under UHII conditions. However, these water sources are on the outskirts of the province, further demonstrating the lack of central surface water in Gauteng and limiting the additional kilometre analysis. Moreover, Jandaghian & Colombo (2024) conclude that urban areas need water presence and open water sources to lower the land surface temperatures and UHI intensification. Bronkhurstspruit Dam notices a subtle increase in urban heat island intensity of about + 1.84°C; this is evident in its yellow shading. Additionally, city centres have a higher UHI intensity of +3.50°C over 40 years. At a local scale, it clearly demonstrates cooling (darker shades) further outward of the city centre. Additionally, water bodies such as the Vaal and Bronkhurstspruit dams exhibit warming over time due to extreme temperatures. North-east of both city centres and the Bronkhurstspruit dam shows a cooling trend; however, further outwards of the dam is outside the province, indicating that Gauteng is possibly warmer than its neighbouring parts.

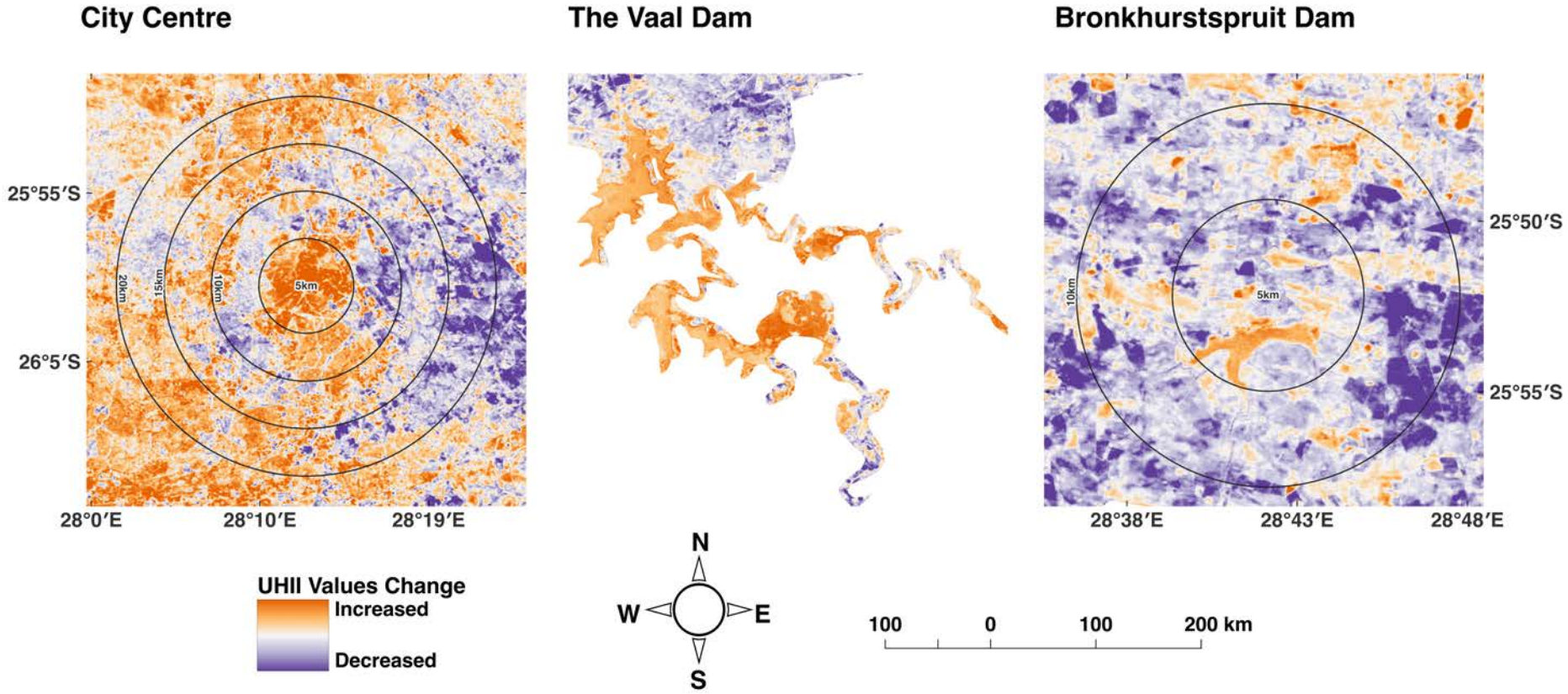



*Figure 4.1 4: Localised long-term change analysis of Urban Heat Island Intensity at a city-scale in Gauteng from 1984 to 2024.*

Table 4.1.3 depicts heatwave characteristics across Gauteng per metropolitan. A heatwave was calculated from the temperatures above the mean for a minimum of three consecutive days.

In 40 years (from 1984 to 2024), Gauteng has had ~36 heatwave events with the average heatwave duration of ~ 3 days. The fewest heatwaves are observed mostly in Sedibeng. The average temperature is increasing, which increases the threshold for heatwaves. In addition, the average duration of heatwaves in the area has increased from ~ 3 to ~ 6 days durations with high frequency reaching 5 for the West Rand in 2024. The lack of heatwave trends across the region over time is similar to Marghidan et al (2023), a study in Mozambique that displayed Tete and Nampula as having no significant trends; however, the results record an increase in frequency for recent years. Additionally, similar results as this paper were observed by Marghidan et al (2023) for the year 2015, of extreme heatwave conditions and frequency across Gauteng. Akin to Fendoung et al (2024) in the analysis of Kribi, Cameroon, our study area is also experiencing water body losses, increased impervious surfaces, and corresponding rises in surface and air temperatures—characteristics of an intensifying Urban Heat Island effect. This demonstrates that as precipitation decreases, surface water reduces, while maximum air temperatures increase. Further, demonstrates the impact and interconnectedness of the variables. Moreover, recent years have seen heatwaves with high frequency and severity.

*Table 4.1 3: Analysis of Heatwave Characteristics in Gauteng*

| Metropolitan | Year | Frequency | Duration | Severity | Intensity | Scale |
|---|---|---|---|---|---|---|
| West Rand | 1984 | 1 | 5 | 7 | 4.3 | 3 |
| No Heatwave Metro | 1989 | 0 | 0 | 0 | 0 | 0 |
| No Heatwave Metro | 1994 | 0 | 0 | 0 | 0 | 0 |
| Tshwane | 1999 | 1 | 3 | 3 | 1.5 | 2 |
| West Rand | 1999 | 1 | 3 | 3 | 1.6 | 2 |
| City of Johannesburg | 1999 | 1 | 3 | 1 | 0.5 | 1 |
| Ekurhuleni | 1999 | 1 | 3 | 1 | 0.5 | 1 |
| Tshwane | 2004 | 1 | 5 | 3 | 0.8 | 2 |
| City of Johannesburg | 2004 | 1 | 3 | 1 | 0.4 | 1 |
| Ekurhuleni | 2004 | 1 | 3 | 1 | 0.4 | 1 |
| No Heatwave Metro | 2009 | 0 | 0 | 0 | 0 | 0 |
| No Heatwave Metro | 2014 | 0 | 0 | 0 | 0 | 0 |
| No Heatwave Metro | 2020 | 0 | 0 | 0 | 0 | 0 |
| City of Johannesburg | 2024 | 4 | 7 | 17 | 3.2 | 3 |
| Ekurhuleni | 2024 | 4 | 7 | 18 | 3.2 | 3 |
| Sedibeng | 2024 | 3 | 8 | 20 | 3.4 | 3 |
| Tshwane | 2024 | 3 | 5 | 17 | 4 | 3 |
| West Rand | 2024 | 5 | 5 | 11 | 3 | 3 |

## 4.2 Effects of Land Cover Types on Triggering Heatwaves and UHI

### 4.2.1 Land Use Land Cover Trend

In Figure 4.2.1, the temporal variation in land covers generated and the estimated changes in area and trends of each class are input into Tables 4.1.1 and 4.1.2. This province is categorised by vegetation land use classes, such as forested land (FL), shrubland (SL), grassland (GL) and cultivated (CL) land. Over time, there is a sporadic trend in areas classified as mining regions (MN) by the random forest classifier. The random forest classifier shows an increase in waterbodies over time; however, development is on the fringe of major waterbodies as seen on maps, with waterbodies being buffered by yellow (cultivated) and brown (built-up). Thus, the results display an increase in waterbodies, with 2014 having a more visible water trend. Similar findings were observed by Sintayehu & Mhangara (2023), that the random forest classifier for land use land cover classification displays an increase in water bodies. This shows that random forest is needed in conjunction with spatial indices to achieve optimum analysis. The increase

in cultivated land (CL) and steady mining percentage over the years corroborates the Gauteng City Region and Gauteng Department of Agriculture and Rural Development (2012). Moreover, urbanisation spreads outwards from city centres, encroaching upon neighbouring land uses, including natural areas and cultivated land, and mine areas. Thus, creating a buffer zone where land use is transitioning. This result is similar to Gauteng City Region article (2015) results on urban expansion in Gauteng between 1990 and 2013, which appears as fringes around older settlement layouts (Nhamo et al., 2021). Therefore, the land use land cover maps depict the expected pattern of urban growth according to literature (Nhamo et al., 2021). Moreover, recent empirical studies in southern Sri Lanka (Wijesinghe et al., 2025) observe a growing city declining in maximum NDVI values over time, increasing Normalised Difference Built-Up Index (built-up areas), and decreasing water presence and content (low NDWI values). These changes corresponded with higher land surface temperatures and heightened UHI intensity (Wijesinghe et al., 2025).

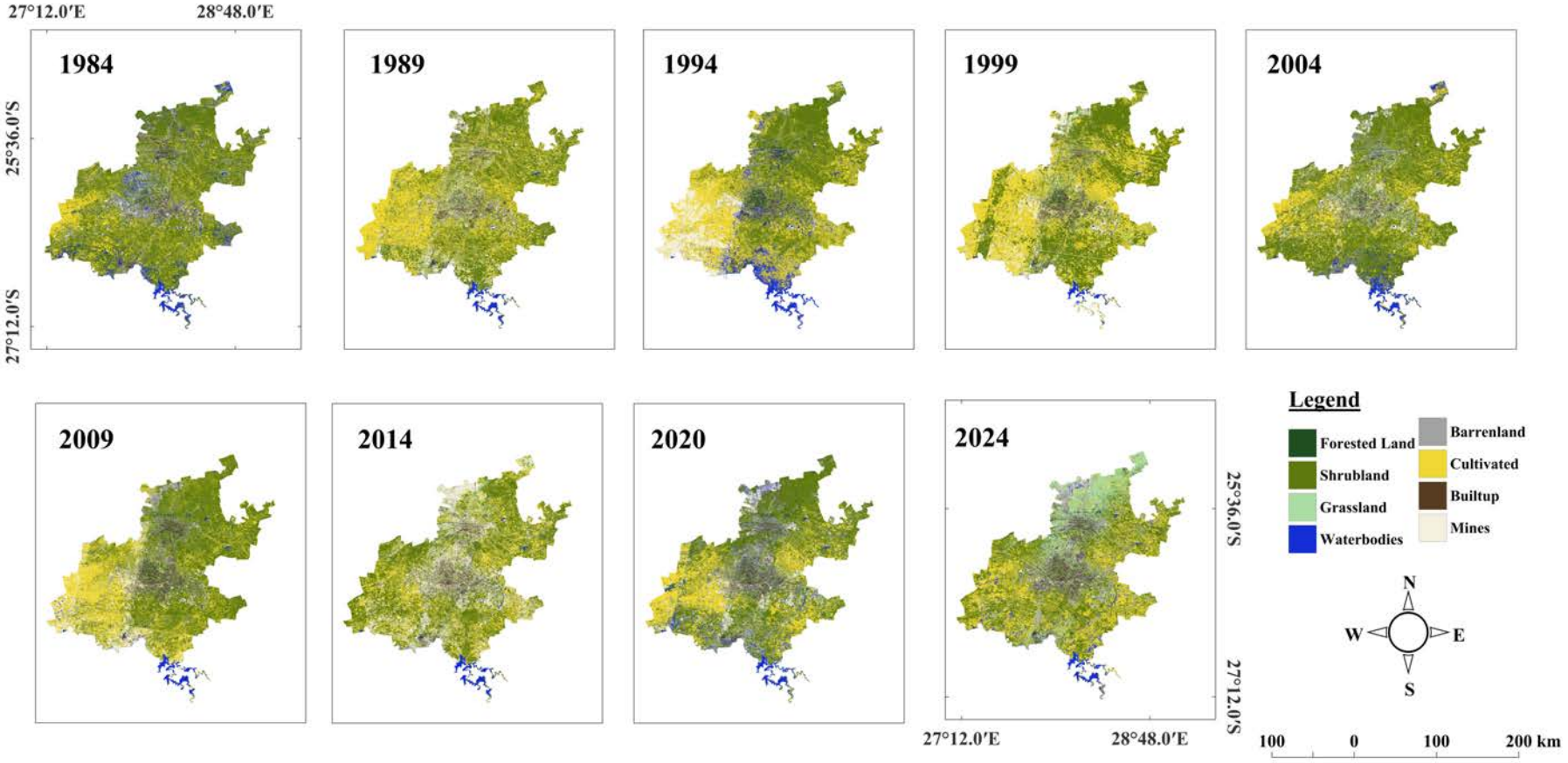



*Figure 4.2. 1: The map above displays the spatiotemporal variation of Land Use in Gauteng*

Table 4.2.1 shows changes in area and area percentages per land use class over time. There is a trend of increasing water bodies over time, while built-up areas and barren land have seen an increase but stagnation in recent years. Additionally, the table states a decrease in vegetation such as cultivated land (CL) and grassland (GL) over time, similar to Munyati & Drummond (2020) and Nhamo et al. (2021), noticing an increase in urban green space in Gauteng. Additionally, Fendoung et al (2024) corroborate the insights that there is a significant correlation between surface temperature and land cover change. In earlier years, before the 2000s, shrubland (SL) was dominant at an average of 35%, while built-up was an average of 12%. However, from the 2000s onwards, recent trends have observed a stagnation in built-up areas and an increase in shrubland land, while forestland and shrubland are increasing in recent times. Furthermore, cultivated (CL) grows gradually in the province over time, creeping into urban regions; however, barren land (BL) is usually noticed as a buffer to built-up areas according to Figure 4.2.1. The extent of surface water (WB) and forestland (FL) increased by 145km2 and 649km2, respectively. This study observes that during the 40 years, cultivated (CL), grassland (GL) and mines increased in size by 4152km2, 919km2 and 30km2, respectively. The presence of diverse and dense vegetation in Gauteng was strongly affecting the classification of barren land, shrub land (which includes bushland) and built-up areas. Built-up regions in richer suburbs were littered with dense forested areas and numerous gardens or cultivated areas (urban farm areas like Krugersdorp and Roodepoort). The overall change from 1984 to 2024 is: the land covers that reduced are shrubland by 25%, barren land by 5%, built-up by 2% and land covers that increased over time are forested land by 3%, grassland by 5%, cultivated land by 22% and mines by 1%. Although the Random Forest-generated LULC maps indicate spatial expansion of certain land cover classes, the magnitude and spatial configuration of mapped change are not directly comparable to on-ground expansion patterns. Even minor misclassification may result in exaggerated transitions when maps are compared across time. This

reflects potential land cover trends rather than exact representations of real-world land transformation. Consequently, discrimination between green water, bare land, and sparsely vegetated grasslands remains challenging, particularly in heterogeneous landscapes.

*Table 4.2 1: Annual Land Use Land Cover Change Table from 1984 to 2024*

| LC | 1984 | | 1989 | | 1994 | | 1999 | | 2004 | | 2009 | | 2014 | | 2020 | | 2024 | |
|---|---|---|---|---|---|---|---|---|---|---|---|---|---|---|---|---|---|---|
| | Area in $km^2$ | % | Area in $km^2$ | % | Area in $km^2$ | % | Area in $km^2$ | % | Area in $km^2$ | % | Area in $km^2$ | % | Area in $km^2$ | % | Area in $km^2$ | % | Area in $km^2$ | % |
| FL | 472 | 3 | 399 | 2 | 865 | 5 | 402 | 2 | 764 | 4 | 776 | 4 | 456 | 2 | 769 | 4 | 549 | 3 |
| SL | 10222 | 55 | 7491 | 41 | 5997 | 32 | 6959 | 38 | 9203 | 50 | 7730 | 42 | 7373 | 40 | 7423 | 40 | 5719 | 31 |
| GL | 220 | 1 | 274 | 1 | 620 | 3 | 1005 | 5 | 601 | 3 | 454 | 2 | 705 | 4 | 628 | 3 | 2597 | 14 |
| WB | 361 | 2 | 83 | 0 | 178 | 1 | 265 | 1 | 273 | 1 | 1019 | 6 | 871 | 5 | 748 | 4 | 1039 | 6 |
| BL | 1474 | 8 | 360 | 2 | 1677 | 9 | 286 | 2 | 1120 | 6 | 420 | 2 | 426 | 2 | 1229 | 7 | 787 | 4 |
| CL | 3865 | 21 | 6621 | 36 | 6428 | 35 | 7293 | 39 | 4643 | 25 | 5162 | 28 | 4452 | 24 | 4309 | 23 | 5583 | 30 |
| MN | 768 | 4 | 683 | 4 | 554 | 3 | 710 | 4 | 498 | 3 | 973 | 5 | 829 | 4 | 781 | 4 | 1105 | 6 |
| BU | 1096 | 6 | 2568 | 14 | 2160 | 12 | 1558 | 8 | 1377 | 7 | 1943 | 11 | 3366 | 18 | 2590 | 14 | 1098 | 6 |
| Total $km^2$ | | 18478 | | | 18478 | | 18478 | | 18478 | | 18478 | | 18478 | | 18478 | | 18478 | |

Table 4.2.2 displays the land cover analysis and confusion metrics generated. This displays the accuracy and ease with which land use class was identified and corrected over the years, per image. Hence, each class performance for each year is tabulated against the confusion metric values. Overall accuracy was ~ 96%  while Kappa coefficients remained above 90% in general. However, the confusion matrix indicates comparatively

higher misclassification among waterbodies, grasslands, and barren land classes. This confusion is often attributed to spectral similarity in multispectral remote sensing data. These conditions include shallow water surfaces, turbidity, green water and acid mine drainage. Such water bodies often reflect characteristics similar to moist soil or sparse vegetation, leading to overlap with grassland and barren classes. Additionally, exposed sand, bare soil, and mining-affected areas share spectral likeness with dried grasslands. As a result, even robust machine learning classifiers such as Random Forest experience reduced distinction among these land cover types, despite overall high classification accuracy. Furthermore, the F-Scores (F-S) exceeded an average of ~86% for both built-up and water body classes. Similar results were obtained by authors who adapted this method (Kouassi et al., 2023). The water bodies were consistently strong in responses to detection, but sensors included shallow vegetation or turbid waters (acid mine drainage), while grassland and shrubland fluctuated over the whole period; however, they were still highly detectable for class association.

*Table 4.2 2: Land Use Cover Analysis Table using CA, PA, F-S, OA, and K- K-coefficient values from 1984 to 2024.*

| LC | 1984 | | | 1989 | | | 1994 | | | 1999 | | | 2004 | | | 2009 | | | 2014 | | | 2020 | | | 2024 | | |
|---|---|---|---|---|---|---|---|---|---|---|---|---|---|---|---|---|---|---|---|---|---|---|---|---|---|---|---|
| | CA% | PA% | F-S | CA% | PA% | F-S | CA% | PA% | F-S | CA% | PA% | F-S | CA% | PA% | F-S | CA% | PA% | F-S | CA% | PA% | F-S | CA% | PA% | F-S | CA% | PA% | F-S |
| FL | 78 | 83 | 80 | 76 | 73 | 74 | 78 | 74 | 76 | 68 | 75 | 71 | 80 | 82 | 81 | 73 | 87 | 79 | 69 | 71 | 70 | 73 | 85 | 78 | 78 | 77 | 77 |
| SL | 91 | 96 | 93 | 92 | 97 | 94 | 93 | 95 | 94 | 98 | 98 | 98 | 95 | 97 | 96 | 95 | 98 | 97 | 94 | 98 | 96 | 97 | 98 | 98 | 96 | 98 | 97 |
| GL | 76 | 66 | 70 | 81 | 87 | 84 | 87 | 80 | 83 | 85 | 81 | 83 | 78 | 67 | 72 | 85 | 69 | 76 | 86 | 70 | 78 | 85 | 77 | 80 | 86 | 73 | 79 |
| WB | 100 | 100 | 100 | 100 | 100 | 100 | 100 | 100 | 100 | 100 | 100 | 100 | 100 | 100 | 100 | 100 | 100 | 100 | 100 | 100 | 100 | 100 | 100 | 100 | 100 | 100 | 100 |
| BL | 100 | 87 | 93 | 100 | 75 | 86 | 94 | 76 | 84 | 88 | 88 | 88 | 94 | 63 | 76 | 100 | 100 | 100 | 95 | 86 | 90 | 100 | 88 | 94 | 89 | 83 | 86 |
| CL | 93 | 87 | 90 | 93 | 90 | 92 | 91 | 91 | 91 | 95 | 98 | 97 | 95 | 94 | 94 | 95 | 93 | 94 | 96 | 92 | 94 | 97 | 97 | 97 | 95 | 96 | 96 |
| MN | 97 | 74 | 84 | 90 | 92 | 91 | 90 | 86 | 88 | 96 | 85 | 90 | 89 | 85 | 87 | 97 | 85 | 91 | 94 | 91 | 93 | 96 | 88 | 92 | 92 | 88 | 90 |
| BU | 98 | 99 | 98 | 100 | 97 | 98 | 100 | 100 | 100 | 99 | 99 | 99 | 99 | 99 | 99 | 99 | 99 | 99 | 98 | 99 | 98 | 98 | 99 | 99 | 99 | 100 | 99 |
| OA% | | 98 | | | 98 | | | 98 | | | 99 | | | 98 | | | 99 | | | 98 | | | 99 | | | | 99 |
| K% | | 95 | | | 96 | | | 96 | | | 98 | | | 97 | | | 97 | | | 97 | | | 98 | | | | 97 |

## 4.2.2 Overview of Vegetation

Figure 4.2.2 depicts NDVI spatio-temporally over Gauteng over 40 years. NDVI is an indicator of vegetation in an area – the abundance or lack thereof. The average values of the NDVI map in Gauteng illustrate the province as having good vegetation health index. NDVI, according to the map (figure 4.2.2), is increasing. City centres have a consistent negative NDVI value spatio-temporally. While peri-urban regions are shown to have an increase in vegetation presence, as the yellow-green pixels increase. Li et al. (2024) state that anthropogenic activities, such as urbanisation, cause variability in interannual NDVI values. Figure 4.2.2demonstrates vegetation stress and decline south-east of the centre, while the northern and southwestern regions of the province increase in NDVI values. Moreover, NDVI values are typically low in city centres due to urban characteristics such as asphalt and other impervious materials. Spatial patterns show dense yellow and red pixels (indicative of low vegetation) concentrated in urban cores, surrounded by greener, vegetation-rich areas. In recent years, NDVI has increased in this region, although this growth is often associated with human-managed landscapes rather than natural ecosystem recovery. This study, like others, found a weak negative correlation between LST and NDVI (r = - 0.29). Other studies have reported a stronger negative correlation (r = – 0.32) with temperature in the designated research area (Opiyo et al., 2025). The modest strength of these relationships indicates that additional and non-climatic drivers also play a significant role in shaping vegetation health within urban environments. Additionally, in Tamil Nadu, India (2014 to 2023), for example, strong spatial variability was observed with some districts showing strong negative correlation with land surface temperature while others had weaker relationships, suggesting that terrain, vegetation type, and rainfall patterns mediate how extreme temperatures affect vegetation and water (Janarth *et al.*, 2024).

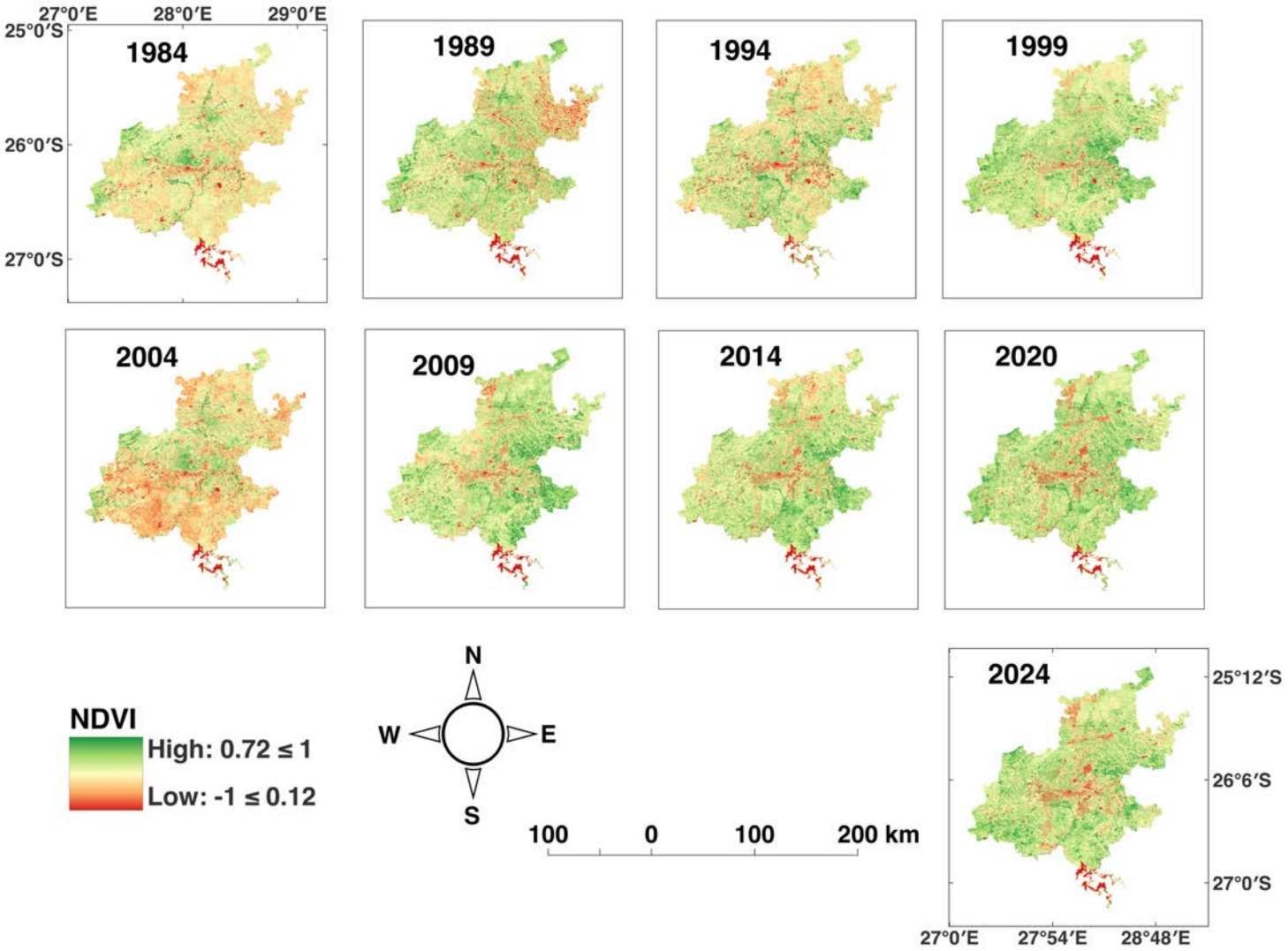



*Figure 4.2. 2: Spatiotemporal variation of NDVI in Gauteng.*

Figure 4.2.3 is the NDVI at a city scale. The NDVI values are low due to the concentration of urban features in the map (Figure 4.2.3). There is a mix of NDVI values, further indicating a difference in land planning. However, NDVI at a city scale depicts the lowest increase in city centres (+0.03) while Bronkhurstspruit Dam and the Vaal show an increase in NDVI by +0.23 and +0.20, respectively, over 40 years. Furthermore, city centres generally remain vegetation-scarce, whereas suburban areas—with leafy trees, planted gardens, and lawns—tend to display higher NDVI values. At a city scale, the 5km demonstrates a lack of healthy vegetation. At all distances, the western areas hold low NDVI values. However, the northern and eastern regions have a strong detection in NDVI values, suggesting more vegetation in cultivated expansion. Most of the strong NDVI values come from shrublands, cultivated lands and botanical gardens (protected green spaces) in cities. Moreover, the development of estates such as golf courses, large gardens, and irrigated urban-agricultural plots has contributed to an increase in NDVI, particularly in affluent residential areas. It is important to note, however, that high NDVI does not necessarily reflect natural vegetation restoration; instead, it frequently represents managed urban vegetation sustained by human factors such as irrigation. Thus, planned development promotes an increase in vegetation through urban green space. While unplanned development contributes to barren land and excess concrete from settlement housing, reducing the green space in the area.

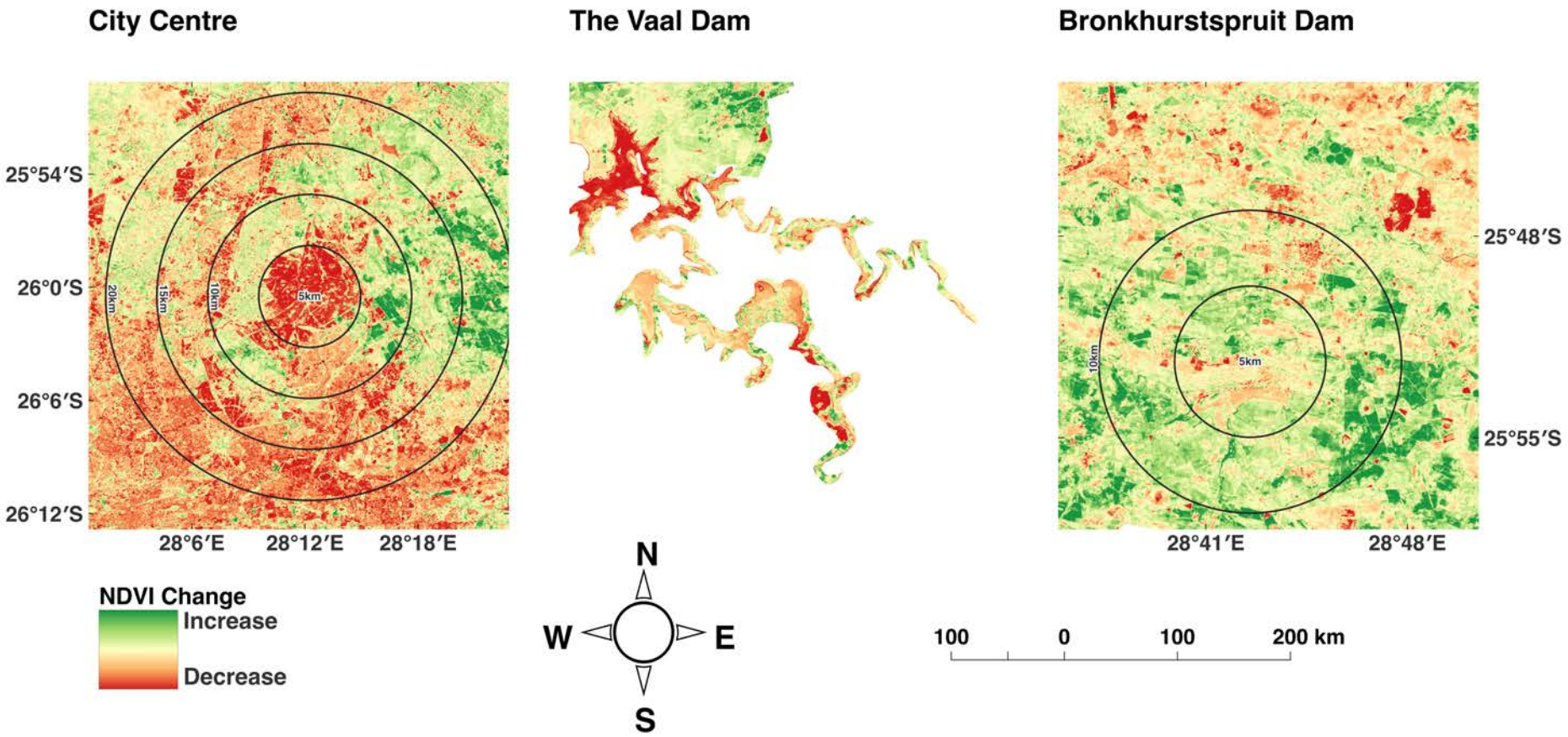



*Figure 4.2. 3: Localised long-term change analysis of NDVI at a city-scale in Gauteng from 1984 to 2024.*

## 4.3 Impacts of Land Cover Dynamics, Heatwaves, Urban Heat Islands on Surface Water Resources

In Figure 4.3.1, the MNDWI is about water presence in an area. Gauteng, according to the maps, is generally a dry region due to the consistent negative MNDWI values over time. However, in 1999, 2004 and 2009, the region noticed an increase in water presence stabilising the MNDWI. In contrast to regional maps, the radial analysis shows a localised trend of MNDWI values. Closer to urban centres, fewer water detections are alluding to urbanisation and the reduction of pervious surfaces from 1984 to 2024. However, 1984, 1994 and the 21st century indicate that the province is water scarce and littered with small waterbodies not great enough to supply the whole province or provide a mass cooling effect. Sintayehu & Mhangara (2023) also report a decreasing trend in MNDWI values in the region. Further, this corroborates with Mondal & Gavsker (2024) noticing city-level low mean MNDWI values in urbanised zones. The decrease in water presence further exacerbates UHI intensity and the effect of water cooling in the area. Therefore, Figure 4.3.1 demonstrates a decrease in surface water detection within urban regions, supporting urbanisation being detrimental to surface water (Wu & Zhang, 2019; Kolath & Egemose, 2023). Similar to this paper's results, research in Bloemfontein Watershed shows that despite some water bodies maintaining presence, overall water body coverage has been relatively stable yet low; meanwhile, land surface temperature has steadily increased over decades (Mshelia & Belle, 2024).

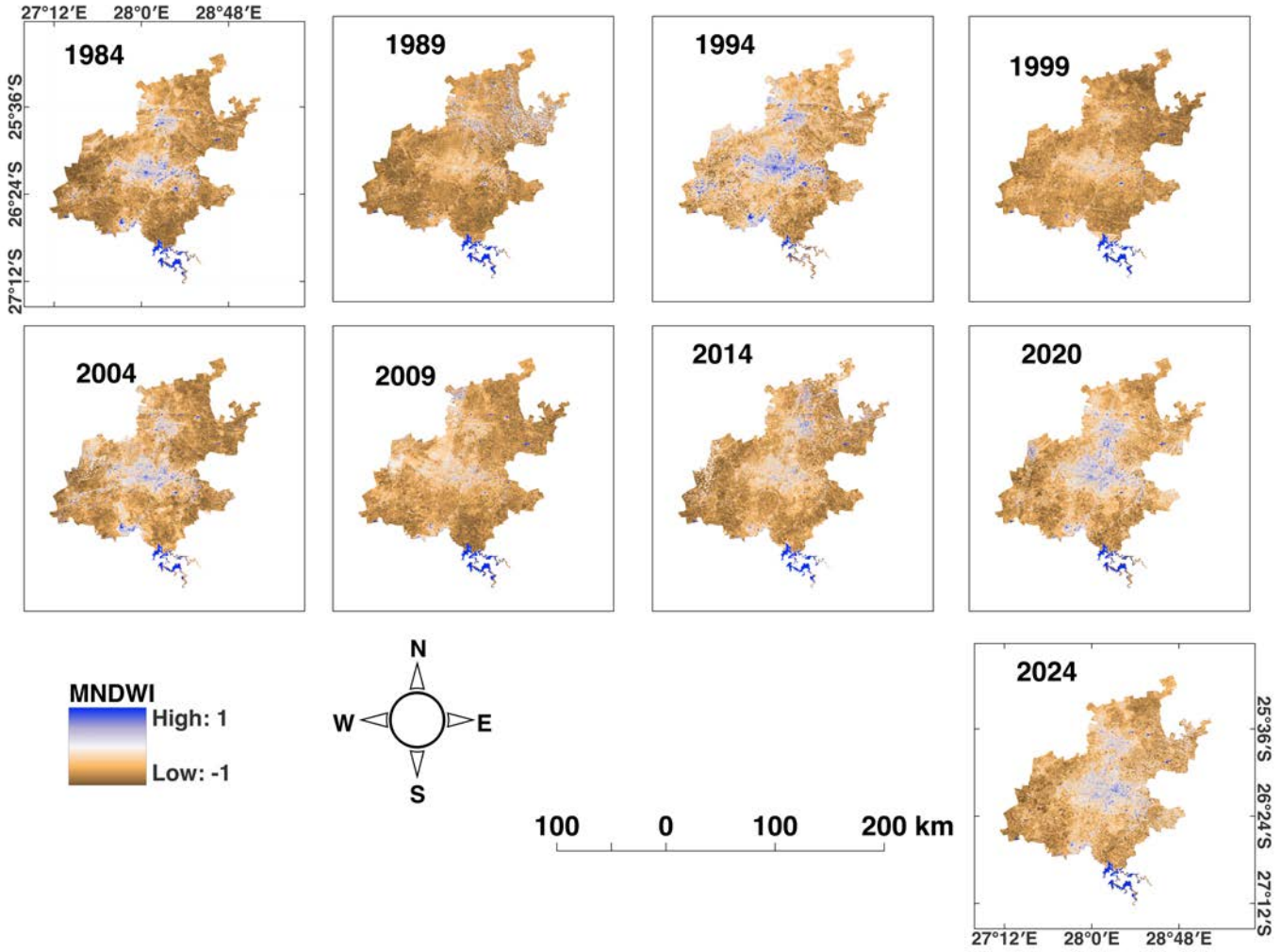



*Figure 4.3. 1The map above displays the spatiotemporal variation of MNDWI in Gauteng.*

Figure 4.3.2 displays MNDWI at a city scale. This allows for the local analysis of MNDWI from 1984 to 2024. MNDWI exhibits no significant trend according to the maps in Figure 4.3.2. Bronkhurstspruit Dam notices no change in MNDWI values over 40 years. While city centres and the Vaal observe a marginal increase of 0.06 and 0.01, respectively. However, further out, MNDWI values become weaker, especially in the western and southern regions beyond 10km. Central Gauteng hosts dense cities such as Johannesburg, which is water-scarce. The limited amount of surface water is observed in other papers (Zhang et al., 2025). Additionally, the maps show stress in both the Vaal and Bronkhurstspruit Dam with red and yellow pixels indicating that the water bodies are experiencing a decreasing trend in MNDWI values. For example, Bronkhurstspruit displays more yellow and red hues, indicating it is at more risk than the Vaal, as certain areas within the Bronkhurstspruit Dam are decreasing over time. City centres show a dominant green shade, demonstrating no change, as water in these areas is low, there is no increase in water presence within the 40 years of this study. South-east of the city centres show a mixed trend of both increase and decrease, possibly relating to cultivation in those areas and the change or rotation of farming zones.

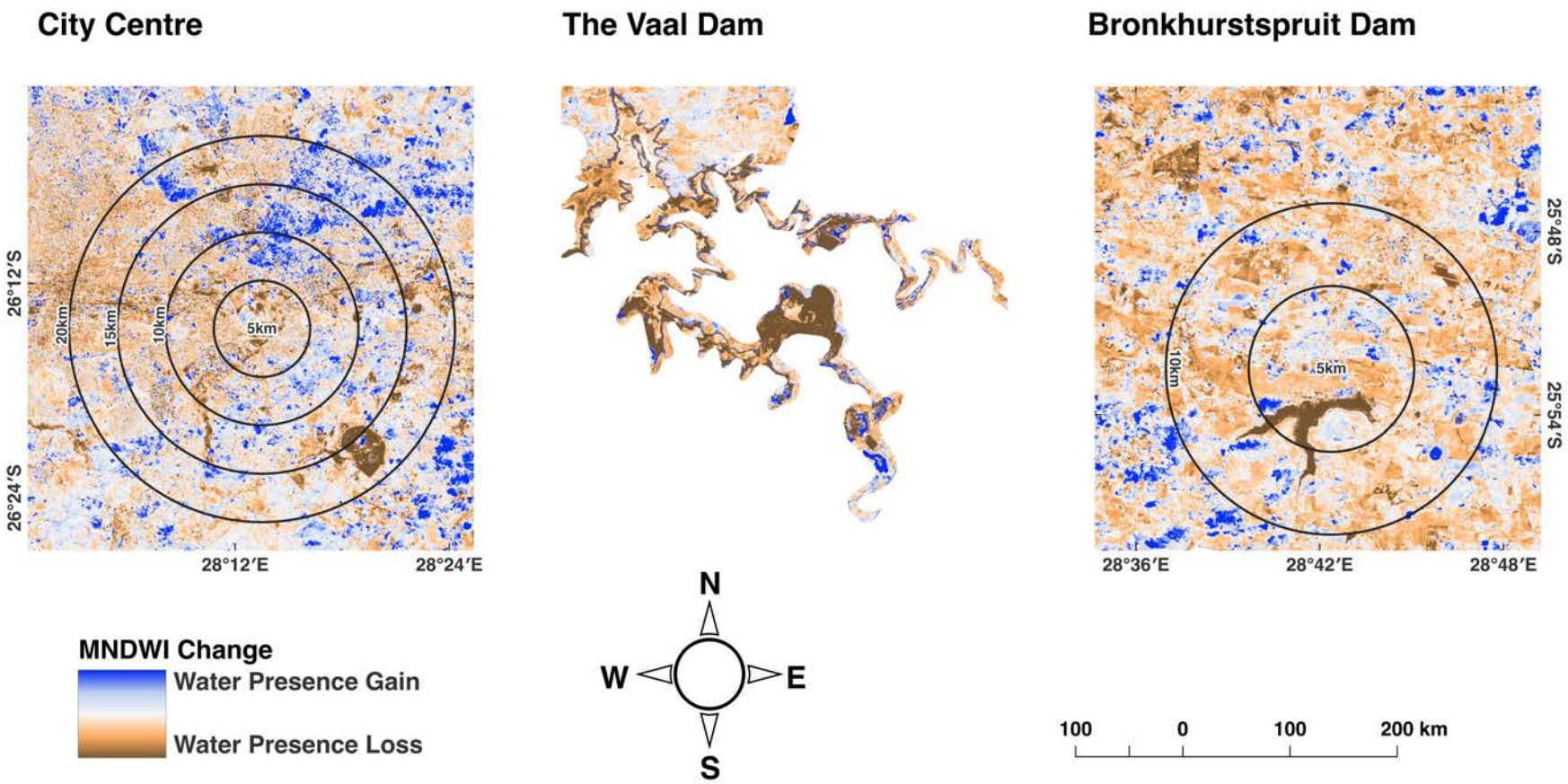



*Figure 4.3. 2: The map above displays a localised long-term change analysis of MNDWI at a city-scale in Gauteng.*

WRI results (figure 4.3.3), designed to capture surface water distribution – water-body identification, range from ~ 0 to 3. The maps above show that certain water bodies decrease in size annually, with a spatial increase or decrease in values. The majority of the waterbodies are on the eastern and southern side of the province, which have maintained consistency of high WRI values due to these bodies being protected structures – the Bronkhorstspruit Dam, Vaal Dam and the Klipdrift Dam. Other natural bodies of water have depleted over time, as shown in the maps with fluctuating blue pixels. Moreover, there is a regional decrease of surface water bodies as the green pixels on the map increase slightly annually, creating a darker shaded map (2004, 2014 and 2024). The more greens (darker shades), the drier the province appears from the WRI index. Hence, the WRI demonstrates that Gauteng has scarce water content throughout the years. Strong (blue pixels) WRI values were mostly during 1984 – 1999. However, in recent years, from 2004, the province has been dominated by green and yellow pixels, indicating low average WRI values (low water content). Nonetheless, the radial maps below better demonstrate surface water bodies from 1984 to 2024 at the city level. The blue pixels indicating positive water detection have diminished, which lends support to Wu & Zhang (2019) and Kolath & Egemose (2023) in stating that land use changes such as urban stream burial and stormwater channelisation reduce surface water presence, exacerbating heat stress. Additionally, Hossain, Mahmud & Islam (2023) used similar methods to assess surface water, although at a city scale and noticed a decreasing trend in surface water for Dhaka city over 30 years.

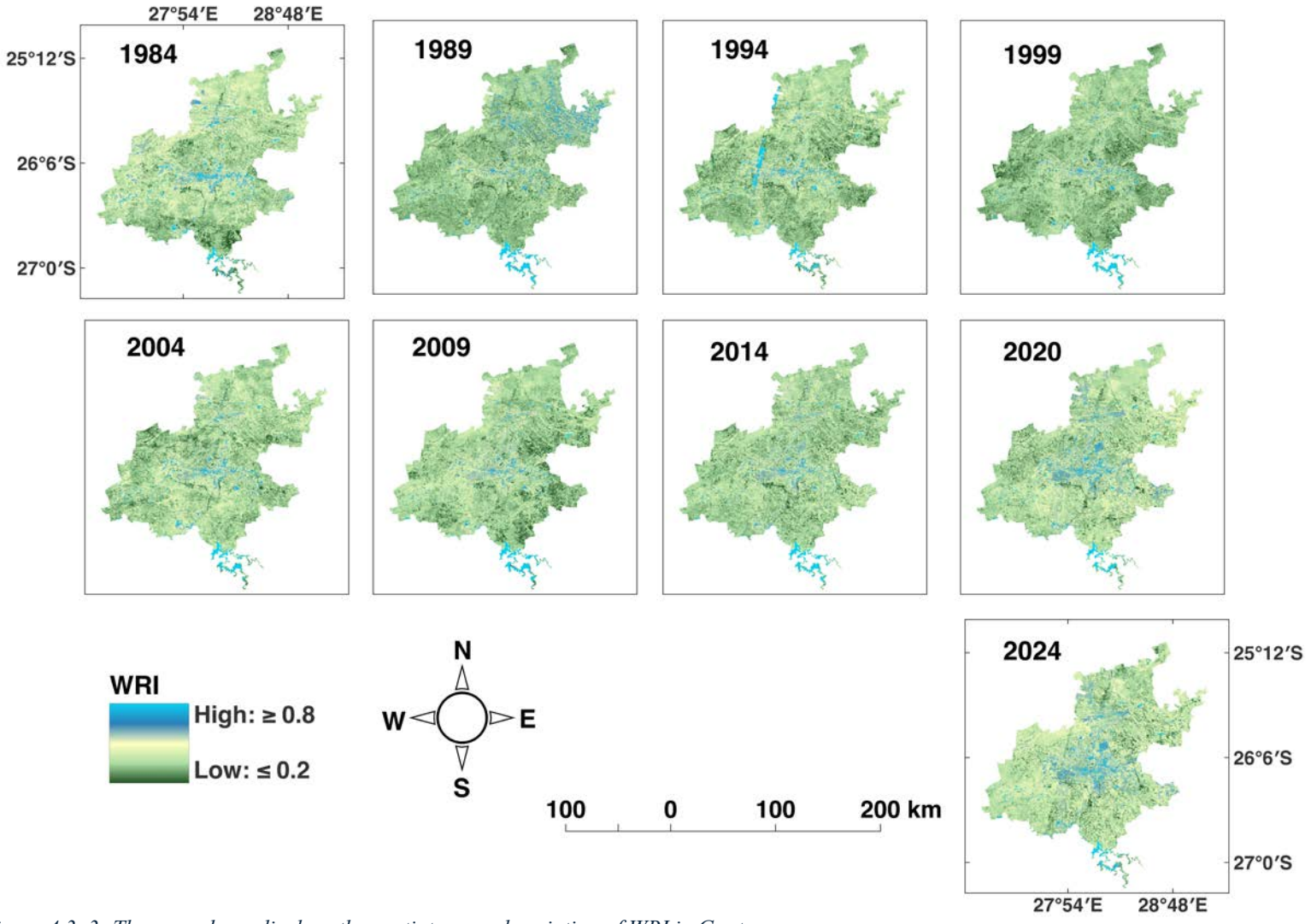



*Figure 4.3. 3: The map above displays the spatiotemporal variation of WRI in Gauteng.*

Figure 4.3.4 displays WRI at a city scale as a change over time. It depicts WRI values decreasing slightly with city centres having a mean increase of ~ + 0.16, while the Vaal and Bronkhurstspruit Dams both increase similarly over time with an average increase over 40 years of + 0.13 and +0.12, respectively. However, the overall trend for the Vaal and Bronkhurstspruit Dams is decreasing WRI values, as the map shows dark green over the water bodies, indicating a negative change. City centres in the maps (figure 4.3.4) display many dry areas with low WRI values. WRI shows low values through the distance of the city centres, and further outwards (north-east), there is an increase in WRI values. This corroborates that city centres have low water presence (yellow shades) and further out are buffered by vegetation or water sources, hinting at poor land planning. Hence, water presence is low, likely due to urban features that have low water retention properties and the deteriorating state of green space. Sintayehu & Mhangara (2023) highlight that water presence through MNDWI at a city-scale is decreasing in Johannesburg (an urban city region).

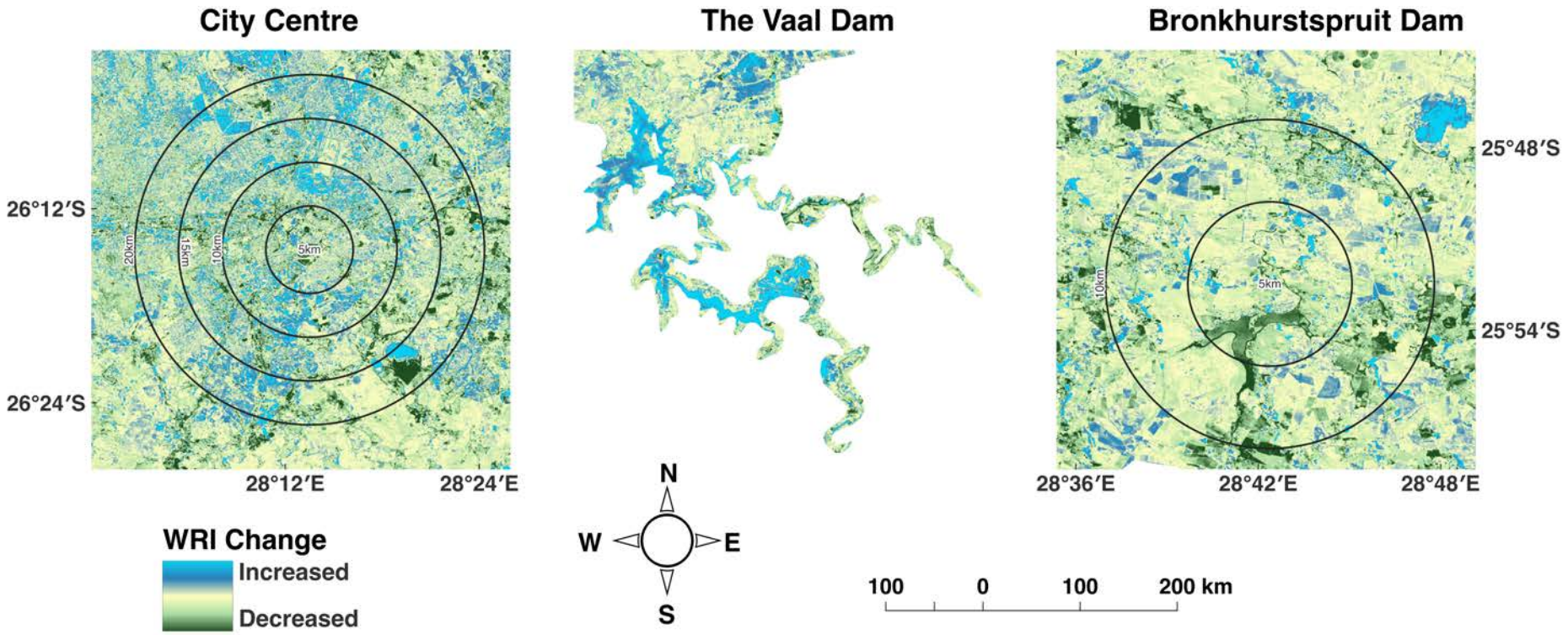



*Figure 4.3. 4: The map above displays a localised long-term change analysis of WRI at a city-scale in Gauteng.*

## 4.4 Vegetation and Climate Indices Correlation

Table 4.4.1 displays the Spearman correlation between Maximum air temperature (TMAX), Land surface temperature (LST), Normalised difference vegetation index (NDVI), Water ratio index (WRI), Modified normalised difference water index (MNDWI) and Precipitation (Precip) annually (from 1984 to 2024) in the Gauteng province. This demonstrates the effect each variable has on the other. LST and TMAX both have a negative correlation with the water variables. NDVI exhibited a strong negative correlation with WRI ($\rho = –0.69$, $p < 0.001$). This alludes to WRI, MNDWI and precipitation having a cooling effect on the surroundings, opposed to LST and TMAX warming the environment. Thus, an increase in WRI, MNDWI and precipitation values can mitigate and reduce high LST or UHI intensification in the region of Gauteng. These findings are corroborated by Dong et al.(2022), stating that the negative correlation between LST-MNDWI across a city-scale analysis of Berlin, Germany. This demonstrates that LST consistently drops as the water presence increases (Manjunath & Jagadeesh, 2024). However, the direct WRI–LST correlation papers are less common than MNDWI–LST, but WRI is repeatedly validated as a water index and covaries with MNDWI. Thus, numerous studies show that increases in water presence result in lower NDVI and LST, which can support the WRI cooling effect (Manjunath & Jagadeesh, 2024). Additionally, NDVI negatively correlates to LST ($\rho = –0.26$, $p < 0.001$). Moreover, consistent with earlier research, MNDWI and LST show a moderately negative correlation of $\rho = –0.40$, $p < 0.001$. This demonstrates that surface water bodies reduce surface heating due to their high heat capacity and evaporative cooling effects.

Similar to the results below, Mahdi et al. (2024) and Zhang et al. (2025) noticed that surface water indices increase with precipitation. Moreover, NDVI negatively correlates with MNDWI ($\rho = –0.39$, $p < 0.001$), indicating that areas with high water correspond to lower vegetation

cover. Moreover, in conjunction with the results, recent work in Western South Africa (1962 to 2022) used the Standard Precipitation and Evapotranspiration Index (SPEI) together with NDVI to show long-term declines in rainfall and rising temperature variability, leading to reduced vegetation density (Opiyo et al., 2025). Further, the high significance of the negative correlation between maximum air temperature and precipitation is observed in European regions on the western coast of the black sea (Vyshkvarkova & Sukhonos, 2022), further reinstating the relationships of these variables.

*Table 4.4. 1: The Statistical Relationship Among Vegetation, Water and Climate Indices*

| | NDVI | MNDWI | WRI | LST | PRECIP | TMAX |
|---|---|---|---|---|---|---|
| NDVI | 1 | | | | | |
| MNDWI | -0.39*** | 1 | | | | |
| WRI | -0.69*** | 0.53*** | 1 | | | |
| LST | -0.26*** | -0.40*** | 0.24*** | 1 | | |
| PRECIP | -0.03 | 0.13 | 0.01 | -0.16* | 1 | |
| TMAX | 0.06 | 0 | -0.26*** | 0.08 | -0.21** | 1 |

## 4.5 Trends of Climate, NDVI and Water Resources in Gauteng

The Mann-Kendall Analysis and Spearman correlation observed the interactions between climate, water and vegetation indices and land surface dynamics. The Mann–Kendall trend (Table 4.5.1) analysis revealed that precipitation ($p = 1.03 \times 10^{-8}$), maximum temperature ($p = 2.87 \times 10^{-11}$), NDVI ($p = 1.99 \times 10^{-15}$) and the Water Ratio Index (WRI) ($p = 1.11 \times 10^{-9}$) exhibited statistically significant monotonic trends over the study period, indicating strong and consistent directional changes in these variables at the provincial scale. Table 4.5.1 displays that there is an increasing trend of maximum temperature while there is a decreasing precipitation, which highlights climatic stress and change. Minimum temperature shows no trend overall within Gauteng. However, the maximum air temperature is on an increasing trend, which relates to global warming. Additionally, the Kendall analysis observed no trend from

land surface temperature within Gauteng, which correlates with recent studies (Chao et al., 2020), noticing temporal heterogeneity in land surface trends, with no significant increase or decrease in some urban settings over time. Furthermore, NDVI displays an increasing trend over time. This alludes to the expansion of urban green areas and the consistent protection of green spaces in Gauteng over the years. Similarly, in China, with the use of climate models and projections, NDVI reported a significant increase over the past two decades (Li et al., 2025). Lastly, the MNDWI displays no noticeable trend over time, indicating a consistent presence of water with no significant decreases or increases for the province over time. However, Sintayehu & Mhangara (2023) report decreases in MNDWI in the province. Additionally, in New Mexico, researchers applied the Modified Normalised Difference Water Index (MNDWI) to monitor surface water bodies across the Middle Rio Grande River Basin between 1994 and 2020 (Belhaj et al., 2022). The analysis revealed a striking decline of more than 66% in surface water extent over the study period (Belhaj et al., 2022). The water ratio index, according to the results, proves to be increasing in Gauteng, but at a city-scale, the WRI values decrease, as noticed in the long-term (1984 to 2024) radial maps of WRI.

*Table 4.5. 1: Long-term Vegetation, Water and Climate Trends*

| Variable | Trend | Tau | p-value | Slope | Interpretation |
|---|---|---|---|---|---|
| Annual Precipitation | Decreasing | -0.18 | $1.03 \times 10^{-8}$) | -0.00084 mm/day/yr | Statistically significant decreasing trend in precipitation |
| Maximum Air Temperature | Increasing | 0.21 | $2.87 \times 10^{-11}$ | 0.00477 °C/year | Statistically significant warming trend |
| Land Surface Temperature | No trend | 0.04 | 0.389 | 0.00797 °C/year | Slight warming, but not statistically significant |
| NDVI | Increasing | 0.39 | $1.99 \times 10^{-15}$ | 0.00030/ year | Strong, significant increase in vegetation |
| Water Ratio Index | Decreasing | -0.30 | $1.11 \times 10^{-9}$ | -0.00024/ year | Strong, significant decrease in water bodies |
| MNDWI | No trend | -0.009 | 0.847 | $-0.142\times 10^{-3}$ / year | Slight decrease in surface water presence. |

# CHAPTER FIVE: CONCLUSION AND FUTURE PROSPECTS

## 5.1 Summary of Key Findings

In conclusion, this paper provides insights into the complex burden of urban heating on surface water resources. The challenges are depicted in the results and literature comparing global studies with this paper and other local research, indicative of the extremes in urban heat islands and land surface temperatures. Gauteng, as a province, exhibits similar trends to global studies, indicating developing regions are facing urban heating due to a lack of green space, land use, land cover change and decreasing water resources.

Key insights from this paper centre on three objectives. First is the analysis of heatwaves and urban heat island intensification over Gauteng from 1984 to 2024. Second, the effects that land use, land cover and vegetation (through normalised difference vegetation index) have on triggering land surface temperatures. Third, a collective impact of land use, land cover, heatwaves and land surface temperatures has on surface water through analysing water indices such as water ratio index and modified normalised difference water index.

Further, this study investigates the interactions between maximum air temperatures, land surface temperatures (LST), vegetation health measured through the Normalized Difference Vegetation Index (NDVI), water-related indices such as the Water Ratio Index (WRI) and the Modified Normalized Difference Water Index (MNDWI), and Land Use/Land Cover (LULC) dynamics in Gauteng Province from 1984 to 2024. By integrating NASA POWER climate data, satellite imagery and applying a Random Forest classifier for LULC, the research provides a comprehensive assessment of urban–environmental relationships. This paper highlights a climatic change, indicating that an increase in maximum temperatures increases

evapotranspiration, thus, coupled with decreased precipitation, inevitably decreases surface water availability, as observed in WRI values decreasing. Further, the central part of Gauteng notices constant temperature highs from UHI intensity, land surface temperatures, and heatwaves in major cities, indicating a warming trend from urban centres. Thus, the results indicate a concentrated approach to development for the Gauteng province. Therefore, major metropolises are at a higher risk of urban warming extremes due to poor urban planning, lack of green and blue space planning, as well as continual urban sprawl. Additionally, the province struggles with water resource availability and the increased heating burdens this issue further. Moreover, heatwaves in Gauteng have increased gradually over the years, with more recent years being at extreme levels. The average frequency was ~3 from 1984 to 2009; however, from 2014 to 2024, the average frequency is ~4. This is evident in Table 4.1.3, analysing heatwaves. The results reveal a significant rise in daily maximum air temperatures, coupled with declining precipitation, while LST exhibited no clear long-term trend. Gauteng is a vegetation-dense province, and the results demonstrated an increase in NDVI overall, suggesting improved greenness despite adverse climatic conditions, demonstrating the complexity of vegetation in regard to climate dependency. Moreover, WRI, like precipitation, displayed a declining trend, highlighting water stress and scarcity in Gauteng. Even though MNDWI displays no visible trend, recent research applying MNDWI at a city scale in Johannesburg reports a decreasing trend. Moreover, the trends of water resources in the paper are juxtaposed with the random forest LULC detected. The mapping of LULC detected an overall increase in water bodies.

## 5.2. Synthesis of Urban Heat Implications on Surface Water Research

These findings underscore the importance of combining remote sensing indices and robust classification techniques with ground truthing in future research. Ground truthing is important regardless of time and expenses in areas like Gauteng with high cloud cover and minimal

research compared to Western nations. Although this research mainly examined environmental causes of urban heat, its results have wider contributions for social and economic aspects of heat risk, including financial expenditures related to shifting to green and blue infrastructure, energy-efficient cooling and urban resilience. The results may aid socio-economic evaluations of environmental injustice and inequalities in urban heat exposure, thus possibly contributing to initiatives and interventions. Furthermore, the study adds to current research in water research, particularly in remote sensing uses when identifying and classifying water bodies, including observing the need for the differentiation between blue, brown and green waters. As this contributes to present problems and becomes crucial to ascertain whether the variations in extent and nature of water bodies are a result of climate-related warming. Nonetheless, this raises questions of climate warming contributing to more eutrophication, sedimentation or reducing water availability. Therefore, maintaining reflexive and holistic approaches in water research is crucial for advancing climate resilience, especially in developing cities where urban expansion and climate vulnerability intersect most acutely. Moreover, from a policy standpoint, this paper's integrated analysis emphasises the need for adaptive vegetation and water governance and sustainable land use planning. This approach will aid in the mitigation of heat risks and declining water availability in South Africa's urbanising provinces like Gauteng. Mitigating climate change in Gauteng needs region-specific data and results to form region-specific strategies and risk plans. Thus, intra-urban studies including minor metropolises (West Rand and Sedibeng) using remote sensing (multi-indices) over longer periods are essential for Gauteng in addressing urban climate and sustainability.

## 5.3. Recommendations and Future Research Directions

Critical additions can be made to enhance this research for improved urban heat mitigation and analysis. The findings build on the understanding of urban heat and its implications for surface

water in Gauteng. Therefore, future research should integrate a more comprehensive set of variables and advanced analytical techniques. This includes adding hydrothermal dynamics, which analyses the heat transfer process between urban surfaces and surface water bodies that affect the local climate gradually. Furthermore, the addition of more complex machine learning or deep learning algorithms can uncover complex, nonlinear relationships between land use changes, surface temperatures, and water quality parameters. This approach would enhance the robustness and scalability of future assessments. Another important addition to future studies is the interaction between groundwater and surface water systems, particularly under conditions of urban heat stress. Understanding this is essential for water resource management in the age of climate variability. Hence, incorporating groundwater temperature monitoring and hydrogeological modelling would provide valuable insights into subsurface thermal regimes and their influence on surface hydrology.

Lastly, the integration of climate models and climate projections allows for long-term trend prediction and analysis of how environmental systems may respond to compounded stressors. Therefore, the additions will provide a more holistic and predictive framework for understanding urban heat implications on water resources. This will further provide a location-specific analysis, enriching future planning and management.

# REFERENCES


Abdullah, S., Adnan, M. S. G., Barua, D., Murshed, M. M., Kabir, Z., Chowdhury, M. B. H., Hassan, Q. K., & Dewan, A. (2022). Urban green and blue space changes: A spatiotemporal evaluation of impacts on ecosystem service value in Bangladesh. *Ecological Informatics*, *70*, 101730.

Adedayo, A. A. (2015). Analysis of impervious surfaces and surface temperature over the Tshwane metropolitan using in situ and remotely sensed data. University of Pretoria (South Africa).

Ademe, D., Zaitchik, B. F., Tesfaye, K., Simane, B., Alemayehu, G., & Adgo, E. (2020). Climate trends and variability at adaptation scale: Patterns and perceptions in an agricultural region of the Ethiopian Highlands. *Weather and Climate Extremes*, *29*, 100263.

Afuye, G. A., Kalumba, A. M., Owolabi, S. T., Thamaga, K. H., Ndou, N., Sibandze, P., & Orimoloye, I. R. (2024). Analysing spatiotemporal variations and dynamics of vegetation over the Amathole district municipality in South Africa. *Environment, Development and Sustainability,* 1-26. https://doi.org/10.1007/s10668-024-05221-0

Ahmad, M., Saqib, M., Ahmad, S. N., Jamal, S., & Mir, A. Y. (2025). Normalised difference spectral indices and urban land cover as indicators of urban heat island effect: a case study of Patna Municipal Corporation. *Geology, Ecology, and Landscapes*, 1-21. https://doi.org/10.1080/24749508.2025.2451479

Akomolafe, G. F., & Rosazlina, R. (2022). Land use and land cover changes influence the land surface temperature and vegetation in Penang Island, Peninsular Malaysia. *Scientific Reports*, 12(1), 21250.

Albut, S. (2024). Land surface temperature (LST) calculation processes with Landsat 8. *Pioneer and Innovative Studies in Engineering*, 133–146.
Angel, S. (2023). Urban expansion: theory, evidence and practice. *Buildings and Cities*, *4*(1), 124–138.

Astell-Burt, T., Feng, X., Mavoa, S., Badland, H. M., & Giles-Corti, B. (2014). Do low-income neighbourhoods have the least green space? A cross-sectional study of Australia's most populous cities. *BMC Public Health*, *14*(1), 292. https://doi.org/10.1186/1471-2458-14-292

Azizi, S., & Azizi, T. (2024). Urban Climate Dynamics: Analysing the impact of green cover and air pollution on Land Surface Temperature—A Comparative Study across Chicago, San Francisco, and Phoenix, USA. *Atmosphere*, *15*(8), 917.
Barriopedro, D., García-Herrera, R., Ordóñez, C., Miralles, D. G., & Salcedo-Sanz, S. (2023). Heat waves: physical understanding and scientific challenges. *Reviews of Geophysics*, *61*(2). https://doi.org/10.1029/2022rg000780

Belgiu, M., & Drăguţ, L. (2016). Random forest in remote sensing: A review of applications and future directions. *ISPRS Journal of Photogrammetry and Remote Sensing*, *114*, 24–31. https://doi.org/10.1016/j.isprsjprs.2016.01.011

Belhaj, O., Mubako, S. T., Tweedie, C. E., Aldouri, R. E., Hargrove, W. L., & Hadia, E. A. (2022). Determination of Change in Surface Waterbodies in The Middle Rio Grande Basin by Modified Normalised Difference Water Index (MNDWI) 1994-2020. *Libyan Journal of Ecological & Environmental Sciences and Technology*, *4*(2), 67–80.

Bessinger, M., Lück-Vogel, M., Skowno, A., Peterson, A. & Conrad, F. (2022). Landsat-8-based coastal ecosystem mapping in South Africa using random forest classification in Google Earth Engine. *South African Journal of Botany*, 150(2), 928-939.

Bhamjee, M., Debary, H., Gaffoor, Z., Govindasamy, T., Mahlasi, C., Fiaz, M., & Kuehnert, J. (2024). Detection and Characterisation of Urban Heat Islands with Machine Learning. *IEEE International Geoscience and Remote Sensing Symposium*, 1693-1699. DOI: 10.1109/IGARSS53475.2024.10641750.

Bhatti, U. A., Bhatti, M. A., Tang, H., Syam, Awwad, E. M., Sharaf, M., & Ghadi, Y. Y. (2023). Global production patterns: Understanding the relationship between greenhouse gas emissions, agricultural greening and climate variability. *Environmental Research*, 245, 118049. DOI: 10.1016/j.envres.2023.118049

Bhungeni, O., Ramjatan, A., & Gebreslasie, M. (2024). Evaluating machine-learning algorithms for mapping LULC of the uMngeni catchment area, KwaZulu-Natal. *Remote Sensing*, 16(12), 2219.

Bille, R. A., Jensen, K. E., & Buitenwerf, R. (2023). Global patterns in urban green space are strongly linked to human development and population density. *Urban Forestry & Urban Greening*, *86*, 127980. https://doi.org/10.1016/j.ufug.2023.127980

Bonetti, S., Sutanudjaja, E. H., Mabhaudhi, T., Slotow, R., & Dalin, C. (2022). Climate change impacts on the water sustainability of South African crop production. *Environmental Research Letters*, 17(8), 84017. https://doi.org/10.1088/1748-9326/ac80cf

Braunisch, V., Coppes, J., Arlettaz, R., Suchant, R., Schmid, H., & Bollmann, K. (2013). Selecting from correlated climate variables: a major source of uncertainty for predicting species distributions under climate change. *Ecography*, 36(9), 971–983.

Chaemiso, S. E., Kartha, S. A., & Pingale, S. M. (2021). Effect of land use/land cover changes on surface water availability in the Omo-Gibe basin, Ethiopia. *Hydrological Sciences Journal*, 66(13), 1936–1962.

Chakwizira, J., Bikam, P., & Adeboyejo, T. A. (2018). Restructuring the Gauteng City region in South Africa: Is a transportation solution the answer? In An Overview of Urban and Regional Planning, IntechOpen eBooks. https://www.intechopen.com/chapters/63405 [Accessed 18 July 2025]

Chao, Z., Wang, L., Che, M., & Hou, S. (2020). Effects of different urbanisation levels on land surface temperature change: Taking Tokyo and Shanghai for example. *Remote Sensing,* 12(12), 2022.

Chawanda, C. J., Nkwasa, A., Thiery, W., & Van Griensven, A. (2024). Combined impacts of climate and land-use change on future water resources in Africa. *Hydrology and Earth System Sciences*, *28*(1), 117–138.

Chen, M., Sun, Z., Newell, B. H., Corr, C. A., & Gao, W. (2020). Missing pixel reconstruction on Landsat 8 analysis-ready data land surface temperature image patches using source-augmented partial convolution. *Remote Sensing*, 12(19), 3143.

Chen, W., Hu, C., Liu, L., Zhang, J., Wang, K., & Liu, S. (2022). Characteristics of built-up land change in resource-based cities and their impact on land surface temperature—Taking Wu'an as an example. *Ecological Informatics*, *68*, 101582. https://doi.org/10.1016/j.ecoinf.2022.101582

Cheval, S., Amihăesei, V., Chitu, Z., Dumitrescu, A., Falcescu, V., Irașoc, A., Micu, D. M., Mihulet, E., Ontel, I., Paraschiv, M., & Tudose, N. C. (2024). A systematic review of urban heat island and heat waves research (1991–2022). *Climate Risk Management*, *44*, 100603. https://doi.org/10.1016/j.crm.2024.100603

Chowdhury, M. S. (2023). Comparison of accuracy and reliability of random forest, support vector machine, artificial neural network and maximum likelihood method in land use/cover classification of urban setting. *Environmental Challenges*, *14*, 100800. https://doi.org/10.1016/j.envc.2023.100800

Council for Scientific and Industrial Research (CSIR). (2019). GreenBook Adapting settlements for the future. *CSIR*. https://greenbook.co.za/ [Accessed 18 July 2025]

D'Ercole, R., Casella, D., Panegrossi, G., & Sanò, P. (2024). A high temporal resolution NDVI time series to monitor drought events in the Horn of Africa. *International Journal of Applied Earth Observation and Geoinformation*, *135*, 104264.

Das, S., Choudhury, M. R., Chatterjee, B., Das, P., Bagri, S., Paul, D., Bera, M., & Dutta, S. (2024). Unravelling the urban climate crisis: Exploring the nexus of urbanization, climate change, and their impacts on the environment and human well-being – A global perspective. *AIMS Public Health*, *11*(3), 963–1001.

De Almeida, C. R., Garcia, N., Campos, J. C., Alírio, J., Arenas-Castro, S., Gonçalves, A., & Teodoro, A. C. (2023). Time-series analyses of land surface temperature changes with Google Earth Engine in a mountainous region. *Heliyon*, 9(8). DOI: 10.1016/j.heliyon.2023.e18846

De Almeida, C. R., Teodoro, A. C., & Gonçalves, A. (2021). Study of the Urban Heat Island (UHI) Using Remote Sensing Data/Techniques: A Systematic Review. *Environments*, 8(10), 105.

De La Iglesia Martinez, A., & Labib, S. (2022). Demystifying normalized difference vegetation index (NDVI) for greenness exposure assessments and policy interventions in urban greening. *Environmental Research*, *220*, 115155. https://doi.org/10.1016/j.envres.2022.115155

Debnath, M., Poddar, I., Saha, A., Islam, N., & Roy, R. (2025). Analysis of land surface temperature and its correlation with urban, water, vegetation, and surface indices in the Siliguri Urban Agglomeration area of the Himalayan foothill region. *Geomatics Natural Hazards and Risk*, *16*(1). https://doi.org/10.1080/19475705.2025.2470393

Department of Water Affairs (DWA), (2010): A Guideline for the Assessment, Planning and Management of Groundwater Resources in South Africa, Edition 2. Pretoria. https://www.dws.gov.za/ghreport/reports/GH4349.pdf [Accessed 15 May 2025].

Department of Water and Sanitation. (2016). The water management areas of South Africa. https://www.dws.gov.za/io/Docs/Starter Pack _Final_FULL (00000003).pdf [Accessed 1 October 2025].

Deuskar, C., Roberts, M., Jones, N., & Park, J. (2023). UNLiVable: What the urban heat island effect means for East Asia's cities. In *Washington, DC: World Bank eBooks*. https://doi.org/10.1596/40771

Diaz, L. R., Santos, D. C., Käfer, P. S., Da Rocha, N. S., Da Costa, S. T. L., Kaiser, E. A., & Rolim, S. B. A. (2021). Atmospheric Correction of Thermal Infrared Landsat Images Using High-Resolution Vertical Profiles Simulated by WRF Model. *The 4th International Electronic Conference on Atmospheric Sciences*, 27. https://doi.org/10.3390/ecas2021-10351

Dinda, A., & Chatterjee, S. (2022). Assessing the local- impacts of heat advection on urban heat islands in Kolkata Metropolitan Area. Urban Climate, 42, 101139. https://doi.org/10.1016/j.uclim.2022.101139

Dippenaar MA, Van Rooy JL, & Diamond RE (2018). Engineering, hydrogeological and vadose zone hydrological aspects of Proterozoic dolomites (South Africa), *Journal of African Earth Sciences*. https://doi.org/10.1016/j.jafrearsci.2018.07.024

Dong, R., Wurm, M., & Taubenböck, H. (2022). Seasonal and diurnal variation of land surface temperature distribution and its relation to land use/land cover patterns. *International Journal of Environmental Research and Public Health*, 19(19), 12738.

Du, C., Ren, H., Qin, Q., Meng, J., & Zhao, S. (2015). A practical split-window algorithm for estimating land surface temperature from Landsat 8 data. *Remote Sensing*, 7(1), 647-665.

Durowoju, O. S., Obateru, R. O., Adelabu, S., & Olusola, A. (2025). Urban change detection: assessing biophysical drivers using machine learning and Google Earth Engine. *Environmental Monitoring and Assessment*, 197(4), 441.

Elbertse, C. (2021). Managing green-burbia: utilising urban management practices to address the Urban Heat Island as a call to adapt to climate change impacts-the case of Melville in Johannesburg (Doctoral dissertation). https://hdl.handle.net/10539/32931

Erol, E. (2023). Assessing the Urban Heat Island Effect in New York City. The University of Arizona. (Dissertation). http://hdl.handle.net/10150/668521

Fadda, M. (2024). Urban planning in a context of rapid urban growth. A large scale review of urban plans in Africa. *arXiv (Cornell University)*. https://doi.org/10.48550/arxiv.2405.00048

Fazel-Rastgar, F., & Sivakumar, V. (2024). A case study on more recent heat wave occurred in South Africa, based on background weather synoptic and dynamic characteristics analysis. *Bulletin of Atmospheric Science and Technology*, 5(1), 5.

Fazel-Rastgar, F., Sivakumar, V., Rostami, M., & Fallah, B. (2025). Study on the associated effects of extreme drought and heatwave on air quality in South Africa during October 2022. *Bulletin of Atmospheric Science and Technology*, 6(1). https://doi.org/10.1007/s42865-025-00101-5

Fendoung, P. M., Moto, F. A. M., & Makuate, M. B. (2024). Impacts of Land Use Change on Urban Heat Islands in Kribi, Cameroon: Assessing Vulnerability and Adaptive Strategies. *European Scientific Journal, ESJ Preprints*, 20(35), 190-190.

Feng, H., Ye, S., & Zou, B. (2020). Contribution of vegetation change to the surface radiation budget: A satellite perspective. *Global and Planetary Change*, 192, 103225. Availablet at: https://doi.org/10.1016/j.gloplacha.2020.103225

Fentaw, A. E., & Abegaz, A. (2024). Analyzing Land Use/Land Cover changes using Google Earth Engine and Random Forest algorithm and their implications to the management of land degradation in the Upper Tekeze Basin, Ethiopia. *The Scientific World Journal*, *2024*(1), 3937558. https://doi.org/10.1155/2024/3937558

Forthofer, R. N., Lee, E. S., & Hernandez, M. (2007). Descriptive methods. *Biostatistics*, 21–69. https://doi.org/10.1016/b978-0-12-369492-8.50008-x

Fuentes, I., Lopatin, J., Galleguillos, M., Ceballos-Comisso, A., Eyheramendy, S., & Carrasco, R. (2024). Is the change deforestation? Using time-series analysis of satellite data to disentangle deforestation from other forest degradation causes. *Remote Sensing Applications Society and Environment*, *35*, 101210. https://doi.org/10.1016/j.rsase.2024.101210

Gauteng Provincial Government. (2010). Gauteng Growth Employment and Development Strategy (GGEDS). https://www.gcro.ac.za/outputs/policy-and-other-outputs/detail/gauteng-growth-employment-and-development-strategy-ggeds/ [Accessed 18 July 2025]

Gidey, E., & Mhangara, P. (2023). An application of a machine-learning model for analysing the impact of land-use change on surface water resources in Gauteng Province, South Africa. *Remote Sensing*, 15(16), 4092.

Gidey, E., & Mhangara, P. (2025). Improving spatial modeling framework to assess the impact of vegetation cover, water content, and surface temperature on urban heat island effects in Johannesburg, South Africa. *Discover Environment*, 3(1), 74.

Gidey, E., Dikinya, O., Sebego, R., Segosebe, E., & Zenebe, A. (2018). Using drought indices to model the statistical relationships between meteorological and agricultural drought in Raya and its environs, northern Ethiopia. *Earth Systems and Environment*, *2*(2), 265–279.

Gislason, P. O., Benediktsson, J. A., & Sveinsson, J. R. (2006). Random forests for land cover classification. *Pattern Recognition Letters*, 27(4), 294-300.

Günen, M. A., & Atasever, U. H. (2024). Remote sensing and monitoring of water resources: A comparative study of different indices and thresholding methods. *The Science of the Total Environment*, *926*, 172117. https://doi.org/10.1016/j.scitotenv.2024.172117

Gyimah, R. R. (2023). The hot zones are cities: Methodological outcomes and synthesis of surface urban heat island effect in Africa. *Cogent Social Sciences*, 9(1). https://doi.org/10.1080/23311886.2023.2165651

Haight, J., De Albuquerque, F., & Frazier, A. (2024). Long-term composited Modified Normalized Difference Water Index (MNDWI) for the greater Phoenix, Arizona, USA, metropolitan area and the surrounding Sonoran Desert derived from annual and seasonal Landsat imagery, 1998 to 2023. *Environmental Data Initiative*. https://doi.org/10.6073/pasta/69700b05a7bc103c2ba17b38af44b8d3

Hardy, C. H., & Nel, A. L. (2015). Data and techniques for studying the urban heat island effect in Johannesburg. *Remote Sensing and Spatial Information Sciences,* 40, 203-206. https://doi.org/10.5194/isprsarchives-XL-7-W3-203-2015

Hossain, M. J., Mahmud, M. M., & Islam, S. T. (2023). Monitoring spatiotemporal changes of urban surface water based on satellite imagery and the Google Earth Engine platform in Dhaka City from 1990 to 2021. *Bulletin of the National Research Centre,* 47(1), 150.

Hsiao, L. H., & Cheng, K. S. (2016). Assessing uncertainty in LULC classification accuracy by using bootstrap resampling. *Remote Sensing*, 8(9), 705.

Hu, L., & Uejio, C. (2024). Ground Urban Heat Island: Strengthening the connection between spaceborne thermal observations and urban heat risk management. *GeoHealth*, 8(7). https://doi.org/10.1029/2024gh001114

Hulley, M. (2012). The urban heat island effect: causes and potential solutions. In Elsevier eBooks (pp. 79–98). https://doi.org/10.1533/9780857096463.1.79

Intergovernmental Panel on Climate Change (IPCC). (2023). Summary for Policymakers. In: Climate Change 2023: Synthesis Report. Contribution of Working Groups I, II and III to the Sixth Assessment Report of the Intergovernmental Panel on Climate Change. IPCC, Geneva, Switzerland, 1-34. https://www.ipcc.ch/report/ar6/syr/

Islami, F. A., Tarigan, S. D., Wahjunie, E. D., & Dasanto, B. D. (2022). Accuracy assessment of land use change analysis using Google Earth in Sadar Watershed, Mojokerto Regency. In IOP Conference Series: Earth and *Environmental Science*, 950 (1), 012091.

Jacobs, S., David, O. O., & Wyk, A. S.V. (2023). The Impact of Urbanisation on Economic Growth in Gauteng Province, South Africa. *International Journal of Economics and Financial Issues*, 13(2), 1–11.

Jamalishahni, T., Turrell, G., Foster, S., Davern, M., & Villanueva, K. (2023). Neighbourhood socio-economic disadvantage and loneliness: the contribution of green space quantity and quality. *BMC Public Health*, *23*(1), 598. https://doi.org/10.1186/s12889-023-15433-0

Janarth, S., Jagadeeswaran, R., Pazhanivelan, S., Balaji, K., Ragunath, K., Sathiyamoorthy, N., Kumar, D. P., & Santhoshkumar, B. (2024). Quantifying the impact of land surface temperature on vegetation moisture for drought monitoring in Tamil Nadu. *Plant Science Today*, 11(4). https://doi.org/10.14719/pst.5547

Jandaghian, Z., & Colombo, A. (2024). The Role of Water Bodies in Climate Regulation: Insights from Recent Studies on Urban Heat Island Mitigation. *Buildings*, 14(9), 2945. https://doi.org/10.3390/buildings14092945

Jombo, S., Adam, E., Byrne, M. J., & Newete, S. W. (2022). Assessing the intraurban differences in vegetation coverage and surface climate in a heterogeneous area. *Transactions of the Royal Society of South Africa*, 77(1), 1-10.

Kabanda, T. H., & Kabanda, T. A. (2019). Urban heat island analysis in Dar es Salaam, Tanzania. *South African Journal of Geomatics*, 8(1), 98-107.

Kagabo, A. S., Safari, B., Gasore, J., Mutai, B. K., & Sebaziga, J. N. (2024). Assessing the impact of Land Use Land Cover changes on land surface temperature over Kigali, Rwanda, in the past three decades. *Environmental and Sustainability Indicators*, 23, 100452. https://doi.org/10.1016/j.indic.2024.100452

Kapwata, T., Gebreslasie, M. T., & Wright, C. Y. (2022). An analysis of past and future heatwaves based on a heat-associated mortality threshold: towards a heat health warning system. *Environmental Health*, 21(1), 112.

Kara, Y., & Yavuz, V. (2025). Urban microclimates in a warming world: Land Surface Temperature (LST) trends across ten major cities on seven continents. *Urban Science*, *9*(4), 115. https://doi.org/10.3390/urbansci9040115

Kareem, H. H., Attaee, M. H., & Omran, Z. A. (2023). Estimation the water ratio index (WRI) and automated water extraction index (AWEI) of bath in the United Kingdom using remote sensing technology of the multispectral data of Landsat 8-OLI. *Water Conservation and Management*, 8(2), 171–178.

Kikon, N., Kumar, D., & Ahmed, S. A. (2023). Quantitative assessment of land surface temperature and vegetation indices on a kilometre grid scale. Environmental Science and Pollution Research, 30(49), 107236-107258.

Kim, S. W., & Brown, R. D. (2021). Urban heat island (UHI) intensity and magnitude estimations: A systematic literature review. *The Science of the Total Environment*, 779, 146389. https://doi.org/10.1016/j.scitotenv.2021.146389

Kliengchuay, W., Phonphan, W., Niampradit, S., Kiangkoo, N., Srimanus, W., Niemmanee, T., Arunplod, C., Wen, B., Guo, Y., Herbreteau, V., & Tantrakarnapa, K. (2025). Variation of vegetation cover and the relationship with land surface temperature across Thailand (2007 to 2022). *Scientific Reports*, 15(1), 27823.

Kolath, A. S., & Egemose, S. (2023). Influences of urban discharges and urban heat effects on stream temperature. *Hydrology*, 10(2), 30.

Kouassi, C. J. A., Qian, C., Khan, D., Achille, L. S., Kebin, Z., Omifolaji, J. K., & Yang, X. (2023). Google Earth Engine for Landsat image processing and assessing LULC classification in southwestern Côte D'ivoire. *Geodesy and Cartography*, 49(1), 37-50.

Kunda, J. J., Gosling, S. N., & Foody, G. M. (2024). The effects of extreme heat on human health in tropical Africa. *International Journal of Biometeorology*, *68*(6), 1015–1033. https://doi.org/10.1007/s00484-024-02650-4

LaDochy, S., Torres, T., & Hsu, Y. (2021). Los Angeles' urban heat island continues to grow urbanization, land use change influences. *Journal of Urban and Environmental Engineering*, 15(2), 103–116.

Lesslie, R., Barson, M., & Smith, J. (2006). Land use information for integrated natural resources management—a coordinated national mapping program for Australia. *Journal of Land Use Science*, 1(1), 45–62.

Li, A., Yin, S., Li, N., & Shi, C. (2025). Comprehensive analysis of the driving forces behind NDVI variability in China under climate change conditions and future scenario projections. *Atmosphere*, 16(6), 738.

Li, X., Stringer, L. C., & Dallimer, M. (2021). The spatial and temporal characteristics of urban Heat Island Intensity: Implications for East Africa's Urban development. *Climate*, *9*(4), 51. https://doi.org/10.3390/cli9040051

Li, X., Stringer, L. C., & Dallimer, M. (2022). The impacts of urbanisation and climate change on the urban thermal environment in Africa. *Climate*, *10*(11), 164. https://doi.org/10.3390/cli10110164

Li, X., Wang, Y., Zhao, Y., Zhai, J., Liu, Y., Han, S., & Liu, K. (2024). Research on the impact of climate change and human activities on the NDVI of arid areas—A case study of the Shiyang River Basin. *Land*, 13(4), 533.

Li, Z. L., Wu, H., Duan, S. B., Zhao, W., Ren, H., Liu, X., & Zhou, C. (2023). Satellite remote sensing of global land surface temperature: Definition, methods, products, and applications. *Reviews of Geophysics*, 61(1).

Li, Z., Shen, H., Weng, Q., Zhang, Y., Dou, P., & Zhang, L. (2022). Cloud and cloud shadow detection for optical satellite imagery: Features, algorithms, validation, and prospects. *ISPRS Journal of Photogrammetry and Remote Sensing*, 188, 89–108.

Liang, J., Qiu, Y. L., Wang, B., Shen, X., & Liu, S. (2025). Impacts of heatwaves on electricity reliability: Evidence from power outage data in China. *iScience*, *28*(2), 111855.

Love, N. L. R., Berkelhammer, M., Tovar, E., Romy, S., Wilson, M. D., & Mir, G. C. N. (2025). Not all green is equal: growth form is a key driver of urban vegetation sensitivity to climate in Chicago. *Remote Sensing*, *17*(17), 2919.

Macarringue, L. S., Bolfe, É. L., Duverger, S. G., Sano, E. E., Caldas, M. M., Ferreira, M. C., & Matias, L. F. (2023). Land use and land cover classification in the northern region of Mozambique based on Landsat time series and machine learning. *ISPRS International Journal of Geo-Information*, 12(8), 342.

Macharia, N. A., Mbuthia, S. W., Musau, M. J., Obando, J. A., & Ebole, S. O. (2022). Dry-season variability in near-surface temperature measurements and Landsat-based land surface temperature in Kenyatta University, Kenya. *Computational Urban Science*, 2(1), 33.

Magagula, N. Q. (2024). Spatio-temporal analysis of urban heat island (UHI) intensity in Mbombela City, Mpumalanga Province, from 2008 to 2023. *Urban Climatology*. https://www.researchgate.net/publication/385098162_Spatio-temporal_Analysis_of_Urban_Heat_Island_Intensity_in_Mbombela_City_Mpumalanga_Province_South_Africa

Magidi, J., & Ahmed, F. (2020). Spatio-temporal variations of land surface temperature using Landsat and MODIS: case study of the City of Tshwane, South Africa. *South African Journal of Geomatics*, 9(2), 379-396.

Magli, S., Lodi, C., Lombroso, L., Muscio, A., & Teggi, S. (2014). Analysis of the urban heat island effects on building energy consumption. *International Journal of Energy and Environmental Engineering*, 6(1), 91–99.

Mahdi, Z. S., Tawfeek, Y. Q., and Al-Jiboori, M. H. (2024). Relationship between monthly surface water derived from Sentinel-2 imagery and meteorological data (precipitation and evaporation) at Baghdad, Iraq. *Water Practice and Technology,* 19(5), 1794–1809.

Maisha, R. T., Ndarana, T., Engelbrecht, F. A., Thatcher, M., Bopape, M. J. M., Van Der Merwe, J., & Masemola, C. (2023). Simulation of the eThekwini Heat Island in South Africa. *Journal of Applied Meteorology and Climatology*, 62(5), 589-609.

Manjunath, D. R., & Jagadeesh, P. (2024). Dynamics of urban development patterns on thermal distributions and their implications on water spread areas of Vellore, Tamil Nadu, India. *Frontiers in Sustainable Cities*, 6, 1462092.

Mankin, K. R., Mehan, S., Green, T. R., & Barnard, D. M. (2025). Review of gridded climate products and their use in hydrological analyses reveals overlaps, gaps, and the need for a more objective approach to selecting model forcing datasets. *Hydrology and Earth System Sciences,* 29(1), 85–108.

Marghidan, C. P., Van Aalst, M., Blanford, J., Guigma, K., Pinto, I., Maure, G., & Marrufo, T. (2023). Heatwaves in Mozambique 1983–2016: Characteristics, trends and city-level summaries using high-resolution CHIRTS-daily. *Weather and Climate Extremes*, 40, 100565. https://doi.org/10.1016/j.wace.2023.100565

Matarira, D., Mutanga, O., & Naidu, M. (2022). Google Earth Engine for Informal Settlement Mapping: A random forest classification using spectral and textural information. *Remote Sensing*, *14*(20), 5130. https://doi.org/10.3390/rs14205130

Maumela, K. G., Mathaba, T. N. D., & Kao, M. (2025). An Integrated Framework for Urban Water Infrastructure Planning and Management: A case study for Gauteng Province, South Africa. *Water*, *17*(15), 2290.

Mawasha, T. S., and Britz, W. (2022). Simulating change in surface runoff depth due to LULC change using soil and water assessment tool for flash floods prediction. *South African Journal of Geomatics*, 9(2), 282–301.

Mbokodo, I. L., Bopape, M. J. M., Ndarana, T., Mbatha, S. M., Muofhe, T. P., Singo, M. V., & Chikoore, H. (2023). Heatwave variability and structure in South Africa during summer drought. *Climate*, 11(2), 38.

Mbokodo, I., Bopape, M. J., Chikoore, H., Engelbrecht, F., & Nethengwe, N. (2020). Heatwaves in the future warmer climate of South Africa. *Atmosphere*, 11(7), 712.

McBride, C. M., Kruger, A. C., & Dyson, L. (2022). Changes in extreme daily rainfall characteristics in South Africa: 1921–2020. *Weather and Climate Extremes*, *38*, 100517. https://doi.org/10.1016/j.wace.2022.100517

McConnachie, M. M., & Shackleton, C. M. (2009). Public green space inequality in small towns in South Africa. *Habitat International*, *34*(2), 244–248.
McFeeters, S. K. (1996). The use of the Normalised Difference Water Index (NDWI) in the delineation of open water features. *International Journal of Remote Sensing*, 17(7), 1425-1432.

Mengistu, A. G., Woyessa, Y. E., Tesfuhuney, W. A., Steyn, A. S., & Lee, S. S. (2023). Assessing the impact of climate change on future extreme temperature events in major South African cities. *Theoretical and Applied Climatology*, *155*(3), 1807–1819.

Meyer, H., Reudenbach, C., Wöllauer, S., & Nauss, T. (2019). Importance of spatial predictor variable selection in machine learning applications – Moving from data reproduction to spatial prediction. *Ecological Modelling*, 411, 108815. https://doi.org/10.1016/j.ecolmodel.2019.108815

Mistry, M. N., Schneider, R., Masselot, P., Royé, D., Armstrong, B., Kyselý, J., Orru, H., Sera, F., Tong, S., Lavigne, É., Urban, A., Madureira, J., García-León, D., Ibarreta, D., Ciscar, J., Feyen, L., De Schrijver, E., De Sousa Zanotti Stagliorio Coelho, M.,

Pascal, M., and Gasparrini, A. (2022). Comparison of weather station and climate reanalysis data for modelling temperature-related mortality. *Scientific Reports*, 12(1), 5178.

Mogonong, B. P., Twine, W., Feig, G. T., Van der Merwe, H., & Fisher, J. T. (2024). Influences of climate Variability on land use and land cover change in rural South Africa. *Remote Sensing*, 16(7), 1200.

Moisa, M. B., & Gemeda, D. O. (2022). Assessment of urban thermal field variance index and thermal comfort level of Addis Ababa metropolitan city, Ethiopia. *Heliyon*, 8(8), e10185.

Monama, T. E. (2016). Evaluating the urban heat island over the city of Tshwane Metropolitan Municipality using remote sensing techniques [Master of Science Thesis, University of Johannesburg]. https://hdl.handle.net/10210/124987

Mondal, S., & Gavsker, K. K. (2024). Investigating the urban eco-environmental quality utilising a remote sensing-based approach: evidence from an industrial city of Eastern India. *Discover Applied Sciences*, 6(12), 666.

Mshelia, Z. H., & Belle, J. A. (2024). A systematic flood risk assessment of Bloemfontein Watershed, South Africa. *Geomatics Natural Hazards and Risk*, 15(1). https://doi.org/10.1080/19475705.2024.2423739

Mudede, M. F., Newete, S. W., Abutaleb, K., & Nkongolo, N. (2020). Monitoring the urban environment quality in the city of Johannesburg using remote sensing data. *Journal of African Earth Sciences*, 171, 103969. https://doi.org/10.1016/j.jafrearsci.2020.1039691

Mughal, M., Li, X., & Norford, L. K. (2020). Urban heat island mitigation in Singapore: Evaluation using WRF/multilayer urban canopy model and local climate zones. *Urban Climate*, 34, 100714. https://doi.org/10.1016/j.uclim.2020.100714

Mugiraneza, T., Hafner, S., Haas, J., & Ban, Y. (2022). Monitoring urbanisation and environmental impact in Kigali, Rwanda, using Sentinel-2 MSI data and ecosystem service bundles. *International Journal of Applied Earth Observation and Geoinformation*, 109, 102775. https://doi.org/10.1016/j.jag.2022.102775

Muller, M., Schreiner, B., Vermeulen, A., Maree, G., & Reddy, T. (2019). Water Security Perspective for the Gauteng City-Region: Securing water for continued growth and well-being. Report prepared by the GCRO for the Office of the Premier of Gauteng. https://www.researchgate.net/publication/351934769_Water_Security_Perspective_for_the_Gauteng_City-Region_Securing_water_for_continued_growth_and_well_being

Munawar, M., McNeil, R., Jani, R., Buya, S., & Tarmizi, T. (2025). Variations in land surface temperature increase in South-East Asian Cities. *Environmental Monitoring and Assessment*, 197(2). DOI: 10.1007/s10661-024-13604-z

Munyati, C., & Drummond, J. H. (2020). Loss of urban green spaces in Mafikeng, South Africa. *World Development Perspectives*, 19, 100226. https://doi.org/10.1016/j.wdp.2020.100226

Mushore, T. D., Dube, T., Manjowe, M., Gumindoga, W., Chemura, A., Rousta, I., & Mutanga, O. (2019). Remotely sensed retrieval of Local Climate Zones and their linkages to land surface temperature in Harare metropolitan city, Zimbabwe. *Urban Climate*, 27, 259-271.

Mutani, G., Scalise, A., Sufa, X., & Grasso, S. (2024). Synergising Machine Learning and Remote Sensing for Urban Heat Island Dynamics: A Comprehensive Modelling Approach. *Atmosphere*, 15(12), 1435

Naserikia, M., Hart, M. A., Nazarian, N., Bechtel, B., Lipson, M., & Nice, K. A. (2023). Land surface and air temperature dynamics: The role of urban form and seasonality. *The Science of the Total Environment*, *905*, 167306. https://doi.org/10.1016/j.scitotenv.2023.167306

Ncongwane, K. P., Botai, J. O., Sivakumar, V., Botai, C. M., & Adeola, A. M. (2021). Characteristics and long-term trends of heat stress for South Africa. *Sustainability*, 13(23), 13249.

Nedd, R., Light, K., Owens, M., James, N., Johnson, E., & Anandhi, A. (2021). A synthesis of Land Use/Land Cover studies: definitions, classification systems, Meta-Studies, challenges and knowledge gaps on a global landscape. *Land*, *10*(9), 994. https://doi.org/10.3390/land10090994

Negesse, M. D., Hishe, S., & Getahun, K. (2024). Urban land use, land cover change and urban microclimate dynamics in Addis Ababa, Ethiopia. *Discover Environment*, *2*(1). https://doi.org/10.1007/s44274-024-00105-6

Nevers, C., Carmeliet, J., Kubilay, A., & Derome, D. (2025). Impact of trees on thermal comfort in adjacent park and neighbourhood in hot-humid climate: A CFD study. *Urban Climate*, 62, 102519. https://doi.org/10.1016/j.uclim.2025.102519

Ngan, T. T., Wang, R., Tate, C., Green, M., Mitchell, R., Hunter, R. F., & O'Neill, C. (2024). Inequality in green space distribution and its association with preventable deaths across urban neighbourhoods in the UK, stratified by Index of Multiple Deprivation. *Journal of Epidemiology & Community Health*, *79*(2), 102–109.

Ngcamu, B. S. (2023). Climate change effects on vulnerable populations in the Global South: a systematic review. *Natural Hazards*, 118(2), 977–991.

Ngie, A., Abutaleb, K., Ahmed, F., Taiwo, O. J., Darwish, A. A., & Ahmed, M. (2016). An estimation of land surface temperatures from Landsat ETM+ images for Durban, South Africa. *Rwanda Journal*, 1. https://research.amanote.com/publication/aY9X1HMBKQvf0BhiBmo2/an-estimation-of-land-surface-temperatures-from-landsat-etm-images-for-durban-south

Nhamo, L., Rwizi, L., Mpandeli, S., Botai, J., Magidi, J., Tazvinga, H., & Mabhaudhi, T. (2021). Urban nexus and transformative pathways towards a resilient Gauteng City-Region, South Africa. *Cities*, 116, 103266.

Opiyo, S. B., Pienaar, L., Piketh, S. J., Burger, R. P., Chikoore, H., & Havenga, H. (2025). Assessment of vegetation density trends in response to long-term climate change impacts in Western South Africa (1962–2022) using SPEI and NDVI time series. *Discover Forests*, 1(29). https://doi.org/10.1007/s44415-025-00030-3

Palliwoda, J., Haase, A., Suppee, C., Rink, D., & Priess, J. A. (2022). Visions for development and management of urban green and blue infrastructure: a citizen's perspective. *Ecology and Society*, *27*(2). https://doi.org/10.5751/es-13129-270208

Parastatidis, D., Mitraka, Z., Chrysoulakis, N., & Abrams, M. (2017). Online global land surface temperature estimation from Landsat. *Remote sensing*, 9(12), 1208.

Parker, C., Mahlasi, C., Govindasamy, T., Radebe, L., Brink, N. B., Jack, C., & Makhanya, S. (2025). Quantifying intra-urban socio-economic and environmental vulnerability to extreme heat events in Johannesburg, South Africa. *International Journal of Biometeorology*, 1-17. https://doi.org/10.1007/s00484-025-02971-y

Peng, J., Xie, P., Liu, Y., & Ma, J. (2015). Urban thermal environment dynamics and associated landscape pattern factors: A case study in the Beijing metropolitan region. *Remote Sensing of Environment*, *173*, 145–155.

Perkins, S. E., & Alexander, L. V. (2012). On the Measurement of Heat Waves. *Journal of Climate*, 26(13), 4500–4517.

Petitcolin, F., & Vermote, E. (2002). Land surface reflectance, emissivity and temperature from MODIS middle and thermal infrared data. *Remote Sensing of Environment*, *83*(1–2), 112–134.

Phan, T. N., Kuch, V., & Lehnert, L. W. (2020). Land cover classification using Google Earth Engine and random forest classifier—The role of image composition. *Remote Sensing,* 12(15), 2411.

Piketh, S.J., Vogel, C., Dunsmore, S., Culwick, C., & Engelbrecht, F. (2025). Climate change and urban development in southern Africa: The case of Ekurhuleni Municipality (EMM) in South Africa. *Water SA*, 40. DOI:10.4314/wsa.v40i4.20

Quante, M., Hanf, F. S., Bär, F., Boettcher, M., Burgemeister, F., Grawe, D., Hoffmann, P., & Schlünzen, H. (2022). Urban-induced modification of precipitation - Findings from a systematic literature review with focus on studies from the last decade. *Conference: EMS Annual Meeting*. https://doi.org/10.5194/ems2022-121

Raj, S., Paul, S. K., Chakraborty, A., & Kuttippurath, J. (2019). Anthropogenic forcing exacerbating the urban heat islands in India. *Journal of Environmental Management*, 257, 110006. https://doi.org/10.1016/j.jenvman.2019.110006

Raj, S., Paul, S. K., Chakraborty, A., & Kuttippurath, J. (2019). Anthropogenic forcing exacerbating the urban heat islands in India. *Journal of Environmental Management*, 257, 110006. https://doi.org/10.1016/j.jenvman.2019.110006

Ramakreshnan, L., Aghamohammadi, N., Fong, C. S., Ghaffarianhoseini, A., Ghaffarianhoseini, A., Wong, L. P., Hassan, N., & Sulaiman, N. M. (2018). A critical review of Urban Heat Island phenomenon in the context of Greater Kuala Lumpur, Malaysia. *Sustainable Cities and Society*, 39, 99–113. https://doi.org/10.1016/j.scs.2018.02.005

Rand Water. (2024). *Addressing Gauteng's impending water crisis*. https://www.swpn.org.za/wp-content/uploads/2024/06/Addressing-Gauteng-Water-Supply-Presentation-June-2024-Rand-Water.pdf

Rao, P., Tassinari, P., & Torreggiani, D. (2023). Exploring the land-use urban heat island nexus under climate change conditions using a machine learning approach: A spatio-temporal analysis of remotely sensed data. *Heliyon*, 9(8), 18423.

Rasebechele, P., Langerman, K., & Kelso, C. (2025). Unveiling local climate action: a case study of mitigation efforts in Gauteng's West Rand District Municipality, South Africa. *Climate Policy*, 25(4), 527-544.

Rinner, C., & Hussain, M. (2011). Toronto's Urban Heat Island—Exploring the Relationship between Land Use and Surface Temperature. *Remote Sensing*, 3(6), 1251–1265.

Roba, Z. R., & Tabor, K. W. (2025). Geospatial analysis of vegetation and land surface temperature for urban heat island mitigation in Hawassa City, Ethiopia. *Scientific Reports,* 15(1), 31786.

Rogalski, S., & Ilunga, M. (2025). Predicting Land Surface Temperature from Rainfall and Elevation Remotely Sensed Data Using Random Forest Machine Learning in Google Earth Engine. *Proceedings*, 119–126. https://www.iiis.org/CDs2025/CD2025Spring/papers/ZA794JM.pdf

Rouault, M., Dieppois, B., Tim, N., Hünicke, B., & Zorita, E. (2024). Southern Africa Climate Over the recent decades: Description, variability and Trends. *Ecological Studies*, 149–168. https://doi.org/10.1007/978-3-031-10948-5_6

Rouse, J.W., Haas, R.H., Schell, J.A. & Deering, D.W. (1973). Monitoring vegetation systems in the great plains with earth resources technology satellite. *Greenbelt*, 309-317. https://ntrs.nasa.gov/api/citations/19740022614/downloads/19740022614.pdf

Salimi, M., & Al-Ghamdi, S. G. (2020). Climate change impacts on critical urban infrastructure and urban resiliency strategies for the Middle East. *Sustainable Cities and Society*, *54*, 101948. https://doi.org/10.1016/j.scs.2019.101948

Sarfo, I., Qiao, J., Yeboah, E., Puplampu, D. A., Kwang, C., Fynn, I. E. M., Batame, M., Appea, E. A., Hagan, D. F. T., Ayelazuno, R. A., Boamah, V., & Sarfo, B. A. (2024). Meta-analysis of land use systems development in Africa: Trajectories, implications, adaptive capacity, and future dynamics. *Land Use Policy*, *144*, 107261. https://doi.org/10.1016/j.landusepol.2024.107261

Schober, P., Boer, C., & Schwarte, L. A. (2018). Correlation coefficients: appropriate use and interpretation. *Anaesthesia & Analgesia*, 126(5), 1763-1768.

Scholes, R. & Engelbrecht, F. (2021). Climate impacts in southern Africa during the 21st Century. *Report for the Centre for Environmental Rights*, 1-9. https://cer.org.za/wp-content/uploads/2021/09/Climate-impacts-in-South-Africa_Final_September_2021.FINAL_.pdf

Sekertekin, A., & Bonafoni, S. (2019). Land surface temperature retrieval from Landsat 5, 7, and 8 over rural areas: Assessment of different retrieval algorithms and emissivity models and toolbox implementation. *Remote sensing*, 12(2), 294.

Senbore, S., & Oke, S. A. (2021). Urban development impact on climate variability and surface water quality in part of Mangaung metropolis of South Africa. *Development Southern Africa*, *40*(2), 293–312.

Senevirathne, D., Jayasooriya, V., Dassanayake, S., & Muthukumaran, S. (2021). Effects of pavement texture and colour on Urban Heat Islands: An experimental study in a tropical climate. *Urban Climate*, 40, 101024.

Shafizadeh-Moghadam, H., Khazaei, M., Alavipanah, S. K., & Weng, Q. (2021). Google Earth Engine for large-scale land use and land cover mapping: An object-based classification approach using spectral, textural and topographical factors. *GIScience & Remote Sensing*, 58(6), 914-928.

Shikwambana, L., and Tsoeleng, L. T. (2020). Impacts of population growth and land use on air quality: a case study of Tshwane, Rustenburg and Emalahleni, South Africa. *South African Geographical Journal*, 102(2), 209–222.

Simpson, N. P., Mach, K. J., Tebboth, M. G., Gilmore, E. A., Siders, A., Holden, P., Anderson, B., Singh, C., Sabour, S., Stringer, L. C., Sterly, H., Williams, P. A., Meyer, A. L., Cundill, G., Rosengaertner, S., Nunow, A., Amakrane, K., & Trisos, C. H. (2024). Research priorities for climate mobility. *One Earth*, *7*(4), 589–607.

Singh, S., Kumar, P., Parijat, R., Gonengcil, B., & Rai, A. (2023). Establishing the relationship between land use, land cover, normalised difference vegetation index and land surface temperature: A case of Lower Son River Basin, India. *Geography and Sustainability*, *5*(2), 265–275.

Skrynyk, O., Aguilar, E., & Cimolai, C. (2025). The sensitivity of heatwave climatology to input gridded datasets: A case study of Ukraine. *Atmosphere*, 16(3), 289.

Soltanifard, H., & Amani-Beni, M. (2025). The cooling effect of urban green spaces as nature-based solutions for mitigating urban heat: insights from a decade-long systematic review. *Climate Risk Management*, *49*, 100731. https://doi.org/10.1016/j.crm.2025.100731

Souverijns, N., De Ridder, K., Veldeman, N., Lefebre, F., Kusambiza-Kiingi, F., Memela, W., & Jones, N. K. (2022). Urban heat in Johannesburg and Ekurhuleni, South Africa: A meter-scale assessment and vulnerability analysis. *Urban Climate*, 46, 101331.

World Meteorological Organisation. (2023). Climate change indicators reached record levels in 2023. https://wmo.int/news/media-centre/climate-change-indicators-reached-record-levels-2023-wmo [Accessed 15 March 2025]

World Meteorological Organisation. (2024). State of the global climate. https://wmo.int/publication-series/state-of-global-climate-2024 [Accessed 20 March 2025].

Streutker, D. (2003). Satellite-measured growth of the urban heat island of Houston, Texas. *Remote Sensing of Environment*, *85*(3), 282–289.

Stringer, L. C., Mirzabaev, A., Benjaminsen, T. A., Harris, R. M., Jafari, M., Lissner, T. K., Stevens, N., & Pahlen, C. T. D. (2021). Climate change impacts on water security in global drylands. *One Earth*, *4*(6), 851–864.

Sultan, M., Saleous, N., Issa, S., Dahy, B., & Sami, M. (2025). Optimising Land Use Classification Using Google Earth Engine: A Comparative Analysis of Machine Learning Algorithms. *ISPRS Annals of the Photogrammetry, Remote Sensing and Spatial Information Sciences*, 863-869. https://doi.org/10.5194/isprs-annals-X-G-2025-863-2025

Talanda, C. E., van Rooyen, P. G., & Rademeyer, J. I. (2015). The potential impact of acid mine drainage on the Vaal River System water resource availability. *Engineers Australia*, 36(1): 1-5.

Taloor, A. K., Parsad, G., Jabeen, S. F., Sharma, M., Choudhary, R., & Kumar, A. (2024). Analytical study of land surface temperature for evaluation of UHI and UHS in the city of Chandigarh, India. *Remote Sensing Applications: Society and Environment*, 35, 101206. https://doi.org/10.1016/j.rsase.2024.101206

Tuan, V. A., Hang, L. T. T., & Quang, N. H. (2019). Monitoring urban surface water bodies change using MNDWI estimated from pan-sharpened optical satellite images. *FIG Working Week, Hanoi, Vietnam*, 22-26. https://www.fig.net/resources/proceedings/fig_proceedings/fig2019/papers/ts07d/TS07D_tuan_hang_et_al_9771.pdf

Tucker, C. J. (1979). Red and photographic infrared linear combinations for monitoring vegetation. *Remote sensing of Environment*, 8(2), 127-150.

Umeh, S. C., & Gil-Alana, L. A. (2024). Trends in temperatures in Sub-Saharan Africa. Evidence of global warming. *Journal of African Earth Sciences*, 213, 105228.

United Nations Children's Fund (UNICEF). (2024). Climate Change – Eastern and Southern Africa. *UNICEF Climate*. https://www.unocha.org/news/seven-things-you-need-know-about-climate-change-eastern-and-southern-africa [Accessed 5 August 2025]

Vahid, R., & Aly, M. H. (2025). A comprehensive systematic review of Machine Learning applications in assessing Land Use/Cover Dynamics and their impact on land Surface Temperatures. *Urban Science*, *9*(7), 234. https://doi.org/10.3390/urbansci9070234

Venter, Z. S., & Sydenham, M. A. (2021). Continental-scale land cover mapping at 10 m resolution over Europe (ELC10). *Remote Sensing*, 13(12), 2301.

Voogt, J., & Oke, T. (2003). Thermal remote sensing of urban climates. *Remote Sensing of Environment*, 86(3), 370–384.

Vyshkvarkova, E., & Sukhonos, O. (2022). Compound extremes of air temperature and precipitation in Eastern Europe. *Climate*, 10(9), 133.

Wijesinghe, D. C., Withanage, N. C., Mishra, P. K., Frenando, W. S., Abdelrahman, K., & Fnais, M. S. (2025). Corrigendum: The impacts of landscape structure changes on urban surface temperature and heat islands formation of a growing city in southern Sri Lanka. *Frontiers in Environmental Science*, 13. https://doi.org/10.3389/fenvs.2025.1615562

Wu, Z., & Zhang, Y. (2019). Water bodies' cooling effects on urban land daytime surface temperature: Ecosystem service reducing heat island effect. *Sustainability*, 11(3), 787.

Wu, Z., Yao, L., & Ren, Y. (2019). Characterising the spatial heterogeneity and controlling factors of land surface temperature clusters: A case study in Beijing. *Building and Environment*, *169*, 106598. https://doi.org/10.1016/j.buildenv.2019.106598

Xu, H. (2006). Modification of the normalised difference water index (NDWI) to enhance open water features in remotely sensed imagery. *International Journal of Remote Sensing,* 27(14), 3025-3033.

Xu, Z., Tang, Y., Connor, T., Li, D., Li, Y., & Liu, J. (2017). Climate variability and trends at a national scale. *Scientific Reports*, 7(1).

Yang, L., Li, Q., Li, Q., Zhao, L., Luo, Z., & Liu, Y. (2024). Different explanations for surface and canopy urban heat island effects in relation to background climate. *iScience*, 27(3).

Yin, C., Yang, Y., Chen, X., Yue, X., Liu, Y., & Xin, Y. (2022). Changes in global heat waves and its socioeconomic exposure in a warmer future. *Climate Risk Management*, *38*, 100459. https://doi.org/10.1016/j.crm.2022.100459

Yu, D., & Fang, C. (2023). Urban Remote Sensing with Spatial Big Data: A Review and Renewed Perspective of Urban Studies in Recent Decades. *Remote Sensing*, 15(5), 1307.

Yu, H., Zahidi, I., & Fai, C. M. (2025). Mitigating Urban Heat Islands (UHI) through vegetation restoration: Insights from mining communities. *Global Challenges*, *9*(3). https://doi.org/10.1002/gch2.202400288

Yuan, F., & Bauer, M. E. (2007). Comparison of impervious surface area and normalised difference vegetation index as indicators of surface urban heat island effects in Landsat imagery. *Remote Sensing of Environment*, 106(3), 375-386.

Zhang, C., Xiao, X., Wang, X., Yi, S., Meng, C., Qin, Y., & Dong, J. (2025). Climate-induced losses of surface water and total water storage in Northeast Asia. *Communications Earth & Environment*, 6(1), 479.

Zhao, S., Tu, K., Ye, S., Tang, H., Hu, Y., & Xie, C. (2023). Land use and land cover Classification Meets Deep Learning: A review. *Sensors*, *23*(21), 8966.

Zhao, T. X., Chan, P. K., & Heidinger, A. K. (2013). A global survey of the effect of cloud contamination on the aerosol optical thickness and its long-term trend derived

from operational AVHRR satellite observations. *Journal of Geophysical Research Atmospheres*, 118(7), 2849–2857.

Zubaidi, S. L., Ortega-Martorell, S., Al-Bugharbee, H., Olier, I., Hashim, K. S., Gharghan, S. K., & Al-Khaddar, R. (2020). Urban water demand prediction for a city that suffers from climate change and population growth: Gauteng province case study. *Water*, 12(7), 1885.

# APPENDIX

UNIVERSITY OF THE WITWATERSRAND, JOHANNESBURG

HUMAN RESEARCH ETHICS COMMITTEE (NON-MEDICAL)
Registration number: REC-101114-044

03 June 2025

Re: Miss Tamiranashe Kuwaza (2428968)

Waiver letter number: HRECNMW25/06/20

To whom it may concern,

Miss Kuwaza is a registered masters' student at the School of Geography, Archaeology and Environmental Studies at the University of Witwatersrand, Johannesburg. This letter is to confirm that, at the time of writing, Miss Kuwaza does not need ethical clearance for the study entitled *"Exploring Heatwaves and Urban Heat Islands: Implications for Water Resource Availability in Gauteng Province, South Africa"*. This decision has been reached based upon a description of the project supplied by Miss Kuwaza to the University Human Research Ethics Committee (Non-Medical), which has been evaluated by the Chairs and Deputy Chairs. If, however, Miss Kuwaza changes the methods of data collection and analysis for this study, this decision may no longer be valid. If such changes take place, this should be communicated to the University Human Research Ethics Committee (Non-Medical) as soon as possible. This waiver letter is valid until 02 June 2028.

Please feel free to contact me should you require any further information.

Thank you.

Yours sincerely,
S Schoeman

**Shaun Schoeman** (Administrative Officer)
Solomon Mahlangu House, 10th Floor, Room 10004, Jorissen Street, Braamfontein, Johannesburg
Private Bag 3, Wits 2050
**T** + 27(0)11 717 1408 | **E** Shaun.Schoeman@wits.ac.za | hrec-medical.researchoffice@wits.ac.za
**www.wits.ac.za/research/about-our-research/ethics-and-research-integrity/**

*Figure 7 1: Ethics Waiver*